

of/de



Resolution Test Chart Labels:

- 1.0
- 1.1
- 1.25
- 1.4
- 1.6
- 1.8
- 2.0
- 2.2
- 2.5
- 2.8
- 3.2
- 3.6
- 4.0

PIONEERS IN METHYLENE BLUE TESTING SINCE 1974



Micro-P
MULTI-BAND FORMING

18000 COUNTY ROAD 5, BURNVILLE, MN 55337, USA
TEL: 612 436 7067 FAX: 612 435 7067 TLX: 610800049



National Library
of Canada

Bibliothèque nationale
du Canada

Acquisitions and
Bibliographic Services Branch

Direction des acquisitions et
des services bibliographiques

395 Wellington Street
Ottawa, Ontario
K1A 0N4

395, rue Wellington
Ottawa (Ontario)
K1A 0N4

Your file *Voire référence*

Our file *Notre référence*

NOTICE

AVIS

The quality of this microform is heavily dependent upon the quality of the original thesis submitted for microfilming. Every effort has been made to ensure the highest quality of reproduction possible.

La qualité de cette microforme dépend grandement de la qualité de la thèse soumise au microfilmage. Nous avons tout fait pour assurer une qualité supérieure de reproduction.

If pages are missing, contact the university which granted the degree.

S'il manque des pages, veuillez communiquer avec l'université qui a conféré le grade.

Some pages may have indistinct print especially if the original pages were typed with a poor typewriter ribbon or if the university sent us an inferior photocopy.

La qualité d'impression de certaines pages peut laisser à désirer, surtout si les pages originales ont été dactylographiées à l'aide d'un ruban usé ou si l'université nous a fait parvenir une photocopie de qualité inférieure.

Reproduction in full or in part of this microform is governed by the Canadian Copyright Act, R.S.C. 1970, c. C-30, and subsequent amendments.

La reproduction, même partielle, de cette microforme est soumise à la Loi canadienne sur le droit d'auteur, SRC 1970, c. C-30, et ses amendements subséquents.

UNIVERSITY OF ALBERTA

**The mineralogy and geochemistry of polymetallic mineral deposits at the
Ketza River Gold Mine, Pelly Mountains, central Yukon Territory**

by



Jacqueline Amelie Staveley

**A thesis submitted to the Faculty of Graduate Studies and Research in partial fulfillment of
the requirements for the degree of Master of Science.**

DEPARTMENT OF GEOLOGY

Edmonton, Alberta

Fall 1992



National Library
of Canada

Bibliothèque nationale
du Canada

Canadian Theses Service Service des thèses canadiennes

Ottawa, Canada
K1A 0N4

The author has granted an irrevocable non-exclusive licence allowing the National Library of Canada to reproduce, loan, distribute or sell copies of his/her thesis by any means and in any form or format, making this thesis available to interested persons.

The author retains ownership of the copyright in his/her thesis. Neither the thesis nor substantial extracts from it may be printed or otherwise reproduced without his/her permission.

L'auteur a accordé une licence irrévocable et non exclusive permettant à la Bibliothèque nationale du Canada de reproduire, prêter, distribuer ou vendre des copies de sa thèse de quelque manière et sous quelque forme que ce soit pour mettre des exemplaires de cette thèse à la disposition des personnes intéressées.

L'auteur conserve la propriété du droit d'auteur qui protège sa thèse. Ni la thèse ni des extraits substantiels de celle-ci ne doivent être imprimés ou autrement reproduits sans son autorisation.

ISBN 0-315-77300-6

Canada

UNIVERSITY OF ALBERTA

RELEASE FORM

NAME OF AUTHOR: Jacqueline Amelie Staveley

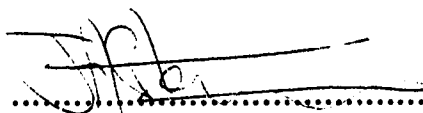
TITLE OF THESIS: The mineralogy and geochemistry of
polymetallic mineral deposits at the
Ketza River Gold Mine, Pelly Mountains,
central Yukon Territory

DEGREE FOR WHICH THIS THESIS WAS PRESENTED: Master of Science

YEAR THIS DEGREE GRANTED: Fall, 1992

Permission is hereby granted to the University of Alberta Library to reproduce single copies of this thesis and to lend or sell such copies for private, scholarly or scientific research purposes only.

The author reserves all other publication and other rights in association with the copyright in the thesis, and except as hereinbefore provided neither the thesis nor any substantial portion thereof may be printed or otherwise reproduced in any material form whatever without the author's prior written permission.



.....


#905, 8708 106th Street
Edmonton
Alberta
T6E 4J5

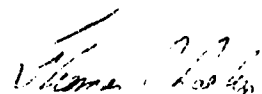
Date: June 8th 1992

UNIVERSITY OF ALBERTA

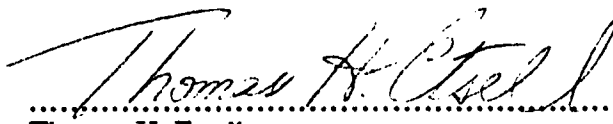
FACULTY OF GRADUATE STUDIES AND RESEARCH

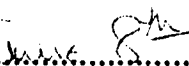
The undersigned certify that they have read, and recommend to the Faculty of Graduate Studies and Research for acceptance, a thesis entitled **THE MINERALOGY AND GEOCHEMISTRY OF POLYMETALLIC MINERAL DEPOSITS AT THE KETZA RIVER GOLD MINE, PELLY MOUNTAINS, CENTRAL YUKON TERRITORY** submitted by **JACQUELINE AMELIE STAVELEY** in partial fulfillment of the requirements for the degree of **MASTER OF SCIENCE**.


.....
Supervisor: Bruce E. Nesbitt


.....
Thomas Chacko


.....
Phillipe Erdmer


.....
Thomas H. Etsell

Date:  1992

Dedicated to the memory of

John Robert Staveley (1940-1991)

and

Diana Berenice Staveley (1942-1982)

my parents.

ABSTRACT

The Ketza River polymetallic mineral deposits are situated in the Pelly Mountains, Central Yukon Territory. The deposits were mined for gold from 1988 to 1990, producing 400 tonnes of oxide ore per day over that period. The Ketza River deposits are hosted by lower Paleozoic sedimentary strata of the parautochthonous Cassiar Terrane. The main host to economic mineralisation is a lower Cambrian, massive, archeocyathid-bearing limestone, which outcrops over much of the Ketza River area.

Four styles of mineralisation are recognised within the Ketza River deposits. Type I mineralisation occurs in the centre of the area and consists of argillite-hosted, Au-quartz-sulphide veins. Sulphide mineralogy is mainly arsenopyrite and pyrite. Type II mineralisation consists of limestone-hosted, massive sulphide mantos and chimneys. The principal sulphide mineralogy of the mantos is pyrrhotite-arsenopyrite-pyrite-chalcopyrite, with quartz and calcite gangue. Gold is present within the arsenopyrite and pyrite. Type III mineralisation consists of limestone-hosted, quartz-sulphide veins and mantos. Mineralogy is similar to the Type II mineralisation, but contains a higher proportion of gangue. Type IV mineralisation consists of Ag-Pb veins. These veins are hosted by a variety of lithologies and represent the outermost extent of Ketza River mineralisation. Sulphide mineralogy is galena-sphalerite-pyrite, with siderite, calcite and quartz gangue.

Oxidation of sulphides in parts of the Ketza River area is deep and pervasive. Areas of oxidation show increased gold grade and were the focus for mining. Oxidation occurs in the heavily fractured central area of the mineralisation, and along the Peel Fault, which extends from the centre of mineralisation towards the east.

Light stable isotope studies indicate that the main mineralising fluid was of meteoric origin ($\delta^{18}\text{O}_{\text{fluid}}=10\text{‰}$, $\delta\text{D}_{\text{fluid}}=-165\text{‰}$). This fluid had evolved in $\delta^{18}\text{O}$ by interaction with Cassiar Terrane rocks before mineralisation occurred. Fluid flow in the limestones was pervasive, and produced a large, approximately 75km^2 , ^{18}O depletion halo around the deposits. The later oxidising fluid was also of meteoric origin ($\delta^{18}\text{O}_{\text{fluid}}=-18\text{‰}$) but shows no evidence of interaction with the sedimentary pile.

Fluid inclusion microthermometry suggests that the temperature of formation of the deposit was around 325°C , at pressures above 600 bars. The mineralising fluid contained approximately 11 mole% $\text{CO}_2\pm\text{CH}_4$, and 5 equivalent weight% NaCl.

ACKNOWLEDGEMENTS

Firstly, I would like to thank my supervisor, Bruce Nesbitt, not because it's the traditional thing to do (which it is), but because he has showed amazing patience at putting up with my idiosyncrasies, side projects and general overenthusiasm for everything I'm not supposed to be doing, and, on top of all this, has supported me financially through much of this research. While on the faculty note, Tom Chacko, Karlis Muehlenbachs and Bob Luth all deserve honorable mentions for helping me sort out problems of untold magnitude, in the fields of geochemistry, thermodynamics and mathematics; and of course for their input into those famous side projects.

Thank you also to the alchemists of the stable isotope lab: Karlis, as mentioned above, Olga, James Steer, Gaileen, and Rob King, who performed isotopic analyses on silicates and fluid inclusions, and without whom this thesis would be largely dataless. The Geology department as a whole has been most supportive, and has made this process a lot easier at times.

Of course, none of this could have happened at all if it wasn't for hard cash (the inevitable bugbear of exploration). Thank you to the Department of Geology, for support in the form of assistantships, also to the Canadian Circumpolar Institute, and Energy, Mines and Resources Canada for supporting me in the field. Thanks to Canamax Resources Inc. for allowing me free access to the Ketzia mine and to pertinent information, and for providing board and lodging at Ketzia River. Special thanks are due to Shirley, Mike and Bruce, the Ketzia geology crew. As I mentioned above, Bruce Nesbitt provided welcome financial support, courtesy of NSERC.

Thanks are well overdue to my friends in the department and elsewhere. Thanks (and purple fishes) to the other two members of the 'terrible trio' - James and Agnes, for moral and emotional support and general goofiness, which kept me sane during the last two years. Thanks to Ralph for advice, critical editing, and chocolate cake crumbs; to Bjarni, Chris, Gerard and Heather for discussion and conversation about work and play, geology and the art of brewing, hockey and stable isotopes. Thanks to everyone else in the University community whom I've come to love or hate, respect and ridicule, have a beer for me!

And finally, in some ways most importantly, thank you to my adopted family of friends: Anna, Robert, Dave, Gunnar, Steph, Krissy and Stephen, for many hours of darts and Star Trek, and for being as crazy as I seem to be. Thanks to Leonard and Lou for plentiful inspiration during hours of dry writing, and to Fuzz, my cat, for just being.

TABLE OF CONTENTS

Chapter:

I: INTRODUCTION TO THE KETZA RIVER MINERAL DEPOSITS.....	1
<i>Exploration and mining history.....</i>	<i>1</i>
<i>Mineralisation in the Cassiar Platform.....</i>	<i>1</i>
<i>Previous work.....</i>	<i>1</i>
<i>Objectives of this study.....</i>	<i>4</i>
 II: GEOLOGY AND TECTONIC SETTING OF THE KETZA RIVER DEPOSIT.....	 5
1. <i>Regional geology of the Pelly Mountains.....</i>	<i>5</i>
<i>Stratigraphy.....</i>	<i>5</i>
<i>Structure.....</i>	<i>7</i>
<i>Igneous activity.....</i>	<i>7</i>
2. <i>Geology of the Ketza River area.....</i>	<i>7</i>
<i>Stratigraphy.....</i>	<i>9</i>
<i>Structure.....</i>	<i>10</i>
 III: MINERALOGY OF THE KETZA RIVER DEPOSIT.....	 12
<i>Type I mineralisation.....</i>	<i>12</i>
<i>Type II mineralisation.....</i>	<i>15</i>
<i>Type III mineralisation.....</i>	<i>20</i>
<i>Type IV mineralisation.....</i>	<i>21</i>
 IV: LIGHT STABLE ISOTOPE STUDY.....	 23
<i>Introduction.....</i>	<i>23</i>
<i>Experimental method.....</i>	<i>23</i>
<i>Results.....</i>	<i>29</i>
<i>Limestones and carbonate veins.....</i>	<i>29</i>
<i>Quartz veins.....</i>	<i>29</i>

TABLE OF CONTENTS (continued)

Chapter:

IV: LIGHT STABLE ISOTOPE STUDY (continued)

<i>Discussion of light stable isotope data.....</i>	35
1. <i>Calcite-quartz geothermometry.....</i>	35
2. <i>Spatial distribution of isotopes and implications for fluid flow.....</i>	38
3. <i>Fluid composition.....</i>	38
<i>Early fluids.....</i>	38
<i>Late fluids.....</i>	41

V: FLUID INCLUSION STUDY..... 44

<i>Introduction.....</i>	44
<i>Results.....</i>	44
<i>Observation of fluid inclusions.....</i>	44
<i>Aqueous inclusions.....</i>	46
<i>CO₂-bearing inclusions.....</i>	46
<i>Microthermometric data from Ketz River fluid inclusions in quartz.....</i>	46
<i>Aqueous inclusions.....</i>	46
<i>CO₂-bearing inclusions.....</i>	49
<i>Fluid composition and density calculations.....</i>	49
<i>Aqueous inclusions.....</i>	49
<i>CO₂-bearing inclusions.....</i>	51
<i>Discussion of fluid inclusion data.....</i>	51
<i>Temperature and pressure of trapping of fluid inclusions.....</i>	53

VI: DISCUSSION AND DEPOSIT MODEL..... 54

<i>Evidence for meteoric fluids: Deposits of the Canadian Cordillera.....</i>	59
<i>Mineral deposits of the Canadian Cordillera: Fluid composition.....</i>	59
<i>A heat source for mineralisation at Ketz River.....</i>	60
<i>Mineralising fluid: 1. Fluid source.....</i>	60
<i>Mineralising fluid: 2. Fluid composition.....</i>	62
<i>A model for the formation of the Ketz River mineral deposits....</i>	62
<i>Implications.....</i>	63

TABLE OF CONTENTS (Appendices)

Appendix:

I:	<i>Fractionation equations used in oxygen isotopic calculations, Chapter IV....</i>	71
II:	<i>Water:rock ratio and mass balance calculations from isotopic data.....</i>	72
III:	<i>Equations used in fluid inclusion salinity calculations, Chapter V.....</i>	74
IV:	<i>Ketza River surface samples.....</i>	75
V:	<i>Sample suites taken along traverses close to underground workings.....</i>	79

LIST OF TABLES

Table:

IV-1	Ketza River regional stable isotope data.....	24
IV-2	Systematic limestone and calcite vein sample series taken from sites close to underground workings.....	27
IV-3	Calcite-quartz oxygen isotope geothermometry for veins of the Ketza River deposit.....	36
V-1	Microthermometric data for vein quartz.....	47
VI-1	Characteristics of the Ketza River mineral deposits.....	55

LIST OF FIGURES

Figure:

1	Tectonic and lithologic units of a. Yukon Territory and b. Pelly Mountains area (b. simplified from Wheeler and McFeely, 1991).....	3
2	Stratigraphic column for the lower Paleozoic of the Pelly Mountains. (After Gabrielse and Wheeler, 1961).....	6
3	Major thrust faults in the Ketza-Seagull district, modified from Abbott (1986).....	8
4	Geology of the Ketza River area, showing hosts to mineralisation.....	11
5	Schematic representation of the features of the four mineralisation styles seen at Ketza River: a. Type I mineralisation: argillite-hosted quartz-sulphide veins; b. Type II mineralisation: limestone-hosted massive sulphide mantos; c. Type III mineralisation: limestone-hosted quartz-sulphide veins and pods; d. Type IV mineralisation: Ag-Pb-bearing quartz-carbonate veins, hosted by a variety of lithologies.....	13
6	Showings and vein groupings used in the text, names given by Canamax and others. 1. Peel; 2. Ridge; 3. Break; 4. Lab/Hoodoo; 5. Penguin; 6. Sauna; 7. Tarn; 8. Upper Tarn; 9. Cliff; 10. Oxo Flats; 11. Oxo; 12. Peel Creek; 13. Gully; 14. QB; 15. Knoll; 16. MMM; 17. Mount Fury; 18. Next Valley; 19. White Creek (north tributary); 20. White Creek; 21. Stump; 22. East Cache Creek; 23. Ketza River (south); 24. Ketza River (north); 25. Misery Creek.....	14
7	Map showing the PEEL and RIDGE zones of oxide and sulphide mineralisation, showing also the surface traces of faults in the area. (After Abercrombie, in press).....	16
8	Oxygen isotopic composition of (a) carbonate veins and (b) limestones in the Ketza River area. Note the two populations of carbonate veins, interpreted from field and petrologic evidence as being from early-stage and late-stage fluids.....	30
9	$\delta^{18}\text{O}$ of carbonate veins in the Ketza River area. Values are quoted as permil (‰) relative to SMOW.....	31
10	Oxygen isotopic composition of quartz veins associated with the four mineralisation types: a. Type I mineralisation; b. Type II mineralisation; c. Type III mineralisation; d. Type IV mineralisation.....	32
11	$\delta^{18}\text{O}$ of quartz veins from the Ketza River area. Figures in italics represent averaged values for several samples from one showing. Values are quoted as permil (‰) relative to SMOW.....	33
12	δD of quartz veins in the Ketza River area. Figures in italics represent averaged values for several samples from one showing. Values are quoted as permil (‰) relative to SMOW.....	34

LIST OF FIGURES (continued)

Figure:

13	Calcite-quartz pairs used for oxygen isotopic geothermometry. The orientation of tie lines for calcite-quartz equilibrium at temperatures of 250°C to 400°C (from the equation of Friedman and O'Neil, 1977) is also shown.....	37
14	Location of evidence for the three fluid types: Fluid I, Fluid II and Fluid III. Fluid I is considered to be responsible for primary mineralisation. Fluid III is considered to be responsible for oxidation of sulphide in parts of the deposit.....	39
15	Plot of δD versus $\delta^{18}O$ for vein forming fluids at Ketz River. The two curves represent fluid evolution with variable water:rock ratios (displayed on the curves) at a temperature of 350°C, for dominantly shale-hosted and dominantly limestone-hosted (<i>italics</i>) systems. Fluid III is plotted along the base of the graph since no δD values are available.....	42
16	Fluid inclusion categories based upon contained phases. Aqueous inclusions are two-phase at room temperature. Carbon dioxide-bearing inclusions are three-phase at room temperature.....	45
17	Isochores for aqueous inclusions trapping Fluid I and Fluid II. Salinity = 5 equiv. wt.% NaCl. Data for 2-phase curve and isochore co-ordinates taken from Haas (1976) and Potter and Brown (1977). Trapping pressure estimates are based on an estimated temperature range of 300 to 350°C. See text for further discussion of fluid pressure and temperature conditions.....	50
18	Isochore for carbon dioxide-bearing inclusions trapping Fluid I. Total fluid density 0.82g/cc, salinity 5 equiv. wt.% NaCl. Isochore co-ordinates taken from Bowers and Helgeson (1983), two-phase curve data from Takenouchi and Kennedy (1965).....	52
19	Model of an hydrothermal cell containing circulating meteoric water, driven by an igneous heat source.....	61
20	Model of the Ketz River hydrothermal system responsible for producing mineralisation styles described in the text - Type I: Au-quartz-sulphide veins; Type II: massive sulphide mantos; Type III: quartz-sulphide bodies; Type IV: Ag-Pb veins. a. Main mineralising event, a pluton-driven hydrothermal cell; b. Oxidising event, influx of low temperature meteoric water.....	64
21	Map as in Figure 7, showing entrances to the underground workings and the surface traces of sample traverses near the underground workings. (After Abercrombie, in press.).....	80

LIST OF PLATES

Plate:

- 1 The Ketz River Gold Mine camp and mill..... 2
- 2 Photomicrographs of polished sections of sample KR-90-81, showing euhedral pyrite separated from pyrrhotite by a thin quartz layer. Scale bar = 100µm. Photographs taken in plane polarised reflected light. po = pyrrhotite, py = pyrite, qtz = quartz..... 18
- 3 Oxide ore from the Ketz River deposits: a. Open pit mining of RIDGE zone oxides; b. outcrop of local oxidation of sulphides of the PENGUIN zone..... 19

CHAPTER I

INTRODUCTION TO THE KETZA RIVER MINERAL DEPOSITS

The Ketza River Gold Mine (Canamax Resources Inc.) is situated in the Pelly Mountains, central Yukon Territory. The minesite (shown in Plate 1) is located at 61° 30' N, 132° 15' W, approximately 90 km southeast of the town of Ross River. Access to the mine is along a 40 km gravel road which leaves the Robert Campbell Highway approximately 50 km east of Ross River.

Exploration and mining history

The original discoveries in the area were silver-lead veins, which were discovered in 1947 by Hudson Bay Mining and Smelting Ltd. on the 'Iona property', a loose description of the Ag-Pb vein deposits which surround the main Ketza River manto mineralisation on three sides. Gold was discovered on the Ketza River property in 1954 and 1955 by Conwest Exploration Co. Ltd. Subsequent exploration work from 1955 to 1960 defined sulphide reserves of 68 000 tonnes with an average grade of 12 g/t Au. Exploration ceased in 1960 due to economic pressures.

In 1984 Pacific Trans-Ocean Resources Ltd. optioned the property and entered into an agreement with Canamax Resources Inc. Three years of exploration defined oxide reserves of 495 000 tonnes grading 18 g/t Au and a sulphide reserve of equal size but lower grade, averaging 9 g/t Au. Mining of oxide ore began in early 1988 and continued until late 1990, when operations were suspended due to exhaustion of exploitable oxide ore and a decrease in gold price. No further mining of the deposit is planned at present.

Mineralisation in the Cassiar Platform

The Ketza River deposits lie in the pericratonic strata of the Cassiar Platform (shown in Figure 1). The host rocks are Lower Paleozoic carbonate and clastic sedimentary rocks deposited along the western margin of ancestral North America (Abbott, 1986). These sedimentary rocks host other mineral deposits in the Yukon and northern British Columbia, at Faro, Midway, Rancheria, and other locations. The Ketza River deposits are unlike the deposits at these other locations in that the primary element of interest is gold; other deposits in the Cassiar platform are primarily Ag-Pb-Zn deposits.

Previous work

The Ketza River deposits have a relatively unique mineralisation style for the Yukon, in terms of mineralogy and morphology. However, little work on this area has

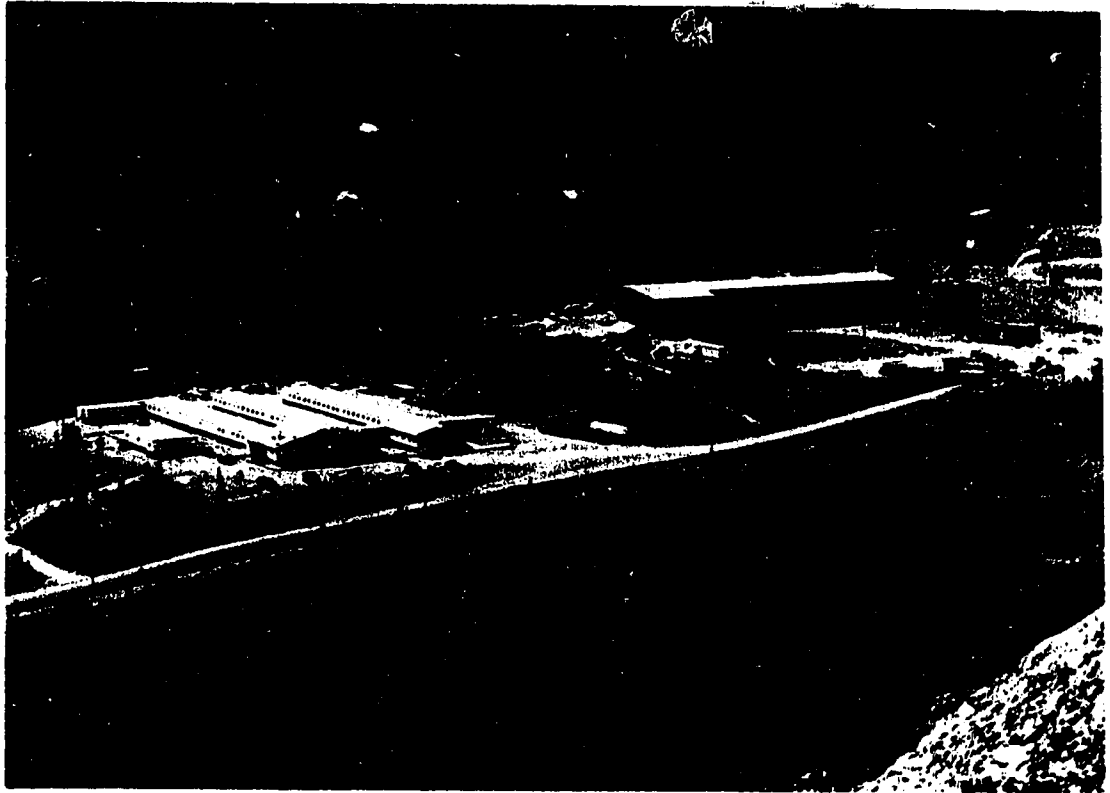


Plate 1: The Ketza River Gold Mine camp and mill.

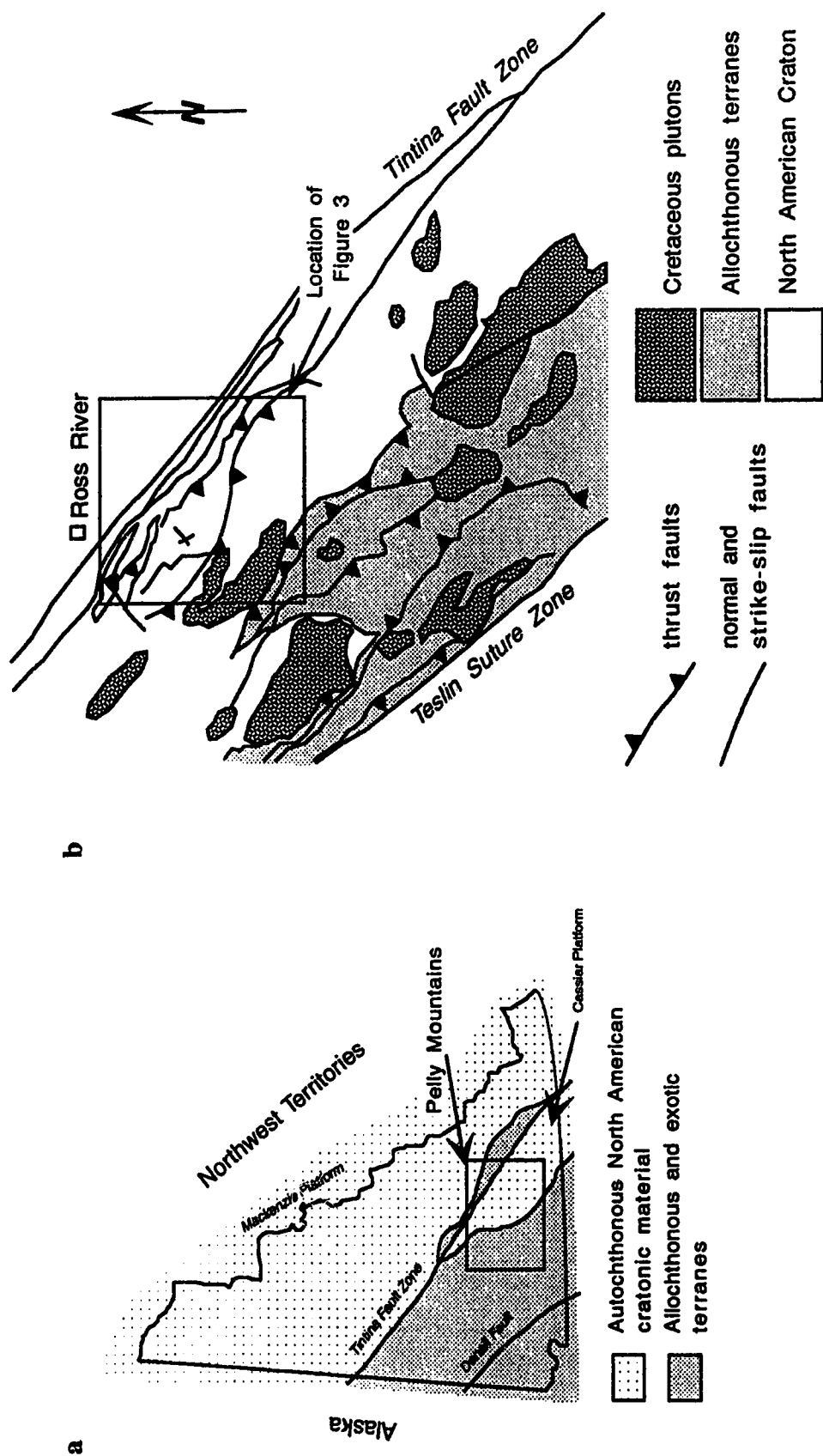


Figure 1: Tectonic and lithologic units of a. Yukon Territory and b. Pelly Mountains area (b. simplified from Wheeler and McFeely, 1991)

been undertaken to date. Abbott (1986) presented a regional description of epigenetic mineralisation in the Ketz River District and in the adjacent Seagull Creek area. This documented a number of mineral occurrences in the two areas, which exhibit similarities which are believed to be related to buried Cretaceous plutons. Cathro (1988) presented preliminary results of a study of the Ketz River deposits, this covers stratigraphy of the area and a description of mineralisation styles. Abercrombie (in press) describes the geology of the oxide ore bodies mined from 1988 to 1990, and the exploration history of the deposit.

Objectives of the present study

Initial aims of this study were to use the techniques of stable isotope geochemistry and fluid inclusion microthermometry to characterise the fluids from which the mineralisation at Ketz River formed. For this, samples of vein quartz and carbonate (calcite, siderite, ankerite) associated with the mineralisation were collected for analysis. Sulphide mineralisation and host rock samples were also collected.

Preliminary results led to a more detailed investigation of fluid flow through the limestones, and fluid-rock interaction within the mineralising system. Isotopic constraints on the water:rock ratio and fluid path were studied. This study aims to present a deposit model for the mineralisation at Ketz River based upon the above geochemical observations and to consider the implications for such a model for other deposits in the Canadian Cordillera and elsewhere.

The study forms part of an ongoing research project into crustal fluids in mineralised and unmineralised areas of the Canadian Cordillera undertaken at the University of Alberta (eg. Nesbitt and Muehlenbachs, 1989; Nesbitt et al., 1989; Nesbitt, 1990).

CHAPTER II

GEOLOGY AND TECTONIC SETTING OF THE KETZA RIVER DEPOSIT

1. Regional geology of the Pelly Mountains

The Pelly Mountains area, shown on Figure 1, lies within the Cassiar Terrane (also known as the Cassiar Platform). The region contains miogeoclinal Proterozoic and Lower Paleozoic strata which are autochthonous and parautochthonous to the North American Craton. The intense deformation seen in these rocks is attributed to arc-continent collision during the Mesozoic, and to Cretaceous plutonism (Abbott, 1986).

This part of the Cassiar Terrane has been displaced to the northwest by strike-slip movement along the Tintina Fault Zone, a large dextral shear zone, which juxtaposes Cassiar Terrane rocks against rocks of the allochthonous Yukon-Tanana Terrane. Approximately 450 km of displacement has occurred on this fault since the mid-Cretaceous (Gabrielse, 1985).

Stratigraphy

The stratigraphy of the Cassiar Platform in the Pelly Mountains has been described by Gabrielse and Wheeler (1961) and Templeman-Kluit et al. (1975,1976). The following summary uses the results of their studies.

The base of the Cambrian in the region is represented by a quartzite unit, overlain by a thick fossiliferous limestone sequence, which contains some argillaceous units. A major depositional hiatus occurred in the Middle Cambrian: Upper Cambrian slates (locally calcareous) and phyllites lie unconformably on the Lower Cambrian limestones. In some locations contain volcanic units of mid- to late-Cambrian age.

The Ordovician and early Silurian throughout the area is represented by graptolitic shales, which are locally graphitic. The shales grade into dolomitic siltstone by the late Silurian.

A second depositional hiatus occurs in the Devonian. This is expressed as a disconformity in some parts of the region, and by an angular unconformity in other parts. The Devonian sedimentary rocks, which lie above this unconformity, are orthoquartzites and fossiliferous dolomites. During the late-Devonian to early-Mississippian, subsidence, volcanism and ultramafic plutonism occurred, marking the transition of the area from passive margin to active subduction, and the incorporation of exotic terrane material into the stratigraphic record.

A stratigraphic column for the Pelly Mountains area is shown in Figure 2.

Structure

The sedimentary strata of the Pelly Mountains have been imbricated by a series of northeasterly directed thrust faults, some of which have been folded. These faults place Cambro-Ordovician rocks above more competent Devonian and Mississippian rocks (Gabrielse and Wheeler, 1961). In places the thrust faults are broken by north-northwesterly trending normal faults; the exact age of these faults is unknown, but they predate at least some of the thrusting, since they do not penetrate all of the thrust faults. Thrusting is thought to be of late-Triassic to early-Cretaceous age (Templeman-Kluit et al, 1976; Abbott, 1986).

Principle faults around the Ketzá-Seagull area (Abbott, 1986) are shown in Figure 3.

Igneous activity

In addition to the Paleozoic volcanism and ultramafic plutonism mentioned above, the region experienced mid-Cretaceous granitic plutonism. The intrusions in the Pelly Mountains occupy the cores of two northwest trending arches within the imbricated miogeoclinal rocks. It is possible that this plutonism is responsible for the folding seen in the thrust faults (Gabrielse and Wheeler, 1961).

2. Geology of the Ketzá River area

The Ketzá River Gold Mine is situated in the northeast portion of the Pelly Mountains, in an area known as the St. Cyr Range. This area is cut by four significant northeasterly directed thrust faults: the McConnell, Porcupine-Seagull, Cloutier and St Cyr thrusts. These faults lie parallel to the Tintina Fault Zone, which separates the Cassiar Platform from the Yukon-Tanana Terrane to the northwest.

The minesite area occupies a prominent northwest-trending window through the Porcupine-Seagull thrust, known as the Ketzá-Seagull Arch (Abbott, 1986). This window shows uplift and doming feature believed to be related to the emplacement of a buried Cretaceous intrusion. The presence of such an intrusion has been indicated by hornfelsing in argillites and by a magnetic anomaly centred on the uplifted area. The Ketzá-Seagull Arch consists of two areas: 1. The Ketzá Uplift, which lies in the centre of the Canamax property, and 2. The Seagull Arch, which lies to the west of the property (Abbott, 1986). These features are shown on Figure 3.

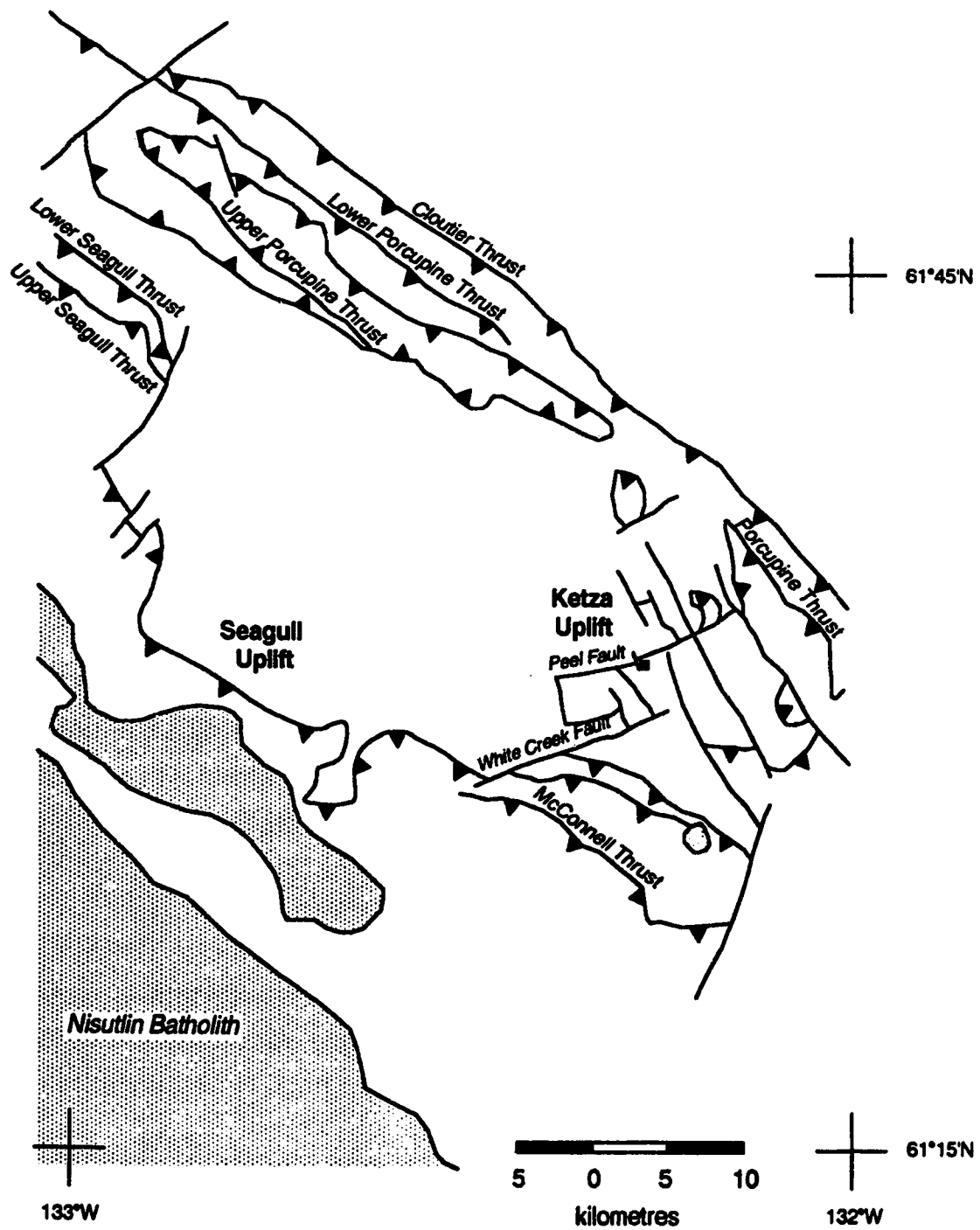


Figure 3: Major thrust faults in the Ketzá-Seagull District, modified from Abbott (1986).

Stratigraphy

The stratigraphy in the minesite area consists of five main lithostratigraphic units (Cathro, 1988) from lower Cambrian to Mississippian in age. The majority of these units are part of the Cloutier thrust sheet, with the uppermost unit occurring as klippen of the overlying Porcupine-Seagull thrust sheet.

Unit 1: Lower Cambrian

The base of this unit is not exposed in the Ketz River area, the upper contact is an unconformity thought to be of Upper Cambrian age (Cathro, 1988). The unit has a total thickness of more than 500m and has been divided into 5 subunits.

Unit 1a consists of siltstone, quartzite and green argillite. It is strongly hornfelsed on the north side of Peel Ridge, which is where the majority of the Ketz River gold deposits are located. Unit 1b is a bed of dark grey-black silty limestone, conformably overlying unit 1a. Unit 1c is a grey-green-brown calcareous phyllitic mudstone containing early Cambrian fossils and large pyrite cubes (Cathro, 1988).

Unit 1d is the main host for the gold mineralisation, consisting of blue-grey archeocyathid bearing limestone. The unit is made up primarily of strongly bioturbated lime mud with interbedded argillaceous layers. The contact between units 1c and 1d is gradational and based upon the lime content of the beds. Some dolomitisation is seen in this bed to the north of the Ketz deposit (Cathro, 1988).

Unit 1e is a phyllitic green mudstone, which in some parts of the area is completely missing, indicating unconformable contact between unit 1 and unit 2. (Cathro, 1988)

Unit 2: Upper Cambrian to Ordovician

The two subunits of unit 2 are recessive and, as such, are difficult to study closely. Unit 2a is a black shale, at least 30-100m thick (Cathro, 1988) unconformably overlying Unit 1. Unit 2b is a calcareous phyllite/shale, containing small quartz-ankerite veins, larger quartz veins and galena-siderite veins.

Unit 3: Ordovician to Devonian

Most parts of unit 3 host galena-siderite veins. The lowermost unit (3a) is conformable with unit 2 and is a graphitic graptolitic shale, containing minor beds of silty and calcareous/muddy shale. Unit 3b is a discontinuous bed of grey silty dolomite and dolomite breccia, containing large coral fragments of Silurian age and some Ag-Pb mineralisation (Cathro, 1988). Unit 3c is a massive orthoquartzite, white to medium grey in

colour, hosting galena-siderite and quartz-pyrite-Au mineralisation. Unit 3d is a dark grey fossiliferous dolostone of Devonian age (Cathro, 1988).

Unit 4: Devonian to Mississippian

Unit 4a lies unconformably on Unit 3c and consists of black slate, cherty siltstone and crystal tuff. The overlying unit 3b contains tuff or siltstone and a calcareous phyllite. The remaining subunit occurs as rare syenite sills and dykes (Cathro, 1988) of Mississippian age. These are concentrated in the southern part of the Ketza River property, outside the main zone of mineralisation.

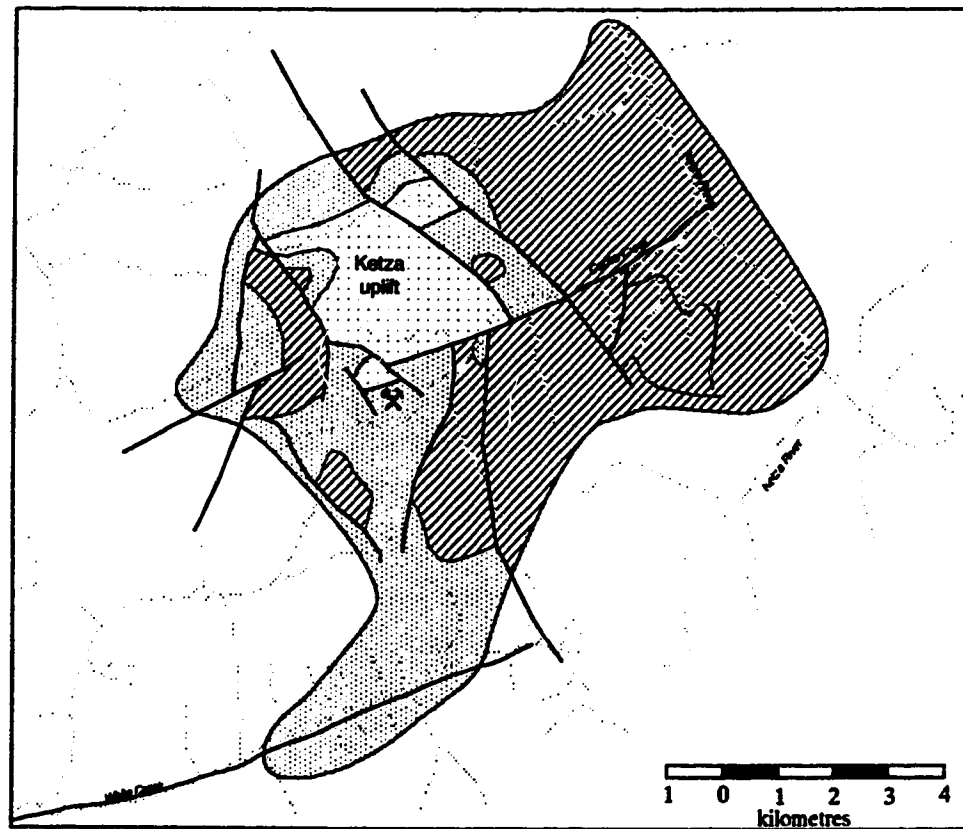
Unit 5: Upper Cambrian to Ordovician

This unit is made up of rocks of the Porcupine-Seagull thrust sheet which form two klippen within the minesite area (Cathro, 1988). The lithologies represented are locally calcareous phyllite and moderately foliated amygdaloidal volcanic flows and agglomerate.

The spatial distribution of units 1a, 1b-e and units 2-5 is shown in Figure 4.

Structure

The Ketza River minesite area is dominated by the Ketza Uplift (Abbott, 1986). The major structures seen are faults. The oldest of these are northeasterly directed thrusts, the effects of which are most easily documented in the Lower Cambrian units. These thrusts are cut by at least three sets of steeply-dipping faults, which are believed to be related to uplift (Cathro, 1988). The majority of silver-lead occurrences are related to northerly-trending faults showing little displacement. Northwest-trending faults provide an important control on Au mineralisation and oxidation of the deposit.



LEGEND

Units	Faults
2-5	Upper Cambrian to Mississippian sediments - shale, siltstone, dolomite, orthoquartzite - hosts for Ag-Pb-bearing distal veins
1b-e	Lower Cambrian calcareous mudstone grading into massive archeocyathid limestone - host to Au-bearing and barren sulphide mantos
1a	Lower Cambrian siltstone, argillites and quartzite - host to Au-bearing quartz-sulphide veins
	Limit of study area

Figure 4: Geology of the Ketza River area, showing hosts to mineralisation.

CHAPTER III

MINERALOGY OF THE KETZA RIVER DEPOSIT

Mineralisation at Ketza River occurs in four distinct types which are spatially related to structure and also to host lithology. The mineralisation is polymetallic and all mineralisation styles include metallic sulphides with quartz and carbonate as the gangue phases. Gold grade appears to be more closely related to structure and to later oxidation than to the style of mineralisation, thus not all zones are auriferous, or economic.

Four types of mineralisation occur in zones extending away from the centre of the Ketza Uplift. These can be termed types I to IV. Type I mineralisation consists of argillite-hosted, Au-bearing quartz-sulphide veins, in which the main sulphides are arsenopyrite and pyrite. This type of mineralisation occurs closest to the centre of the Ketza Uplift, where the argillites are extensively hornfelsed. The area forms the north limb of the Peel Creek anticline (Abercrombie, in press). Type II mineralisation, found primarily on the southern flank of the Peel Creek anticline and extending westwards, consists of limestone-hosted, massive sulphide pods with quartz and calcite as gangue phases. The pods are known as mantos where they are approximately stratiform; vertical pods are termed chimneys. In parts of the deposit, these pods have been extensively oxidised and it is in the oxidised parts of these bodies that the majority of gold ore is found, with an average grade of 12.8g/t (Abercrombie, in press). Few of the sulphide pods contain significant gold; none contain grades as high as the oxides. Type III mineralisation is made up of limestone-hosted, quartz-sulphide veins and pods, containing locally extensive boxwork, which are generally Au-poor or barren. Type IV mineralisation surrounds the central deposits on three sides. This primarily takes the form of Ag-Pb veins, containing galena and pyrite with carbonate and quartz as gangue phases.

The major features of each of the mineralisation types I to IV are shown in Figure 5, and discussed in more detail below. Figure 6 shows the locations of named mineral occurrences and vein groupings used by the author and is referred to in the sections below.

Type I mineralisation

The QB, GULLY, KNOLL, MMM, and PEEL CREEK zones, which are representative of this type of mineralisation, are shown on Figure 6. The main mineralogy is quartz, arsenopyrite and lesser amounts of pyrite, with trace calcite. Oxidation in this area has led to replacement of the sulphides by scorodite and limonite and to the production of clay minerals. Gold grades are highest where oxidation has occurred, locally reaching as high as 1000g/t (Cathro, 1988), although average grades are much lower. None of the

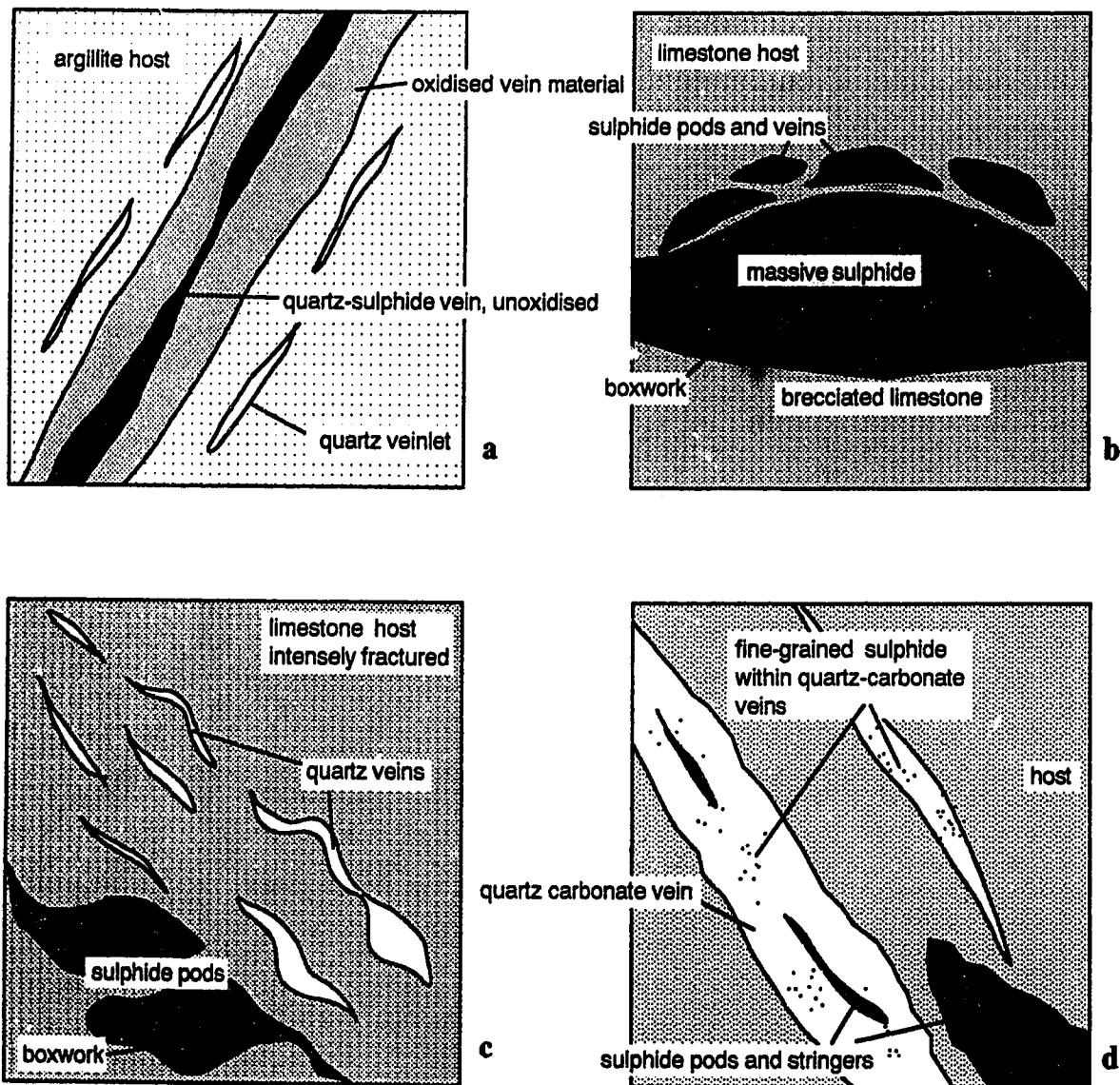


Figure 5: Schematic representation of the features of the four mineralisation styles seen at Ketza River: a. Type I mineralisation: argillite-hosted quartz-sulphide veins; b. Type II mineralisation: limestone-hosted massive sulphide mantos; c. Type III mineralisation: limestone-hosted quartz-sulphide veins and pods; d. Type IV mineralisation: Ag-Pb-bearing quartz-carbonate veins, hosted by a variety of lithologies.

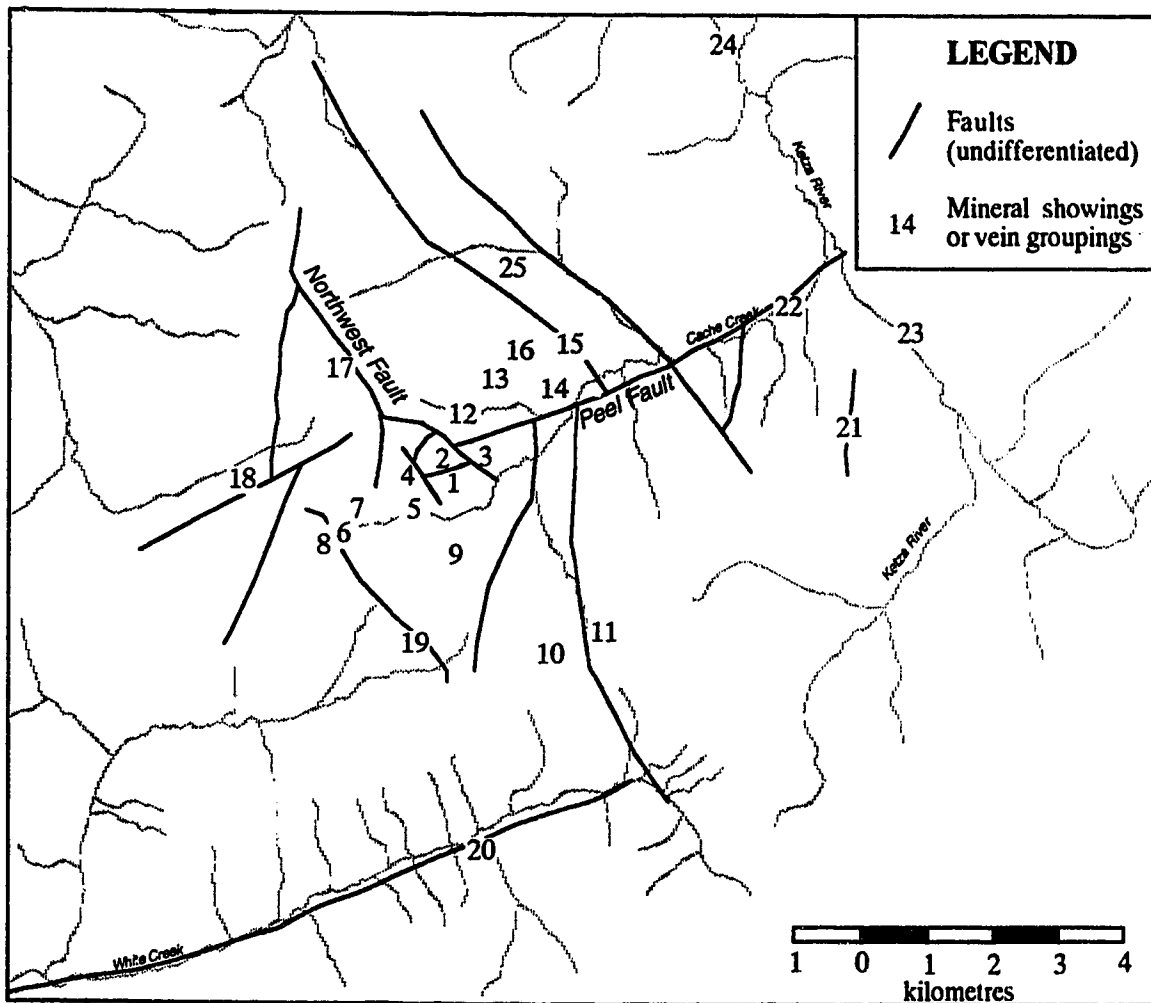


Figure 6: Showings and vein groupings used in the text, names given by Canamax and others. 1. Peel; 2. Ridge; 3. Break; 4. Lab/Hoodoo; 5. Penguin; 6. Sauna; 7. Tarn; 8. Upper Tarn; 9. Cliff; 10. Oxo Flats; 11. Oxo; 12. Peel Creek; 13. Gully; 14. QB; 15. Knoll; 16. MMM; 17. Mount Fury; 18. Next Valley; 19. White Creek (north tributary); 20 White Creek; 21. Stump; 22. East Cache Creek; 23. Ketza River (south); 24. Ketza River (north); 25. Misery Creek.

veins are extensive and this mineralisation type is responsible for only a small part of the gold tonnage mined at Ketzah River. The veins strike north to northeast and dip steeply, usually being close to vertical. Vein orientation may be related to a suite of normal faults which developed in response to the emplacement of the Cretaceous stock thought to lie beneath the centre of the Ketzah Uplift (Cathro, 1988; Abbott, 1986).

The largest quartz-sulphide vein of this group is the GULLY zone, which contains quartz, scorodite, some arsenopyrite and minor pyrite. Brecciation is reasonably common in much of the vein and in the most oxidised parts, the quartz is broken and rubblely. Limonitic staining of the quartz is visible, although large pods of limonite are not seen. The QB (quartz breccia) zone also consists of quartz, scorodite and arsenopyrite, but is less extensive than the GULLY zone and contains some gangue phase carbonate. The KNOLL zone contains mainly quartz-carbonate veins, with limonitic staining, and lesser amounts of sulphide. The MMM zone consists of a quartz-arsenopyrite vein, partially oxidised to scorodite and clay around a central sulphide core.

Type II mineralisation

This style of mineralisation is found in the PEEL, RIDGE, BREAK, PENGUIN and TARN zones shown on Figure 6, and was the major focus of mining activity at Ketzah from 1988 to 1990. The PEEL and RIDGE zones, two deeply and pervasively oxidised bodies which occur close to the junction of the Peel Fault and the Northwest Fault (shown on Figure 7), are situated in an area of intense faulting south of the centre of the Ketzah Uplift. The pods are composed primarily of sulphide or oxide minerals, with minor quartz and carbonate (calcite and siderite) veining, usually around the edges of the pods, or along fissures. Pyrrhotite is the main sulphide phase present, with arsenopyrite, pyrite and chalcopyrite present in variable, but considerably smaller, quantities. The pyrrhotite is generally massive, but in places occurs as aggregates of small, euhedral grains. Arsenopyrite is present in local areas of concentration within massive pyrrhotite. Pyrite occurs as euhedral cubic crystals, up to 1mm in diameter, within the massive pyrrhotite, often associated with gangue phases which are quartz and calcite. Chalcopyrite is present only in very small quantities, usually associated with pyrite.

Oxide mineralogy consists of a complex assemblage of hydrous Fe oxides, including limonite, hematite and hisingerite - a banded yellow, orange, red and black amorphous mineral which is invariably associated with the highest gold grades. Very little alteration of the limestone is seen at the edges of the sulphide or oxide pods, although in some areas local bleaching of the surrounding limestone has been noted (Cathro, 1988).

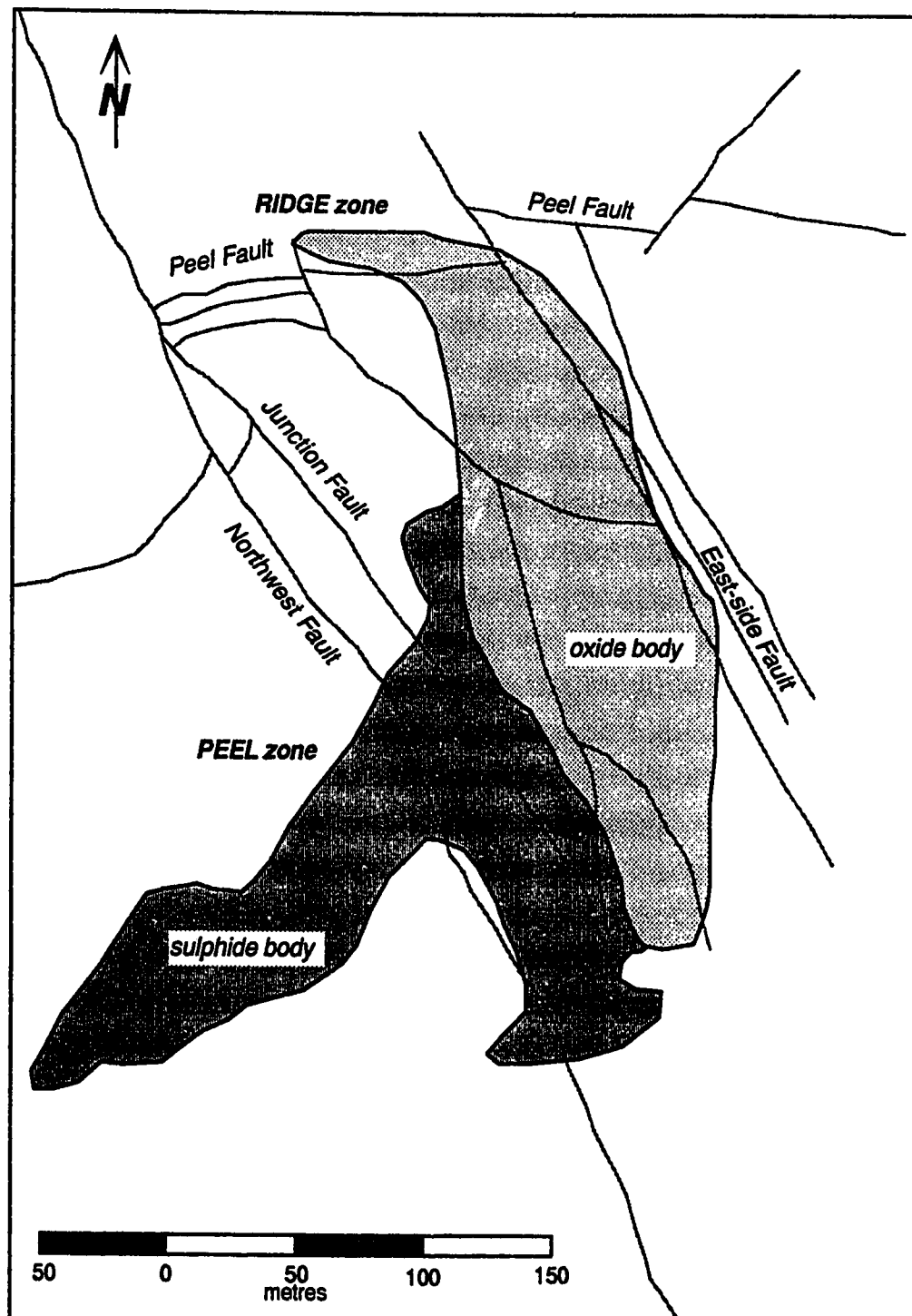


Figure 7: Map showing the PEEL and RIDGE zones of oxide and sulphide mineralisation, showing also the surface traces of the main faults in the area. (After Abercrombie, in press.)

The PEEL and RIDGE zones produced the majority of the gold tonnage mined at Ketz River. These are shown in Figure 7. The PEEL zone is a manto which consists of two parts. These are separated by the steep, northwest trending Junction Fault. The western part of the manto contains sulphides; the eastern part has been thoroughly oxidised. The PEEL sulphides grade approximately 9g/t Au, which is higher than any of the other sulphides, but generally less than the oxides, and is sub-economic at current gold prices. The major sulphide is massive pyrrhotite, which is intergrown with quartz in some parts of the manto. Pyrite occurs as euhedral to subhedral crystals, often separated from the pyrrhotite by thin bands of quartz. Plate 2 shows photomicrographs of PEEL sulphides and illustrates this relationship between the pyrrhotite, pyrite and quartz. Gold occurs as disseminated grains of native gold up to 25 microns in diameter, and less frequently as electrum. It is found in fracture zones within arsenopyrite or pyrite, and is commonly associated with native bismuth or chalcopyrite (Abercrombie, in press).

The PEEL oxides form the lower part of the ore mined at Ketz River. Limonite, hisingerite, quartz, clay and trace pyrite are found within the oxide body. Two distinct textures occur; the lower part of the oxide body consists of massive to boxwork limonite, whereas the upper part contains fine-grained, red-orange, banded hisingerite and limonite. As for the sulphide zone, gold occurs as free grains up to 25 microns in diameter within oxide minerals. The presence of submicroscopic gold has also been indicated by metallurgical tests (Abercrombie, in press). The highest gold grades occur nearest to the hangingwall of the oxide body, and are associated with the presence of hisingerite in the banded oxide.

The RIDGE oxides form a chimney extending upwards from the PEEL zone, with which they are continuous. Mineralogy of the RIDGE zone is the same as that seen in the PEEL oxides, but there is no associated sulphide pod. Oxide material from the RIDGE zone is shown in Plate 3. Gold occurs in the central part of the chimney in fine-grained, bright coloured oxides, surrounded by lower grade, boxwork textured oxide (Abercrombie, in press).

The PENGUIN zone is a stratiform sulphide manto showing some oxidation. It is associated with quartz veins which extend into the surrounding limestone. Oxidation appears to be mainly surficial, but with some more extensive limonitic boxwork in the southern part of the showing.

The TARN zone contains oxide and sulphide material, with some associated quartz veining. Boxwork is common in the oxide parts of the zone. These oxides are limonite, scorodite and hisingerite, and contain gold in sub-economic quantities. The sulphide parts of the showing contain pyrrhotite, arsenopyrite and pyrite, and are usually more massive in



Plate 2: Photomicrographs of polished sections of sample KR-90-81, showing euhedral pyrite separated from pyrrhotite by a thin quartz layer. Scale bar = 100 μ m. Photographs taken in plane polarised reflected light. po = pyrrhotite, py = pyrite, qtz = quartz.

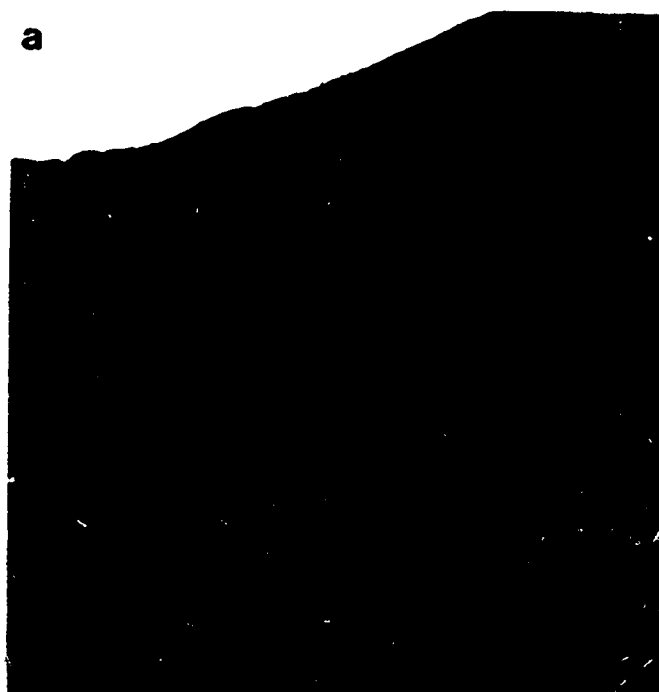


Plate 3: Oxide ore from the Ketz River deposits: a. Open pit mining of RIDGE zone oxides; b. Outcrop of local oxidation of sulphides of the PENGUIN zone.

nature than the oxidised parts which suggests that the oxidised fluid may have flowed more readily through the boxwork. The extent of this sulphide/oxide body is not certain, due to limited exposure.

Type III mineralisation

This type of mineralisation is found in the LAB/HOODOO, CLIFF, MOUNT FURY, SAUNA, UPPER TARN, OXO and MISERY CREEK zones which are shown in Figure 6. These showings, which are hosted by lower Cambrian limestone, contain sulphide boxwork and quartz veining. Some occurrences show oxidation, although to a lesser extent than the PEEL and RIDGE zones of the sulphide mantos: oxidation is generally confined to near surface and to those areas along the Peel Fault, a large east-northeast trending structure which cuts across most of the mineralised area. Type III mineralogy is similar to the limestone-hosted mantos, and consists of quartz, limonite, hisingerite ($\text{Fe}_2\text{Si}_2\text{O}_5(\text{OH})_4 \cdot 2\text{H}_2\text{O}$), pyrrhotite, pyrite, arsenopyrite, scorodite, and some calcite. The ratio of quartz to sulphide found in these occurrences varies greatly. Some appear to consist primarily of quartz, with little sulphide, whereas others resemble the massive sulphide mantos of the more central area, but are smaller and contain higher proportions of gangue phase.

The SAUNA zone contains extensive quartz veining in the host limestone, and shows moderate-sized areas of sulphide/oxide boxwork. Mineralogy is mainly pyrrhotite and pyrite, oxidised to limonite and hisingerite, but there are local concentrations of arsenopyrite and associated scorodite. The mineralogy is similar to that seen in the TARN zone, but quartz veining associated with the sulphides is more ubiquitous, and parts of this zone show limonite stained quartz veins with no associated sulphides. Extensive fracturing occurs, with quartz and oxide stringers extending into the limestone. This zone contains some of the highest gold grades of this group of occurrences.

The CLIFF zone contains a number of small north-south striking pods of massive pyrrhotite and pyrite, locally oxidised to produce limonite-pyrite banding. As for the PENGUIN zone, the host limestone contains extensive quartz veining around the pods. However, the veining does not appear to extend into the sulphide itself.

Extensive oxidised stockwork is found in the LAB/HOODOO zone, associated with pods of brecciated and limonite stained quartz, but little veining. The host in this area is extensively fractured and shows limonitic staining. Microveins of quartz and calcite occur and are generally sub-parallel to bedding, where seen. The CLIFF and LAB/HOODOO occurrences can be thought of as transitional between the massive sulphide manto mineralisation and the barren quartz-sulphide veins more distant from the Ketzia Uplift.

The OXO showing contains quartz and carbonate veins associated with massive sulphide pods, in a limestone host. Veining in the limestone is concentrated around the sulphide bodies. The sulphides present are pyrrhotite, pyrite and galena.

Type IV mineralisation

This final group includes the OXO FLATS, STUMP and WHITE CREEK occurrences and the Ketz River, East Cache Creek, and Next Valley areas shown in Figure 6. This group is the most diverse, both in mineralogy and host rock types. The majority of occurrences of this type are silver-lead veins, which lie to the east, south and north of the Ketz Uplift (Cathro, 1988). These occurrences are hosted in Upper Cambrian to Mississippian rocks of units 2 to 5 of the local stratigraphy (Cathro, 1988). Mineralogy is generally quartz, carbonate (siderite, calcite and ankerite in varying proportions), pyrite, galena and Fe-oxides, but may also include sphalerite, chalcopryrite, arsenopryrite and pyrrhotite. In contrast to the more proximal deposits in the Ketz River area, these deposits contain less pyrrhotite, more galena, and a larger proportion of ferroan carbonate. Some of the larger quartz-carbonate veins contain multiple stages of carbonate veining, associated with pyrite or galena. Veins within the East Cache Creek area - along the eastern extension of the Peel Fault - show oxidation and a higher proportion of siderite than other veins in the Ketz River area. Cathro (1988) reports grades of 300-800 g/t Ag, 10-25% Pb and trace to 2g/t Au for siderite-galena veins.

Due to access difficulties, many of these silver-lead occurrences were not visited during the present study and information has been gathered from the few showings visited and from work by previous authors (eg Cathro, 1988; Abbott, 1986).

The STUMP occurrence consists of quartz-calcite-siderite-galena veins hosted by grey-green Cambro-Ordovician phyllite. It has been reported to contain 47,800 tonnes of ore grading 20% Pb and 719 g/t Ag (Cathro, 1988). Quartz and carbonate are the main phases and appear to be intergrown. Although limonitic weathering occurs on the surface of the quartz vein material, pyrite is not seen as a sulphide phase. Brecciation of both veins and host is common. Smaller, unnamed showings situated north of Cache Creek at its eastern end contain oxidised sulphides, galena and sphalerite, in upper Cambrian to Devonian orthoquartzites and phyllites. Other showings in this area are sulphide-carbonate veins hosted by black shales.

Cathro (1988) reports that most silver-lead veins strike approximately north-south, and dip steeply. Some of the veins form along faults but displacement on these faults is difficult to determine, and is thought to be minimal. Vein width varies from 10cm to 5m, with the sulphides forming bands up to 10-20cm wide. Type IV veins cut units both above

and below the Porcupine-Seagull thrust, which is exposed on the property. Lack of displacement of the veins across these faults indicates that the emplacement occurred after thrusting.

CHAPTER IV

LIGHT STABLE ISOTOPE STUDY

Introduction

Light stable isotope studies (C-O-H) of gangue phases in hydrothermal mineral deposits have been demonstrated to be important in determination of the origin and evolution of mineralising fluids (eg Taylor, 1979; Sheppard et al., 1971; Kerrich, 1987; Nesbitt, 1990). In the Ketz River deposit, vein quartz and carbonate are intimately associated with sulphide and oxide mineralisation and are considered to be coeval with the mineralisation. These veins were analysed in order to determine the isotopic characteristics of the fluids from which they formed. Stable isotope ratios for the limestone host to types II and III mineralisation were also determined. This was done to investigate the dynamics of the fluid system, whether flow was pervasive throughout the host or channelised along pathways now represented by veining.

Experimental method

Whole rock limestone samples showing little or no visible alteration were selected from sites adjacent to sulphide bodies and quartz-sulphide veining. Some regional limestone samples were also collected. Carbonate veins were separated from the host limestones by cutting. All samples were crushed to a fine powder. $\delta^{18}\text{O}$ and $\delta^{13}\text{C}$ values were obtained using the H_3PO_4 technique of McCrea (1950).

Quartz samples were separated from silicate and carbonate hosts by cutting. Crushed samples of quartz were then cleaned by boiling in aqua regia for one hour. A small amount of 30% H_2O_2 was added to the acid solution to oxidise and remove sulphides. The samples were then washed and hand picked to ensure purity. $\delta^{18}\text{O}$ of the quartz veins was analysed using the BrF_5 technique of Clayton and Mayeda (1963). Direct extraction of inclusion fluids within vein quartz was conducted by bulk thermal decrepitation. Clean quartz samples were heated to 1100°C under vacuum to decrepitate the inclusions. The aqueous phase liberated during decrepitation was reduced to hydrogen by reaction with Zn pellets at 400°C (Coleman et al., 1982) and then analysed for D/H ratios.

Tables IV-1 and IV-2 show light stable isotope data from the Ketz River study area. $\delta^{18}\text{O}$ and δD values are quoted relative to standard mean ocean water (SMOW), whilst $\delta^{13}\text{C}$ values are quoted relative to Pee Dee Belemnite (PDB). Uncertainties for ^{18}O are $\pm 0.1\text{‰}$, for D $\pm 3\text{‰}$ and for ^{13}C $\pm 0.1\text{‰}$.

Table IV-1: Ketz River regional stable isotope data

Location¹	Sample² number	Mineral³	$\delta^{18}\text{O}$ ‰SMOW	δD^4 ‰SMOW	$\delta^{13}\text{C}$ ‰PDB
Underground	KR-90-U-1	quartz	16.6		
	KR-90-U-2	quartz	15.8		
	KR-90-U-3	quartz	16.4		
	KR-90-U-4	quartz	14.6		
Peel Zone	KR-90-79	quartz	15.4		
	KR-90-86	calcite	-3.9		0.3
Break Zone	KR-90-66	calcite	13.1		-0.9
	KR-90-66	limestone	13.0		0.8
Lab/Hoodoo	KR-90-33	quartz	16.3		
	KR-90-35	calcite	13.6		-4.4
Penguin Zone	KR-90-76	quartz	19.0		
	KR-90-110	quartz	18.1		
Mount Fury	KR-90-60	quartz	19.2		
	KR-90-61	quartz	19.1		
Sauna Zone	KR-90-24	quartz	14.5		
	KR-90-25	quartz	15.4	-170	
	KR-90-25*	quartz	15.8		
	KR-90-52	quartz	18.7	-120	
	KR-90-53	calcite	12.0		-2.7
	KR-90-53	limestone	12.5		-3.1
Upper Tarn	KR-90-78	quartz	17.7		
	KR-90-78	limestone	14.2		0.0
Next Valley	KR-90-44	quartz	13.6	-85	
	KR-90-44*	quartz		-83	
	KR-90-45	quartz	13.2	-124	
	KR-90-45*	quartz		-123	
	KR-90-46	calcite	10.6		5.1
	KR-90-90	quartz	9.5	-104	
	KR-90-91	quartz	17.3		
White Creek (N trib)	KR-90-107	quartz	14.6		
	KR-90-108	quartz	15.1		
White Creek	KR-90-97	quartz	15.7	-161	
	KR-90-98	quartz			
	KR-90-99	quartz	14.5	-158	
	KR-90-99	calcite	13.7		-5.3

Table IV-1: Ketz River regional stable isotope data (continued)

Location ¹	Sample ² number	Mineral ³	$\delta^{18}\text{O}$ ‰SMOW	δD ⁴ ‰SMOW	$\delta^{13}\text{C}$ ‰PDB
Peel Creek	KR-90-69	quartz	13.1		
	KR-90-70	quartz	13.7	-151	
	KR-90-71	calcite	-1.3		0.9
Gully Zone	KR-90-62	quartz	15.5		
	KR-90-65	quartz	19.4		
	KR-90-74	quartz		-160	
	KR-90-114	quartz	13.9	-145	
	KR-90-115	quartz	13.2	-152	
	KR-90-116	quartz	13.2		
	KR-90-123	quartz	14.7	-124	
	KR-90-123	calcite	12.8		-3.1
	KR-90-123*	calcite	12.7		-3.1
	KR-90-124	quartz	13.5	-164	
	KR-90-124*	quartz	13.9		
	KR-90-125	quartz	15.1	-165	
MMM Zone	KR-90-75	quartz	14.7		
	KR-90-119	quartz	14.8		
QB Zone	KR-90-20	quartz		-169	
	KR-90-22	quartz	18.3	-149	
	KR-90-117	quartz	14.5		
	KR-90-118	quartz	12.9		
Knoll Zone	KR-90-120	quartz	18.3		
	KR-90-120	calcite	15.4		-1.2
	KR-90-121	quartz	18.1	-154	
	KR-90-121*	quartz		-146	
	KR-90-121	calcite	15.6		-1.3
Misery Creek	KR-90-58	quartz	14.0	-156	
	KR-90-132	quartz	15.3		
	KR-90-132*	quartz	14.6		
	KR-90-133	quartz	12.3	-111	
East Cache Creek	KR-90-13	calcite	-6.3		0.2
	KR-90-14	siderite	-1.7		-2.6
	KR-90-14*	siderite	-1.9		-2.6
	KR-90-18	calcite	16.7		-1.4
	KR-90-38	quartz		-173	
	KR-90-39	quartz	17.7	-168	
	KR-90-42	quartz	21.3	-183	
	KR-90-42	calcite	15.8		-2.5
	KR-90-43	quartz	19.4	-170	
	KR-90-43	calcite	16.9		-1.7

Table IV-1: Ketz River regional stable isotope data (continued)

Location ¹	Sample number ²	Mineral ³	$\delta^{18}\text{O}$ ‰SMOW	δD^4 ‰SMOW	$\delta^{13}\text{C}$ ‰PDB
Oxo Showing	KR-90-103	quartz	16.7	-182	
	KR-90-104	limestone	14.0		-0.0
	KR-90-105	calcite	13.9		-3.0
Oxo Flats	KR-90-135	quartz	17.9	-145	
	KR-90-136	calcite	15.1		-2.6
Stump Mine	KR-90-5	quartz		-173	
	KR-90-5	calcite	15.2		-2.6
	KR-90-7	quartz	19.7	-171	
	KR-90-8	quartz	20.1	-179	
	KR-90-8*	quartz	20.9	-177	
	KR-90-9	quartz	19.8		
Ketz River South	KR-90-2	quartz	16.3		
	KR-90-2	limestone	13.2		
	KR-90-3	quartz	22.5		
	KR-90-12	quartz	16.8	-161	
	KR-90-12	siderite	13.3		
	KR-90-50	ankerite	12.3		-3.6
	KR-90-50*	ankerite	12.6		-3.6
	KR-90-50	quartz	18.3		
	KR-90-50*	quartz	18.1		
	KR-90-51	quartz	17.2	-166	
	KR-90-51*	quartz	17.7		
Ketz River North	KR-90-1	limestone	21.5		0.3
	KR-90-1*	limestone	21.2		0.2
	KR-90-94	quartz	18.1		
	KR-90-112	quartz	18.6	-182	

Notes:

- ¹ see Figure 6, page 14 for key to locations.
- ² asterisk denotes repeat analyses.
- ³ 'limestone' is used to denote analyses of host rock samples, distinct from vein calcite.
- ⁴ δD analyses of inclusion fluids in quartz.

Table IV-2: Systematic limestone and calcite vein sample series taken from sites close to underground workings

Location ¹	Sample ² number	Mineral ³	$\delta^{18}\text{O}$ ‰SMOW	$\delta^{13}\text{C}$ ‰PDB
1510, series 1	KR-90-140	calcite	14.2	-1.5
	KR-90-140	limestone	14.1	-0.1
	KR-90-141	limestone	14.3	0.7
	KR-90-142	limestone	13.3	0.6
	KR-90-145	limestone	13.8	0.1
	KR-90-146	limestone	13.3	-0.0
	KR-90-148	limestone	11.3	0.5
	KR-90-149	limestone	13.0	0.7
	KR-90-150	limestone	12.1	0.1
	KR-90-152	calcite	14.9	-1.5
	KR-90-152	limestone	13.8	-0.6
	KR-90-153	limestone	13.2	-2.8
	KR-90-155	limestone	13.0	-0.1
	KR-90-156	limestone	14.8	1.0
	KR-90-156*	limestone	15.9	1.2
	KR-90-157	calcite	13.0	-2.2
	KR-90-157	limestone	13.5	-0.2
	KR-90-158	limestone	11.7	-0.1
	KR-90-159	limestone	12.0	-3.3
	KR-90-160	calcite	10.2	-1.8
	KR-90-160	limestone	11.2	0.4
1510, series 2	KR-90-163	limestone	17.1	-0.0
	KR-90-164	limestone	15.2	-0.5
	KR-90-165	limestone	16.7	0.4
	KR-90-167	limestone	14.6	0.0
1510, series 3	KR-90-168	calcite	14.8	-1.6
	KR-90-168	limestone	17.3	-0.2
	KR-90-169	calcite	11.8	-2.2
	KR-90-169	limestone	15.0	0.2
1430, series 1	KR-90-170	limestone	13.7	-0.1
	KR-90-172	limestone	14.8	-1.0
	KR-90-173	limestone	13.7	-2.6
	KR-90-174	limestone	13.6	-2.6
	KR-90-175	limestone	11.9	-3.5
	KR-90-176	calcite	13.0	-0.8
	KR-90-176	limestone	13.5	0.5
	KR-90-178	limestone	15.5	1.2
	KR-90-179	limestone	14.8	-2.6
	KR-90-181	limestone	12.7	-3.9
	KR-90-182	limestone	14.6	0.1
	KR-90-183	limestone	13.7	0.5
	KR-90-184	limestone	14.5	1.0

Table IV-2: Systematic limestone and calcite vein sample series taken from sites close to underground workings (continued)

Location¹	Sample² number	Mineral³	$\delta^{18}\text{O}$ ‰SMOW	$\delta^{13}\text{C}$ ‰PDB
1430, series 2	KR-90-186	limestone	14.2	-1.7
	KR-90-187	calcite	13.4	-2.8
	KR-90-187*	calcite	13.6	-2.7
	KR-90-187	limestone	14.2	-0.7
	KR-90-188	limestone	14.3	-1.0
	KR-90-190	calcite	14.1	-1.9
	KR-90-190	limestone	14.0	-0.8
	KR-90-191	calcite	13.6	-2.2
	KR-90-191	limestone	14.0	0.7
	KR-90-192	limestone	15.0	2.3
	KR-90-193	limestone	14.5	0.3

Notes:

¹ see Figure 6, page 14 for key to locations.

² asterisk denotes repeat analyses.

³ 'limestone' is used to denote analyses of host rock samples, distinct from vein calcite.

Results

Limestones and carbonate veins

Figure 8 shows histograms of $\delta^{18}\text{O}$ for limestones and carbonate veins. Within the study area (approximately 75 km²) the average $\delta^{18}\text{O}$ of the limestones is $13.9 \pm 1.3\text{‰ (SMOW)}$. This value is strongly depleted in ^{18}O relative to average Cambrian limestone. Marine limestones of Cambrian age give $\delta^{18}\text{O}$ values of 20.6 to 25.8‰ (SMOW) (Veizer, 1983). Carbonate veins and veinlets (dominantly calcite, with minor ankerite and siderite) within the limestones have a similar average $\delta^{18}\text{O}$ to the limestones ($13.7 \pm 1.6\text{‰}$). A sample of limestone collected ~23km from the centre of mineralisation (outside the map area shown in Figure 9) yielded a $\delta^{18}\text{O}$ value of 21.5‰ which is within the range expected for Cambrian limestone. Consequently, the carbonate veins and limestones surrounding mineralisation define a large ^{18}O depletion zone. The total extent of this depletion zone is unknown, and will only be determined by further sampling of limestones around the deposit.

Isotopic analyses of vein carbonate from the central portion of the area (associated with Type I mineralisation) and from a number of locations along the Peel Fault (KR-90-71, KR-90-13, KR-90-14) have very low $\delta^{18}\text{O}$ values (Figure 9), averaging $-3.3 \pm 2.0\text{‰}$. Such veins are associated with oxidation of sulphides.

$\delta^{13}\text{C}$ values for veins and limestone hosts generally lie in the range +1 to -4‰ (PDB) (Tables IV-1 and IV-2). A single carbonate vein from the west of the study area gives a $\delta^{13}\text{C}$ of 5.1‰.

Quartz veins

The $\delta^{18}\text{O}$ values obtained from quartz veins are shown in Figures 10 and 11. The values lie in the range 12 to 23‰ (SMOW). Slightly lighter average values were obtained for the central, Type I mineralisation veins ($15.1 \pm 2.1\text{‰}$) and for vein material within the oxide mantos ($15.8 \pm 0.7\text{‰}$) than for the outer areas of the system (average $\delta^{18}\text{O}$ for Ag-Pb veins is $18.0 \pm 2.2\text{‰}$). δD values obtained by bulk extraction of inclusion fluids in quartz are generally in the range -140 to -180‰ (SMOW). The distribution of δD values is shown in Figure 12.

In the western part of the study area quartz veins more distal to the centre of mineralisation (KR-90-44, KR-90-45, KR-90-90) give consistently lower values of $\delta^{18}\text{O}$ (9 to 14‰; average $12.8 \pm 2.7\text{‰}$) and consistently higher values of δD (-85 to -125‰; average $-104 \pm 20\text{‰}$) than the other quartz veins sampled (Figures 11 and 12). No overlap in the range of δD values shown by these samples and the range shown by the majority of samples is seen.

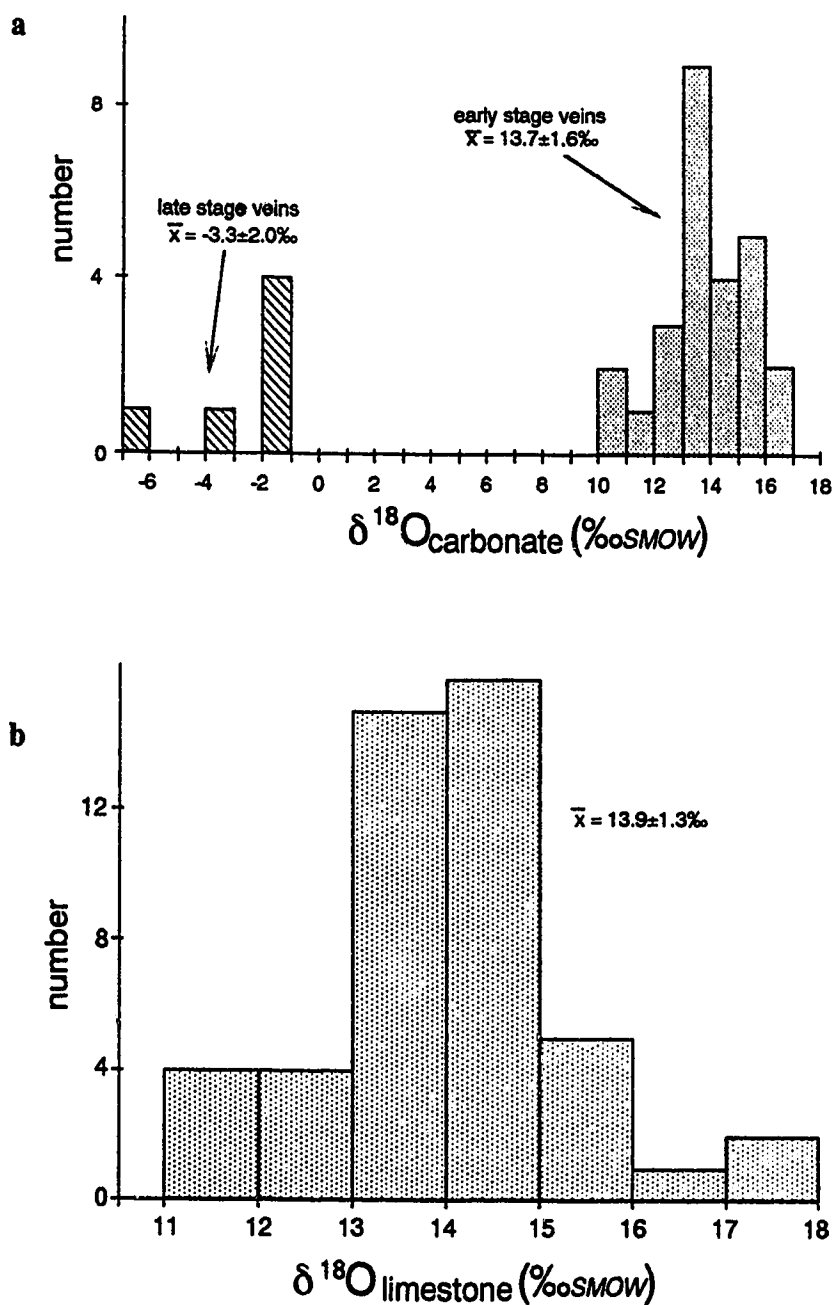


Figure 8: Oxygen isotopic composition of (a) carbonate veins and (b) limestones in the Ketzá River area. Note the two populations of carbonate veins, interpreted from field and petrologic observations as being formed from early-stage and late-stage fluids.

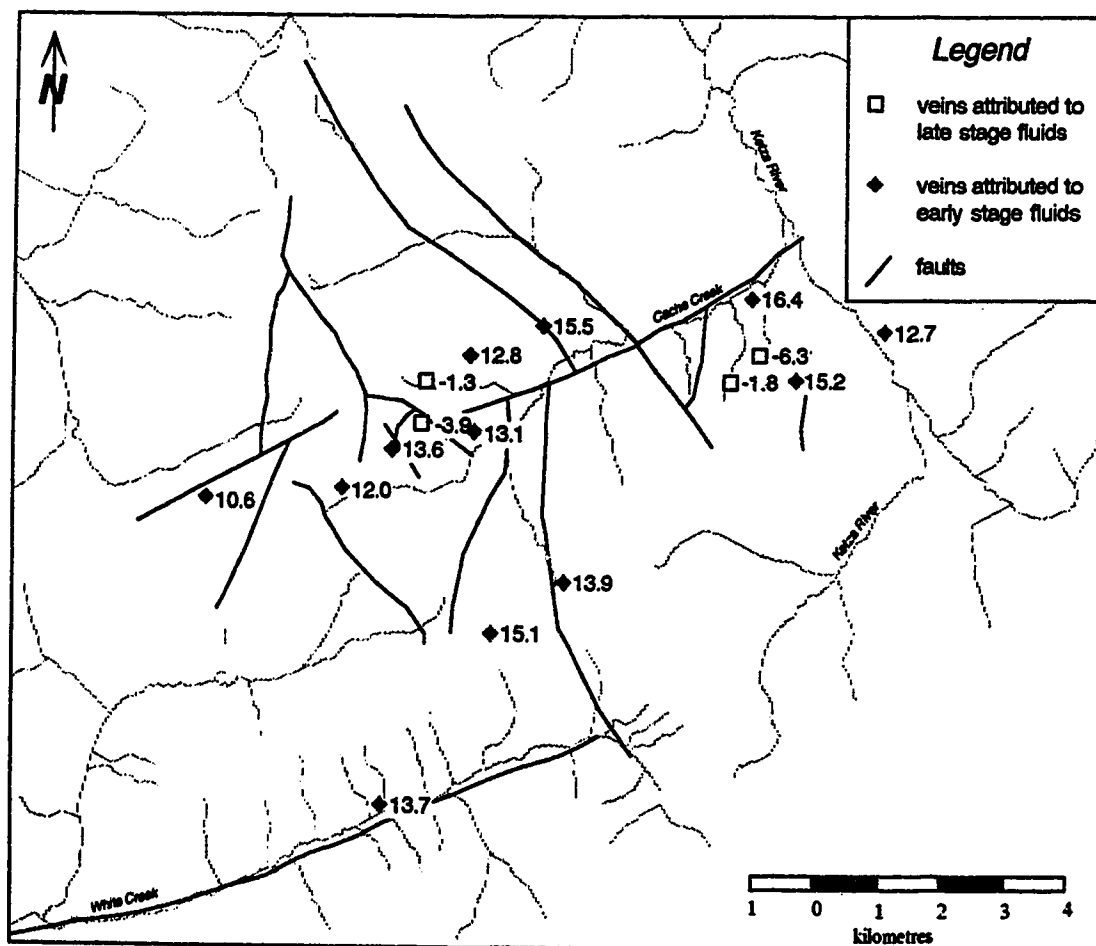


Figure 9: $\delta^{18}\text{O}$ of carbonate veins in the Ketzá River area. Values are quoted as permil (‰) relative to SMOW.

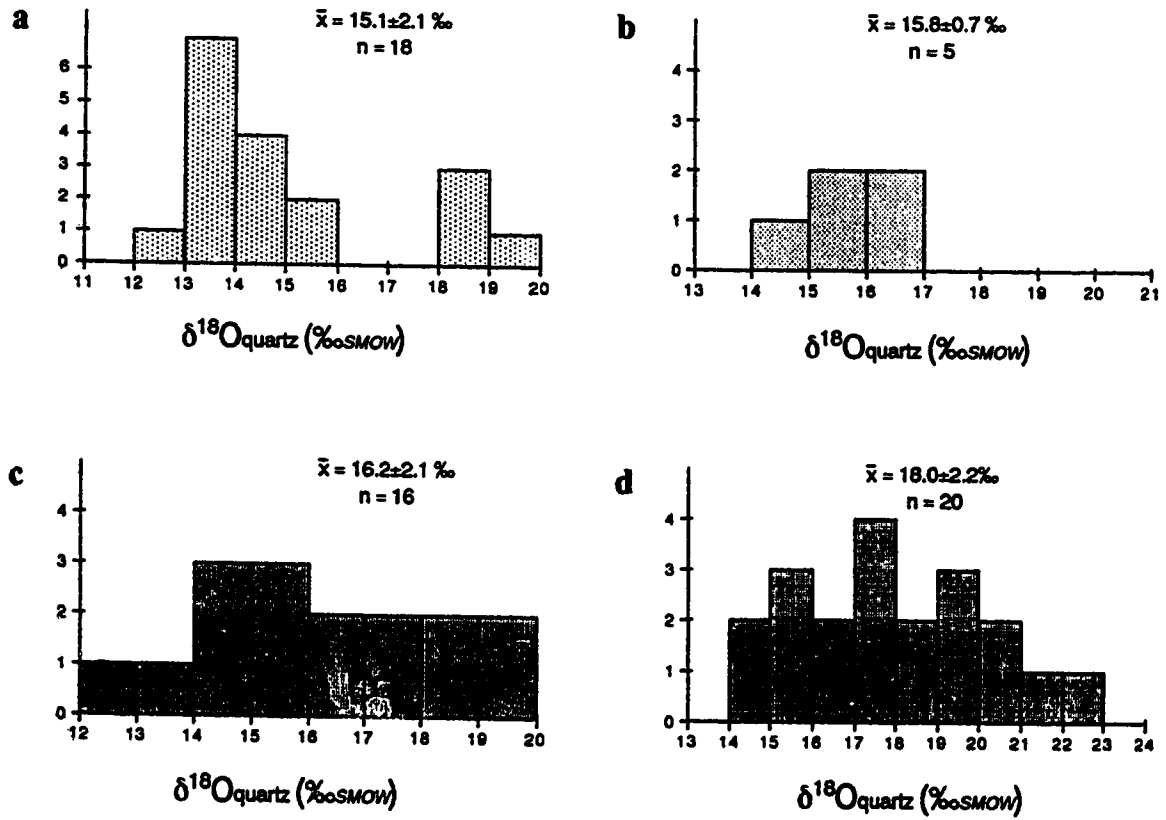


Figure 10: Oxygen isotopic composition of quartz veins associated with the four mineralisation types: a. Type I mineralisation; b. Type II mineralisation; c. Type III mineralisation; d. Type IV mineralisation.

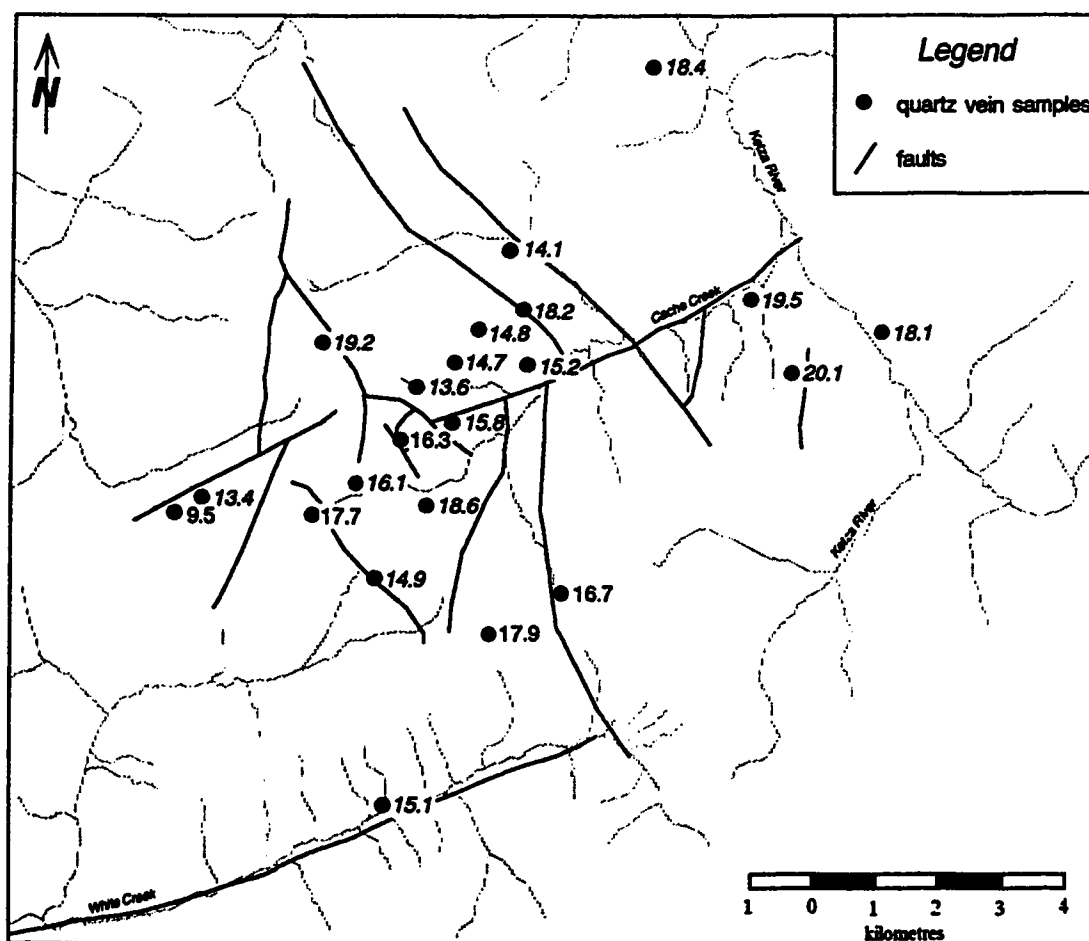


Figure 11: $\delta^{18}\text{O}$ of quartz veins in the Ketz River area. Figures in italics represent averaged values for several samples from one showing. Values are quoted as permil (‰) relative to SMOW.

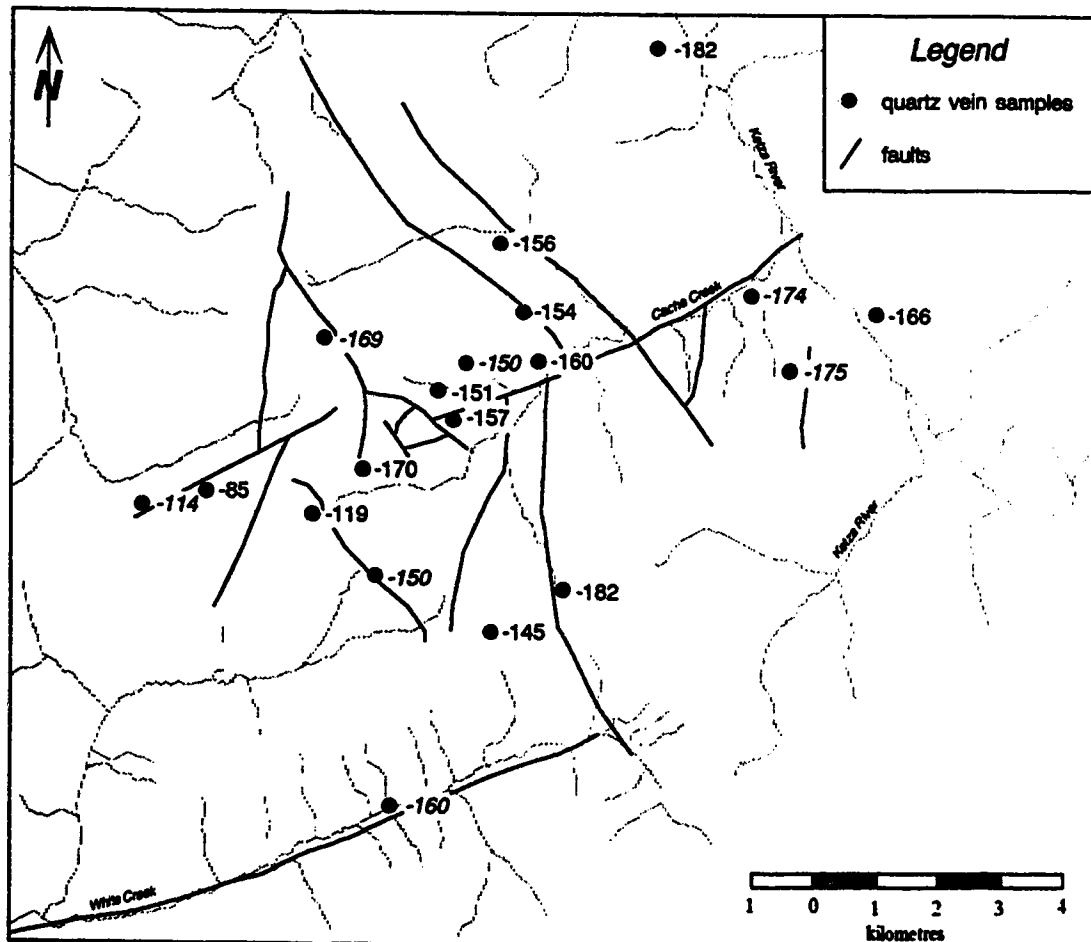


Figure 12: δD of quartz veins in the Ketz River area. Figures in italics represent averaged values for several samples from the same showing. Values are quoted as permil (‰) relative to SMOW.

Discussion of light stable isotope data

1. Calcite-quartz geothermometry

The application of geothermometers to the Ketz River mineralisation is limited by the restricted mineralogy of the veins and mantos. The only widespread mineral pair available for geothermometry is calcite-quartz. However, use of a calcite-quartz oxygen isotope geothermometer is problematic. Problems include the relative ease with which carbonates exchange oxygen isotopes with fluids (Clayton et al., 1968) and the small oxygen isotope fractionation between quartz and calcite which results in large temperature uncertainties (Friedman and O'Neil, 1977). Calcite and quartz are frequently not in isotopic equilibrium with each other, and, as such, temperatures obtained using the calcite-quartz geothermometer are often inconclusive and in disagreement with temperatures obtained using other thermometric techniques (Kerrick, 1987).

Three calibrations of the calcite-quartz geothermometer were tested. The first is the calcite-quartz fractionation expression of Friedman and O'Neil (1977), the second is derived by combining the quartz-water fractionation expression of Matsuhisa et al. (1979) with the calcite-water fractionation expression of O'Neil et al. (1969) and the third is the calcite-quartz fractionation determined from experiments by Clayton et al. (1989), with extrapolation below 500°C using the equations of Clayton and Kieffer (1991). Temperatures obtained from these three calibrations are shown in Table IV-3. The range of calculated temperatures, especially that from samples which are spatially close to each other (KR-90-120, KR-90-121 from the GULLY zone and KR-90-42, KR-90-43 from the East Cache Creek sampling area), is sufficiently large to conclude that the samples cannot be relied upon to show isotopic equilibrium between quartz and calcite. Figure 13 shows diagrammatically the $\delta^{18}\text{O}$ values for the quartz-calcite pairs, together with the expected equilibrium fractionation for the temperature range 250–400°C, calculated from the calcite-quartz fractionation expression of Friedman and O'Neil (1977). Many other hydrothermal deposits form at temperatures between 250 and 400°C (Kerrick, 1987), thus this range was chosen for comparison. From the diagram it is obvious that the isotopic composition of many pairs are not consistent with calcite-quartz temperatures of 250 to 400°C. This may be due to continued exchange of oxygen isotopes between calcite and another phase (likely a fluid phase) after deposition and below the temperature at which quartz-fluid exchange occurs, or to a slight difference in fluid temperature between calcite precipitation and quartz precipitation.

Sample #	Location*	$\delta^{18}\text{O}_{\text{quartz}}$ ‰ _{SMOW}	$\delta^{18}\text{O}_{\text{calcite}}$ ‰ _{SMOW}	temperature ¹ °C	temperature ² °C	temperature ³ °C
KR-90-42	East Cache Creek	21.3	5.8	58	48	162
KR-90-43	East Cache Creek	19.4	6.9	246	208	238
KR-90-99	White Creek	14.5	13.7	940	609	416
KR-90-120	Knoll	18.3	15.4	202	173	222
KR-90-121	Knoll	18.1	15.6	246	208	238
KR-90-123	Gully	14.7	12.8	341	282	271

Notes:

- * see Figure 6, page 14 for key to locations.
- ¹ temperature based on the equation of Friedman and O'Neil (1977) for quartz-calcite fractionation.
- ² temperature based on a combination of the equations of Matsuhisa et al. (1979) for quartz-water fractionation and O'Neil et al. (1969) for calcite-water fractionation.
- ³ temperature based on the experimental calibration of calcite-quartz fractionation of Clayton et al. (1989) and the corrections of Clayton and Kieffer (1991) for extrapolation below 500°C.

Table IV-3: Calcite-quartz oxygen isotope geothermometry for veins of the Ketza River Deposit.

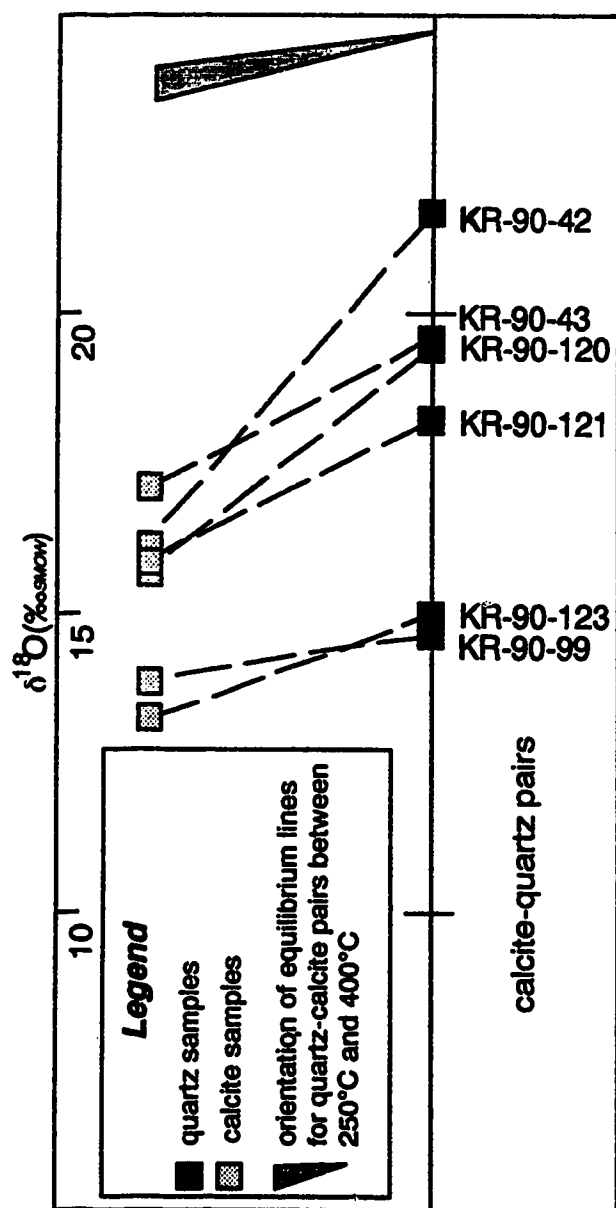


Figure 13: Calcite-quartz pairs used for oxygen isotopic geothermometry. The orientation of tie lines for calcite-quartz equilibrium at temperatures of 250°C to 400°C (from the equation of Friedman and O'Neil, 1977) is also shown.

2. Spatial distribution of isotope values and implications for fluid flow

Average $\delta^{18}\text{O}$ for limestones ($13.9 \pm 1.3\text{‰}$) and carbonate veins ($13.7 \pm 1.6\text{‰}$) is identical within the limits of the analytical method used. This suggests that the fluid responsible for vein formation was also responsible for ^{18}O depletion of the limestones. Furthermore, this correlation indicates that fluid flow was pervasive throughout the limestones within the ^{18}O depletion halo.

There is an increase in $\delta^{18}\text{O}$ quartz away from the central, Type I mineralisation to the distal, Type IV mineralisation (Figure 11). This increase may be attributed either to a drop in temperature away from the centre of mineralisation, or to a change in fluid composition across the area. The first explanation is reinforced by the available fluid inclusion data. This temperature zonation around the centre of mineralisation suggests that the Ketza River deposits formed from a large fluid convection cell. The upflow zone of this fluid cell would occur in the area where the highest temperature values are observed. This is in the centre of the mineralised area, and corresponds to the position hypothesised for a buried pluton, as suggested by geophysical evidence and by hornfelsing of the argillites.

3. Fluid composition

Ketza River stable isotope data shows evidence for the action of three isotopically distinct fluids on the rocks of the study area. These fluids can be distinguished by their discrete hydrogen and oxygen isotopic patterns. These have been designated Fluid I, Fluid II, Fluid III. The spatial distribution of evidence for the three fluids is shown in Figure 14.

The relative timing of Fluids I and II cannot be determined unambiguously, since no relationships between minerals formed from these fluids are evident. However, they are both responsible for early vein formation and are considered to be early stage fluids. Evidence for Fluid III is found only in those parts of the deposit which have undergone oxidation, and represents a later stage in the development of the Ketza River deposit.

Early fluids

Fluid I is the most pervasive of the three fluids seen in the study area (Figure 14). This fluid is responsible for the majority of vein formation and for ^{18}O depletion of the limestone host to types II and II mineralisation. This fluid is interpreted as the main mineralising fluid, from which the sulphide and gangue mineralogy of types I -IV mineralisation formed.

It is possible to determine the oxygen isotopic composition of a mineralising fluid from the $\delta^{18}\text{O}$ of the gangue minerals if the temperature of vein formation is known

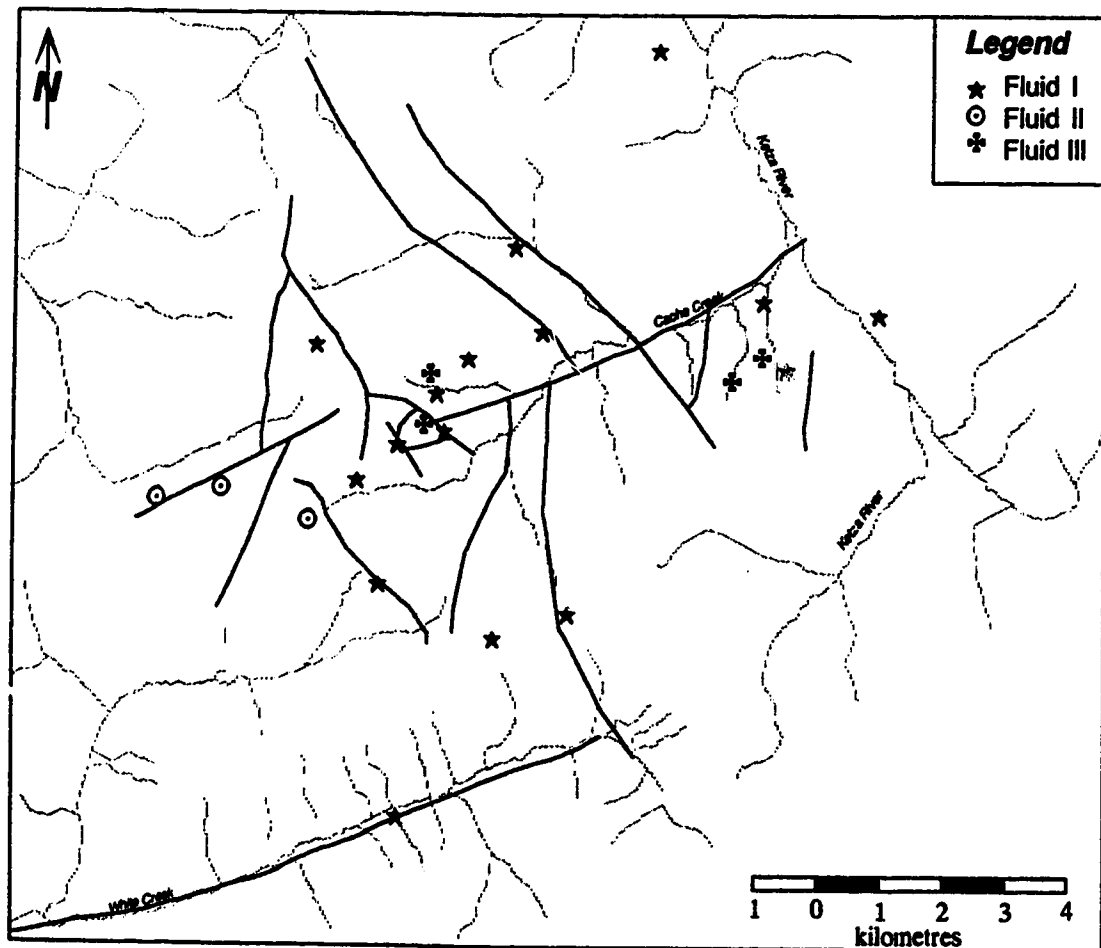


Figure 14: Location of evidence for three fluid types: Fluid I, Fluid II and Fluid III. Fluid I is considered to be responsible for primary mineralisation. Fluid III is considered to be responsible for oxidation of sulphide in parts of the deposit.

(Taylor, 1979; Field and Fifarek, 1985). Calculation of fluid isotopic composition requires three major assumptions: (1) that the minerals are in isotopic equilibrium with the fluid from which they formed; (2) that the gangue minerals formed from the mineralising fluid and (3) that the temperature of formation is known. Quartz-calcite pairs at Ketza River do not, in general, show isotopic equilibrium, as discussed above. However, this may be due to a difference in closure temperature, below which isotopic exchange does not occur, and thus does not necessarily imply disequilibrium between fluid and minerals. It is also possible that quartz and calcite precipitation occurred at different stages in the mineralising event, and that formation temperatures for the two minerals are slightly different.

For the Ketza River deposits, temperature estimates based on limited fluid inclusion homogenisation temperatures, and upon comparison with other carbonate-hosted sulphide deposits, suggest a temperature of mineralisation in the range 300-350°C. No more precise determination of mineralising temperature is available, thus this range of temperatures is used in calculations of fluid $\delta^{18}\text{O}$ for the main mineralising event. Average $\delta^{18}\text{O}$ of quartz veins in the centre of mineralisation (Type I mineralisation) gives a fluid $\delta^{18}\text{O}$ range of 8.3 to 9.9‰, using the equation of Matsuhisa et al. (1979), over the temperature interval 300-350°C.

The ^{18}O depletion of limestones over a large area at Ketza River indicates pervasive flow of large volumes of low ^{18}O fluid. For calculations of water:rock ratios a volume of ^{18}O depleted limestone of 75km³ is used (75km² area observed x 1 km depth assumed). The original oxygen isotopic composition of the limestone is assumed to be 22‰(SMOW) (Veizer, 1983). Final average oxygen isotopic composition of the limestone is 14‰, with a limestone-water oxygen isotope fractionation of 4.5‰ (O'Neil et al., 1969).

If this fluid was of magmatic origin, with an average $\delta^{18}\text{O}$ of 7‰ (Sheppard, 1986) then the water:rock ratio required to produce the ^{18}O depletion halo would be 1.7, using the equation of Field and Fifarek, (1985) to obtain mass ratios. If the fluid was of meteoric origin (-22‰) then the required water:rock ratio would be 0.1 (see Appendix II for calculations). It would therefore take a large volume of magmatic-derived water to produce this alteration, which would require a pluton with a minimum volume of 2500km³ as a source. This assumes a water content of 5% for a granitic pluton (Whitney, 1989). This pluton volume would suggest a plutonic area much larger than the mineralised area. The amount of meteoric water needed to cause the ^{18}O depletion of the limestones is much smaller than the amount of magmatic water. A pluton with a minimum volume of 33km³ would be capable of driving the convection cell for the circulation of meteoric water, based upon the equation of Cathles (1981) for pluton driven hydrothermal circulation systems.

The majority of δD values obtained by thermal decrepitation of inclusion fluids from quartz veins lie in the range -140 to -180‰. This range suggests that the fluids responsible for vein formation are of meteoric origin. Magmatic fluids generally show δD values >-100 ‰ (Sheppard, 1986).

Thus whilst the $\delta^{18}O$ of Fluid I does not preclude either a magmatic or a meteoric origin, the meteoric model is preferred, based upon the ^{18}O depletion seen in the limestone, and upon the δD values of inclusion fluids. Some magmatic component in the fluid cannot be ruled out, but the fluid has a dominant meteoric signature. A metamorphic origin for the fluids is unlikely, since the area contains no rocks of sufficiently high metamorphic grade.

A plot of δD vs $\delta^{18}O$ for the three fluid types seen at Ketza River is shown in Figure 15. This plot also shows the fields for metamorphic and magmatic waters (Sheppard, 1986) and the meteoric water line (Craig, 1961). Calculated compositions for Fluid I plot in the lightly stippled box, which intersects projected isotopic evolution curves for reaction between Cretaceous, Yukon, meteoric water and shale/limestone dominated sedimentary rocks at a range of water:rock ratios. These curves were calculated using the equations of Field and Fifarek (1985). If Fluid I is of meteoric origin, as suggested above, then it is likely that it evolved in $\delta^{18}O$ by interaction with the Paleozoic sedimentary rocks which host the mineralisation.

Evidence for Fluid II comes from quartz veins in the western part of the study area (Figure 14). This fluid does not appear to be associated with any major mineralisation. The western part of the study area contains some pyrite, but is generally barren. The calculated isotopic compositional range for Fluid II is shown by the striped box in Figure 15, which overlaps with the magmatic water box of Sheppard (1986). Fluid II appears to be dominated by a magmatic fluid component. This fluid also contains appreciable amounts of CO_2 (with some CH_4), as seen in the abundant and large fluid inclusions found in samples from the western part of the study area.

Further study of the Seagull Uplift and its associated mineralisation would enable better characterisation of the temporal and geographical distribution of fluid regimes and the extent of magmatic and meteoric fluid involvement in mineralisation. The distinct nature of Fluids I and II, without any evidence for intermediate compositions, suggests that the veins produced by these fluids are of different ages, but no field evidence to confirm or disprove this was noted.

Late fluids

Carbonate veins associated with oxide parts of the deposit provide evidence for Fluid III. These carbonate veins are isotopically distinct from veins associated with

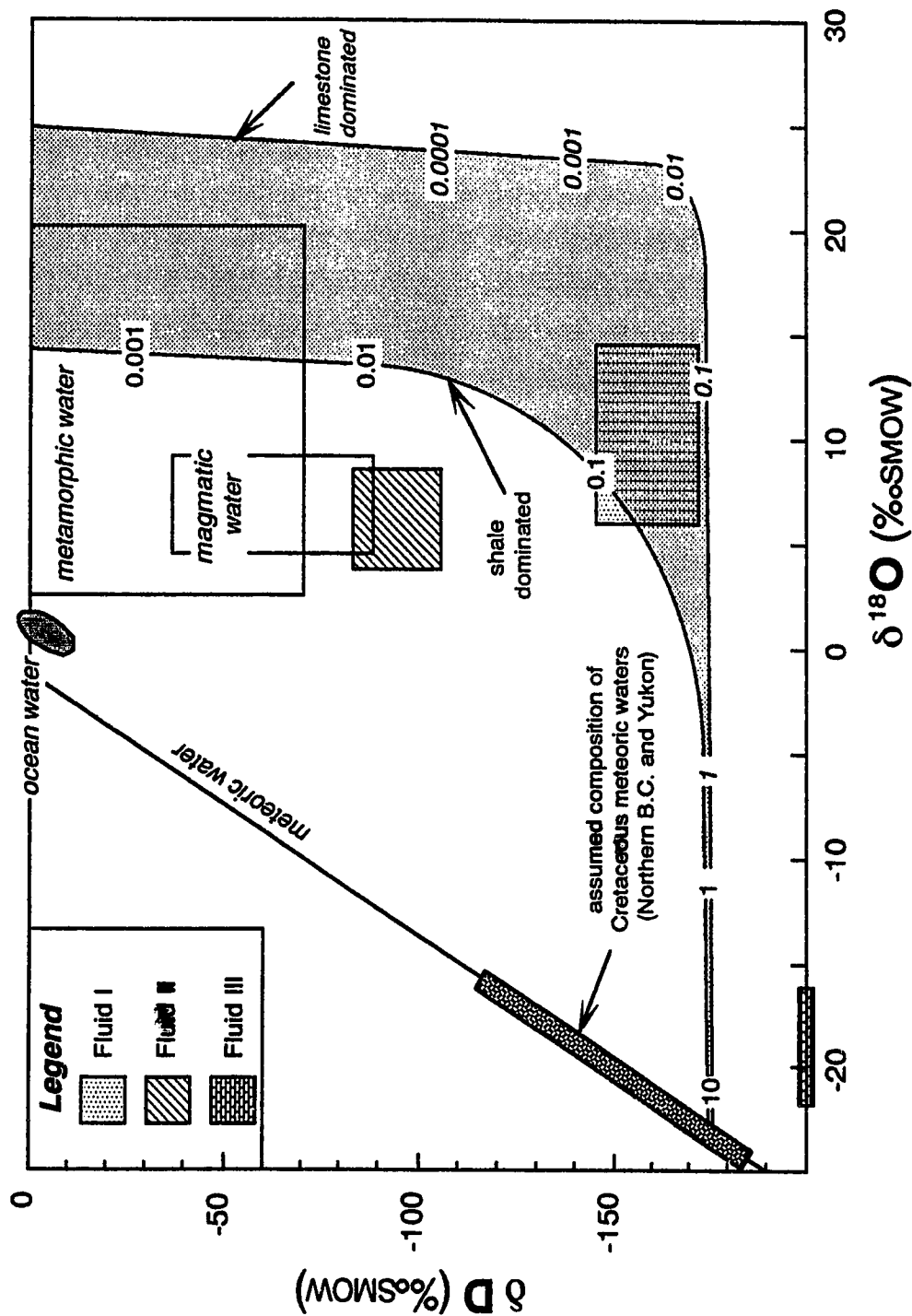


Figure 15: Plot of δD versus calculated $\delta^{18}O$ for vein forming fluids at Ketza River. The two curves represent fluid evolution with variable water:rock ratios (displayed on the curves) at a temperature of $350^{\circ}C$, for dominantly shale-hosted and dominantly limestone-hosted (*italics*) systems. Fluid III is plotted along the base of the graph since no δD values are available.

Fluid I. This fluid is interpreted as responsible for oxidation of sulphides in the centre of the mineralised area and along the Peel Fault to the east. Quartz veins in, or close to, equilibrium with these carbonates are not found.

$\delta^{18}\text{O}_{\text{fluid}}$ values (Fluid III) calculated from $\delta^{18}\text{O}$ of late stage carbonate veins at Ketz River are shown on Figure 15. Isotopic evidence for Fluid III comes solely from carbonate veins. Isotopic analyses of fluid inclusions were performed exclusively on quartz samples, hence no δD data for this fluid are available. The $\delta^{18}\text{O}$ values for Fluid III are therefore plotted along the base of Figure 15.

$\delta^{18}\text{O}_{\text{fluid}}$ values for Fluid III were calculated using an assumed temperature of 100°C . This is likely to represent an upper limit for the temperature of this fluid. The range of $\delta^{18}\text{O}_{\text{fluid}}$ values calculated at 100°C is -18 to $-23\text{‰}_{(\text{SMOW})}$, at 50°C this $\delta^{18}\text{O}_{\text{fluid}}$ would be -25 to $-30\text{‰}_{(\text{SMOW})}$. $\delta^{18}\text{O}_{\text{fluid}}$ values for Fluid III are much lower than for other fluids involved in the formation of the Ketz River deposits. No quartz values in equilibrium with these carbonates are found. The carbonate veins from which these $\delta^{18}\text{O}_{\text{fluid}}$ values are calculated are associated with oxidised portions of the deposit and occur along the Peel Fault.

Fluid III is interpreted as consisting of low temperature ($<100^{\circ}\text{C}$), infiltrating meteoric water, and is considered to be responsible for deep supergene oxidation of the deposit and formation of late stage carbonate veins (calcite and siderite). This fluid appears to have penetrated deeply into the intensely faulted central area of the deposit, oxidising the sulphides in much of the Types I and II mineralisation, but to have had little effect on the oxygen isotopic composition of the quartz veins, since no very light $\delta^{18}\text{O}$ values were recorded in quartz veins.

CHAPTER V

FLUID INCLUSION STUDY

Introduction

In addition to the light stable isotope study presented in Chapter IV, a fluid inclusion study of vein quartz at Ketz River was undertaken, in order to characterise the P-V-T-X conditions of the mineralising fluids. Preliminary investigations revealed that much of the vein quartz was unsuitable for fluid inclusion analysis, due to poor optical clarity of the quartz and to the small size of the majority of inclusions visible. However, observations of inclusions from 7 samples of vein quartz were possible, and these analyses, although limited in number, contribute to an understanding of the properties of the fluids responsible for mineralisation at Ketz River.

Inclusions in doubly polished quartz wafers were investigated using standard microthermometric techniques. A modified USGS gas-flow heating-freezing stage was used in the analyses. Calibration of the stage was performed using liquid nitrogen, natural CO₂ inclusions from Alpine vein quartz, a distilled ice-water bath and Merck standards. Errors in microthermometric data are $\pm 0.2^{\circ}\text{C}$ for freezing and $\pm 2.0^{\circ}\text{C}$ for heating to 400°C .

The limited number of samples containing inclusions of sufficient size for analysis prevents detailed comparisons between sample locations, mineralisation styles and fluid types within the Ketz River system. However, samples of vein quartz from locations associated with the different mineralising styles were investigated as much as possible. The fractured nature of the vein quartz, and the abundance of secondary inclusions made identification and selection of primary inclusions for analysis a difficult task.

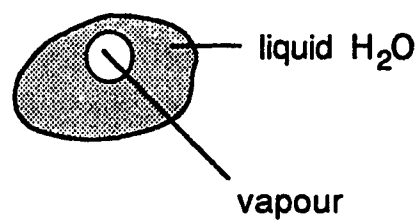
In the previous chapter, Fluids I, II and III are defined based upon isotopic evidence from quartz and carbonate vein material. Fluid inclusions are classified using the same fluid designations, by the location of the host sample.

Results

Observation of fluid inclusions

All inclusions analysed fall into two visual categories, being either two-phase or three-phase at room temperature. These categories correspond to different inclusion compositions, demonstrated by freezing/heating behavior. Schematics of the two types of inclusions are shown in Figure 16. Aqueous inclusions are two-phase at room temperature, containing an aqueous liquid and a vapour bubble, and no discernable CO₂.

Aqueous inclusions



Carbon-dioxide bearing inclusions

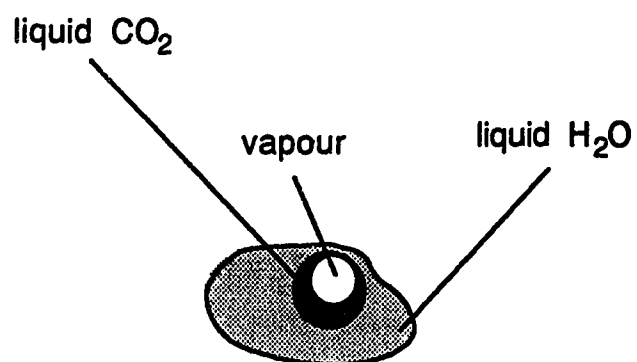


Figure 16: Fluid inclusion categories based upon contained phases. Aqueous inclusions are two-phase at room temperature. Carbon dioxide-bearing inclusions are three-phase at room temperature.

CO₂-bearing inclusions are all three-phase at room temperature, containing an aqueous liquid, an immiscible carbonic liquid and a vapour bubble.

Table V-1 shows observational and microthermometric data for vein quartz samples at Ketz River.

Aqueous inclusions

These inclusions are found in samples from Mount Fury and the Next Valley parts of the Ketz River deposit. Location names are given in Figure 6, page 14. These inclusions contain 70-90% liquid (by volume, estimated) and show low salinities. The majority of aqueous inclusions are from samples which are believed to have formed from Fluid II, although some aqueous inclusions of Fluid I are found.

CO₂-bearing inclusions

CO₂-bearing inclusions sample both Fluid I and Fluid II. These inclusions are found in samples from the PEEL, QB, Next Valley and OXO areas of the Ketz River deposits (Figure 6, page 14). CO₂-bearing inclusions exhibit degrees of fill (volume % estimation of the aqueous liquid phase) of 55 to 95%. Most CO₂-bearing inclusions studied are believed to be primary or pseudosecondary in origin, some inclusions from KR-90-45 may be of secondary origin. CO₂-bearing inclusions generally show the presence of CO₂-hydrate (clathrate) on cooling. In some inclusions the presence of clathrate was not detected, probably due to the small size of the inclusions.

Inclusions measured in sample KR-90-79 (PEEL sulphide zone) were adjacent to a pyrrhotite grain. Other samples do not show such close association with mineralisation.

Microthermometric data from Ketz River fluid inclusions in quartz

Aqueous inclusions

Aqueous fluid inclusions exhibit a range of ice melting temperatures (T_{mice}) from 0 to -5°C. The equation of Potter et al. (1978) was used to calculate the salinity, as an equivalent weight% NaCl. The presence of even trace amounts of dissolved CO₂ in a system can depress the melting point of ice, thus these salinities should be regarded as maximum values. Average salinity for Fluid I is 6.6±0.9 equiv. wt.% NaCl and for Fluid II is 5.8±0.4 equiv. wt.% NaCl.

Total fluid inclusion homogenisation temperatures (Th_{tot}) range from 240 to 280°C. Average Th_{tot} for Fluid I is 244.3±0.5°C; average for Fluid II is 280.4±0.6°C. All aqueous inclusions studied homogenised to the liquid phase. Some inclusions leaked upon heating, and a few decrepitated violently before homogenisation.

Table V-1: Microthermometric data for vein quartz.

Location ¹	Sample ² # -chip	Fluid ³	Incl. ⁴ origin	Incl. ⁵ type	Phase ⁶ assem.	Vol % ⁷ H ₂ O	TmCO ₂ ⁸	Tmice ⁹	Tmclath ¹⁰	ThCO ₂ ¹¹	Th _{tot} ¹²	Eq. wt. ¹³ % NaCl
Peel	79-B	I	?P	C	L-?L-V	70	-57.4	-	9.5	not seen	not seen	1.0
		I	P	C	L-L-V	70	-57.7	-	9.0	28.7	227.3	2.0
		I	P	C	L-L-V	70	-57.5	-	9.1	not seen	256.1	1.8
		I	?P	C	L-?L-V	60	not seen	-	9.1	not seen	324.1	1.8
		I	P	C	L-L-V	60	not seen	-	8.9	not seen	313.8	2.2
		I	P	C	L-?L-V	70	not seen	-	not seen	not seen	324.4	-
QB	22-A	I	?P	C	L-?L-V	70	-56.8	-4.3	-	not seen	not seen	6.9
		I	?	C	L-L-V	70	-	-4.4	-	-	not seen	7.0
		I	?	C	L-L-V	90	-57.7	-	not seen	(2.9)	not seen	-
		I	?	C	L-?L-V	70	not seen	-3.4	-	not seen	231.4	5.5
		I	?	C	L-?L-V	80	-57.6	-	not seen	(3.0)	282.4	-
		I	?	C	L-?L-V	90	not seen	-	not seen	not seen	251.5	-
		I	?P	C	L-?L-V	70	-57.6	-	not seen	not seen	300.1	-
		I	?P	C	L-L-V	70	-57.3	-	11.4	not seen	310.4	-
		I	?P	C	L-?L-V	70	-57.0	-	not seen	not seen	316.8	-
		I	?P	C	L-L-V	90	-57.0	-	not seen	not seen	284.6	-
Mount Fury	60-B	I	?P	?C	L-L-V	70	not seen	-	not seen	not seen	342.0	-
		I	?P	C	L-L-V	95	-57.7	-	not seen	not seen	not seen	-
		I	?P	aq	L-V	90	-	-5.3	-	-	244.8	8.2
		I	?P	C	L-L-V	80	-58.0	-	7.1	not seen	220.8	5.6
		I	?P	aq	L-V	70	-	-3.8	-	-	243.8	6.1
		I	?P	C	L-L-V	95	-57.7	-	not seen	not seen	not seen	-
Next Valley	45-A	II	PS/S	C	L-L-V	60	not seen	-	not seen	not seen	245.4	-
		II	PS/S	C	L-L-V	60	-57.3	-	10.3	28.7	248.3	-
		II	PS/S	C	L-L-V	60	-57.5	-	9.8	28.6	260.5	0.4
		II	PS/S	C	L-L-V	50	-57.4	-	9.7	not seen	260.7	0.6
		II	PS/S	C	L-L-V	55	-57.4	-	9.5	not seen	266.1	1.0
		II	PS/S	C	L-L-V	55	-57.4	-	9.5	not seen	266.1	1.0

Table V-1: Microthermometric data for vein quartz (continued).

Location ¹	Sample ² # -chip	Fluid ³	Incl. ⁴ origin	Incl. ⁵ type	Phase ⁶ assem.	Vol % ⁷ H ₂ O	T _{mCO₂} ⁸	T _{mice} ⁹	T _{mclath} ¹⁰	ThCO ₂ ¹¹	Th _{tot} ¹²	Eq. wt. ¹³ % NaCl
Next Valley	90-A	II	?P	aq	L-V	75	-	-3.1	-	-	279.8	5.1
		II	?P	aq	L-V	90	-	-3.7	-	-	280.5	6.0
		II	?P	aq	L-V	80	-	not seen	-	-	280.6	-
		II	?P	aq	L-V	90	-	-3.5	-	-	281.0	5.7
	90-D	II	?P	aq	L-V	80	-	-3.4	-	-	280.1	5.5
		II	?P	aq	L-V	90	-	0.4	-	-	260.1	0
		II	?P	aq	L-V	90	-	0.4	-	-	259.1	0
		II	?P	aq	L-V	90	-	-3.6	-	-	280.4	5.8
		II	?P	aq	L-V	95	-	-4.0	-	-	279.9	6.4
		I	P/PS	C	L-L-V	90	-57.8	-	not seen	25.8	309.1	-
		I	P/PS	C	L-L-V	90	-58.2	-	not seen	not seen	(351.0)	-
		I	?	C	L-L-V	95	not seen	-	not seen	not seen	393.5	-
		I	?P	C	L-?L-V	90	not seen	-	not seen	not seen	402.7	-
		I	?P	C	L-?L-V	80	-58.0	-	not seen	not seen	304.1	-
Oxo	103-A	I	P/PS	C	L-L-V	90	-57.8	-	not seen	25.8	309.1	-
		I	P/PS	C	L-L-V	90	-58.2	-	not seen	not seen	(351.0)	-
		I	?	C	L-L-V	95	not seen	-	not seen	not seen	393.5	-
		I	?P	C	L-?L-V	90	not seen	-	not seen	not seen	402.7	-
		I	?P	C	L-?L-V	80	-58.0	-	not seen	not seen	304.1	-

Notes

- See Figure 6, page 14 for explanation of location names
- All samples are KR-90-##. Letters denote individual quartz chips
- Fluid descriptions for fluids I and II are given in chapter IV. Fluid I is considered responsible for mineralisation.
- P - primary inclusions; PS - pseudosecondary inclusions; S - secondary inclusions
- aq: aqueous inclusion; C: CO₂-bearing inclusion
- L-V: 2-phase inclusions at room temperature; L-L-V: 3-phase inclusions at room temperature
- Estimate of degree of fill of inclusion. For aqueous inclusions this is vol.% H₂O(liquid)
- Temperature of CO₂ melting (°C)
- Temperature of ice melting (°C)
- Temperature of CO₂-hydrate (clathrate) melting (°C)
- Temperature of homogenisation of volatile phase (°C). Inclusions homogenised to liquid except Q which homogenised to vapour
- Temperature of total homogenisation (°C) *Italics* represent inclusions which decrepitated before homogenisation.
- Calculated salinity (using equations of Potter, 1978 and Bozzo et al., 1975) expressed as equivalent weight % NaCl

CO₂-bearing inclusions

CO₂-bearing inclusions show a T_{mCO_2} of -57.0 to -58.2°C. This depression of the melting point of CO₂ suggests that there is CH₄ or N₂ present in the CO₂. Clathrate melting temperatures (T_{mclath}) for CO₂-bearing inclusions lie in the range 7.1 to 11.4 °C averaging $9.4 \pm 1.0^\circ\text{C}$. This gives a salinity of 0 to 6 equiv. wt.% NaCl using the equation of Bozzo et al. (1975). For samples where $T_{mclath} > 10^\circ\text{C}$ the equation of Bozzo et al. (1975) cannot be used to calculate fluid salinity. The presence of CH₄ or N₂ in the volatile phase increases T_{mclath} , thus the salinities calculated should be regarded as minimum values. In general, salinities calculated for CO₂-bearing inclusions are lower than those calculated for aqueous inclusions.

Carbonic phase homogenisation is not seen in the majority of CO₂-bearing inclusions due to the small size of many inclusions. Where observations were possible, volatile homogenisation to the liquid phase occurred. Observed temperatures of homogenisation of CO₂ (Th_{CO_2}) range from 25.8 to 28.7°C, and exhibit sub-critical behavior. Two inclusions from sample KR-90-22 (QB zone) exhibited homogenisation of CO₂ at 3.0°C, by homogenisation to the vapour phase. The reason for this low temperature and change in mode is uncertain, but could be due to a combination of pressure changes and the presence of other volatiles (CH₄ or N₂) in the carbonic phase.

Temperature of total homogenisation (Th_{tot}) for CO₂-bearing inclusions lie in the range 227 to 403°C. Only one sample (KR-90-103, OXO showing) gave $Th_{tot} > 350^\circ\text{C}$. A large number of CO₂-bearing inclusions decrepitated before homogenisation. A single inclusion in sample KR-90-103 was observed to homogenise to the vapour phase, other inclusions homogenised to liquid. Insufficient data are available to establish the presence or absence of gradients in Th_{tot} across the mineralised area.

Fluid composition and density calculations

Aqueous inclusions

Fluid densities were calculated from Th_{tot} and calculated salinities using the data of Haas (1976). Samples of Fluid II from aqueous inclusions have an average density of 0.80g/cc; aqueous inclusions containing Fluid I have an average density of 0.85g/cc. Isochores calculated from these fluids are shown in Figure 17. Isochore co-ordinates are taken from the data of Potter and Brown (1977) for the system NaCl-H₂O.

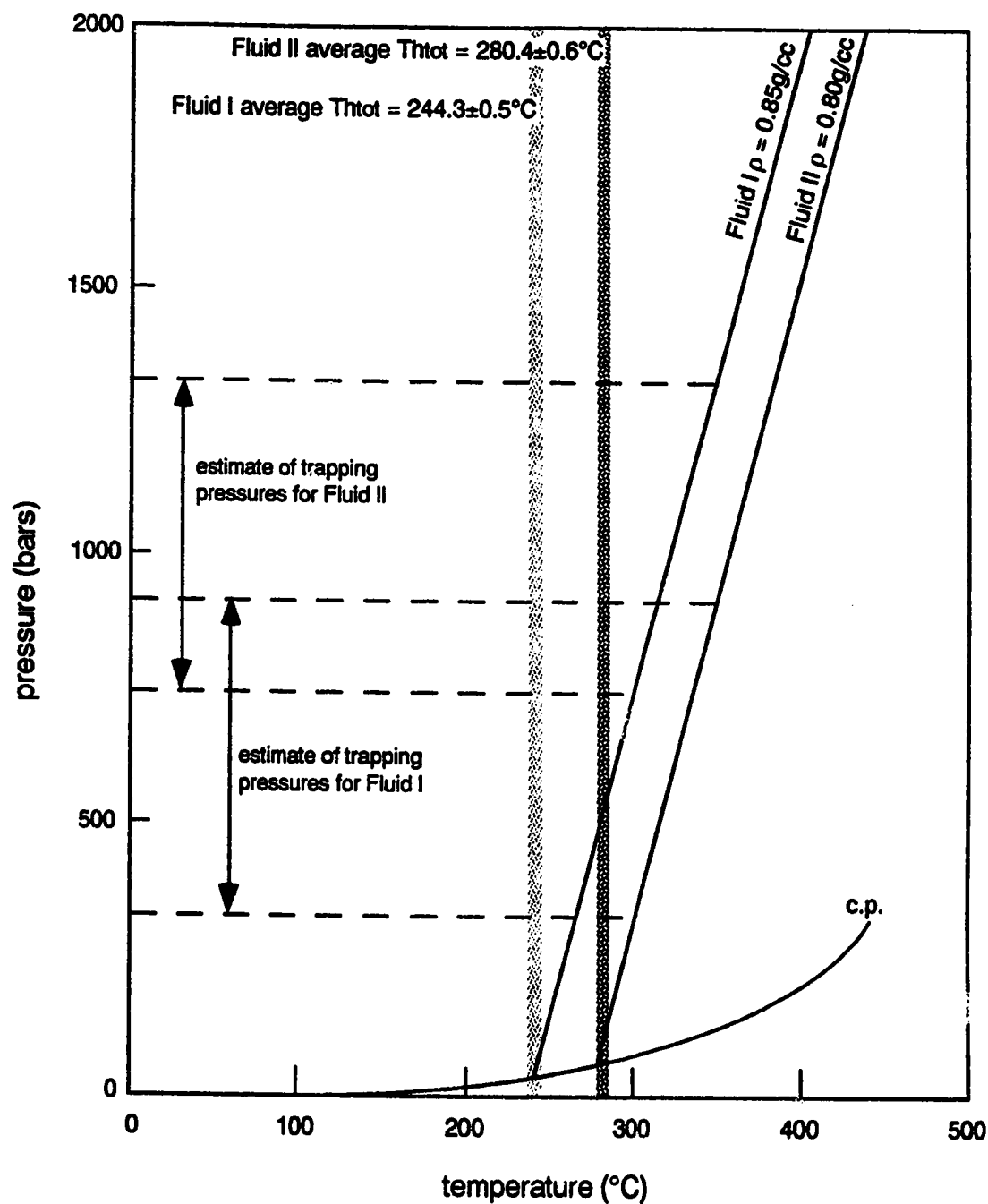


Figure 17: Isochores for aqueous inclusions trapping Fluid I and Fluid II. Salinity = 5 equiv. wt.% NaCl. Data for 2-phase curve and isochore co-ordinates taken from Haas (1976), Potter and Brown (1977). Trapping pressure estimates are based on an estimated temperature range of 300 to 350°C. See text for further discussion of fluid pressure and temperature conditions.

CO₂-bearing inclusions

The slight depression of T_{mCO_2} seen in the inclusions from Ketza River indicates a CH₄/N₂ component in the carbonic (volatile) phase. Assuming that this is CH₄, the construction of Heyen et al. (1982) can be used to determine the mole fraction of methane (XCH₄) in the volatile (carbonic) phase. For the CO₂-bearing inclusions XCH₄ in the volatile phase is 0.05 to 0.10. From the construction of Swanenberg (1979) equivalent CO₂ densities of 0.60 to 0.65g/cc can be determined for the CO₂-bearing inclusions, in which the carbonic phase homogenised to liquid. In sample KR-90-22, the carbonic component of the CO₂-bearing inclusions homogenised to the vapour phase, and the equivalent CO₂ density calculated is 0.13g/cc.

XCO₂(±CH₄±N₂) for CO₂-bearing inclusions is determined from the graphical construction of Schwartz (1989) based upon visual estimates of the volume fraction of the carbonic phase in the inclusion, and the density of the carbonic phase. Despite the obvious potential for error in visual estimates, the work of Diamond (1986) suggests that predictions of XCO₂ using this method are reliable and of sufficient accuracy. XCO₂ for CO₂-bearing inclusions at Ketza River ranges from 0.04 to 0.16, with an average XCO₂ of 0.11±0.04.

Total fluid densities for CO₂-bearing inclusions range from 0.74 to 0.84g/cc, with an average of 0.81±0.03g/cc. Again, the data set is too small to establish any systematic variations in fluid density across the mineralised area.

An isochore plot for CO₂-bearing inclusions trapping Fluid I is shown in Figure 18. Estimated minimum trapping pressures for these inclusions are 650 to 900 bars. In the absence of an independent temperature determination, true trapping pressures and temperatures cannot be determined.

Discussion of fluid inclusion data

The size of the fluid inclusion data set precludes any investigation into spatial variations in fluid conditions within the Ketza River deposits. However, the data do provide useful information about fluid parameters for Fluid I and Fluid II. No characterisation of Fluid III is possible since this fluid does not interact with vein quartz.

Fluid inclusion data for Fluids I and II show greater similarity between these two fluids than is suggested by the isotopic data (Chapter IV). Both fluids are low salinity, with XCO₂ = 0 to 0.16. The relationship between aqueous and CO₂-bearing inclusions for the same fluid is not known, but may be due to variable CO₂ contents of the original fluid. It is possible that there was effervescence of CO₂ from the fluid during quartz precipitation, but the data set is too small for this to be established.

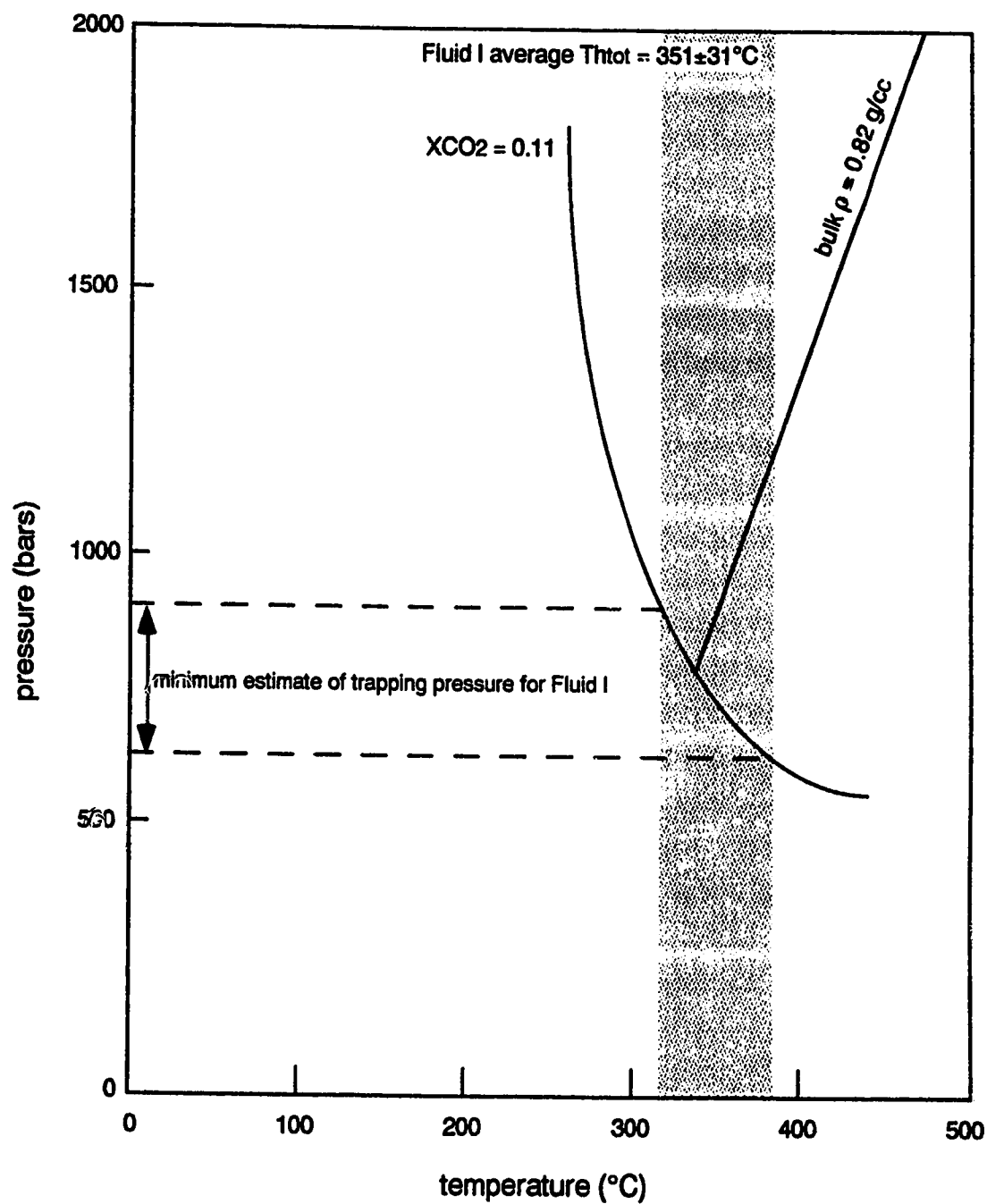


Figure 18: Isochore for carbon dioxide-bearing inclusions trapping Fluid I. Total fluid density 0.82g/cc, salinity 5 equiv. wt.% NaCl. Isochore co-ordinates taken from Bowers and Helgeson (1983), two-phase curve data from Takenouchi and Kennedy (1965).

Temperature and pressure of trapping of fluid inclusions

Although a reliable independent temperature estimate (from mineral pair geothermometry) is not available for the Ketza River deposit, it is possible to estimate temperatures of formation of the deposit by comparison with studies of other deposits. This is discussed in Chapter IV, and a temperature range of 300 to 350°C is suggested for deposit formation. If this is used as an estimate of trapping temperature (T_{trap}) of the inclusions, then estimated trapping pressures (P_{trap}) can be calculated from the fluid isochores.

For aqueous inclusions of Fluid I, a range of T_{trap} of 300-350°C gives a range of P_{trap} of 300 to 900 bars. For Fluid II the same range in T_{trap} gives a range of P_{trap} of 700 to 1300 bars. These pressure estimates are shown in Figure 17. Minimum trapping pressures of CO₂-bearing inclusions are shown on Figure 18, calculated from the range in T_{hot} .

CHAPTER VI

DISCUSSION AND DEPOSIT MODEL

The mineralogical and geochemical characteristics of the Ketza River deposit are summarised in Table VI-1. The four mineralisation styles occur in approximately concentric zones about the Ketza Uplift, which lies in the centre of the mineralised area. A lithologic association is evident in mineralisation types I, II and III. Type I mineralisation occurs only in the central, hornfelsed lower Cambrian argillites immediately above the inferred position of the pluton. Types II and III mineralisation are restricted to the lower Cambrian archeocyathid-bearing limestone. Type IV mineralisation shows no preferential host lithology.

Light stable isotope and fluid inclusion studies of gangue phases in the Ketza River deposit have enabled characterisation of three fluids involved in mineralisation. Fluid I is an $\text{H}_2\text{O}-\text{CO}_2-\text{NaCl}$ fluid with a calculated $\delta^{18}\text{O}$ of 10‰, and a δD of -165‰ (determined directly from fluid inclusions). Average fluid inclusion homogenisation temperature is 325°C, average XCO_2 is 0.11 and average fluid salinity is 5 equivalent weight % NaCl. This is interpreted to be an evolved meteoric fluid, and is considered to be responsible for the main mineralising event (See Chapter IV). Fluid II occurs only in a limited part of the study area (shown in Figure 14, page 39). This is also an $\text{H}_2\text{O}-\text{CO}_2-\text{NaCl}$ fluid, but homogenisation temperatures are lower than for Fluid I, averaging 280°C. Calculated $\delta^{18}\text{O}$ for Fluid II is 7‰, δD from inclusion fluids is -95‰. Fluid salinities and XCO_2 are as for Fluid I. This fluid is interpreted to contain a magmatic fluid component, from comparison with the isotopic data of Sheppard (1986). Fluid III is evident only from stable isotopic analysis of carbonates. This fluid has a calculated $\delta^{18}\text{O}$ of -18‰. No compositional or thermometric data are available for this fluid. This fluid is interpreted to be a percolating meteoric fluid responsible for oxidation of sulphide minerals at a late stage in the formation of the Ketza River deposit.

The Ketza River deposit shares many features with other Au and polymetallic sulphide deposits in the North American Cordillera. Relative to current models of mineralisation, the Ketza River deposit shows similarities with manto-type, carbonate-hosted sulphide deposits and with mesothermal gold mineralisation.

Nelson (1991) defines manto-type deposits as carbonate-hosted sulphide replacement bodies of irregular shape, sub-parallel to bedding (true mantos) or crosscutting bedding (chimneys). These deposits are implicitly associated with intrusive systems which provide a heat and/or fluid source. Manto-type deposits form at temperatures of

Table VI-1: Characteristics of the Ketz River mineral deposits

characteristic mineralogy	I quartz+arsenopyrite
	II pyrrhotite+arsenopyrite+pyrite ±chalcopryite±quartz±calcite
	III quartz+pyrrhotite+pyrite
	IV quartz+galena+sphalerite±calcite ±siderite
$\delta^{18}\text{O}_{\text{fluid}} (\text{‰SMOW})^1$	Fluid I 10‰
	Fluid II 7‰
	Fluid III -18‰
$\delta\text{D}_{\text{fluid}} (\text{‰SMOW})^2$	Fluid I -165‰
	Fluid II -95‰
fluid salinity ³	5 equiv. wt.% NaCl
$\text{XCO}_{2\text{fluid}}^4$	0 to 16%
Th_{tot} (fluid temp) ⁵	Fluid I 325°C
	Fluid II 280°C

Notes:

- ¹ average, calculated from $\delta^{18}\text{O}_{\text{quartz}}$ at 300-350°C for Fluid I and Fluid II, from $\delta^{18}\text{O}_{\text{calcite}}$ at 100°C for Fluid III
- ² from direct analysis of fluid inclusions in quartz
- ³ average value for fluids I and II, calculated from microthermometric fluid inclusion data
- ⁴ calculated from microthermometric fluid inclusion data, range applies to fluids I and II
- ⁵ minimum temperatures of trapping, from average fluid inclusion homogenisation temperatures

approximately 200 to 350°C, which are between those of Mississippi Valley Type deposits and skarn deposits.

Manto deposits have been described from several areas of the North American Cordillera, and from Mexico, Peru, China, and Korea. Sulphide mineralogy is usually dominated by pyrite, galena and sphalerite. Fluids are generally of moderate salinity and are low in CO₂, commonly containing no detectable CO₂. Fluid inclusion homogenisation temperatures generally range from 230 to 330°C.

Beatty et al. (1986) and Beatty (ed., 1990) suggest that manto-type Ag-Pb-Zn deposits in Colorado and Idaho are the result of circulation of magmatic-derived fluids within extensively faulted carbonate hosts. Precipitation of sulphides is the result of an increase in fluid pH as the carbonate host is dissolved.

Nesbitt et al. (1989) define mesothermal gold deposits as those in which the principal economic element is Au, where the temperature of formation ranges from 250-350°C and the pressure of formation is greater than 700 bars. Mesothermal gold deposits are usually hosted by metamorphic terranes, and are characterised by Au-quartz-sulphide veins. Fluids responsible for mesothermal gold mineralisation are found to be uniform over large geographic areas. These fluids show low salinities (<3 wt.% NaCl equivalent) and contain significant CO₂, up to 20 mole % (Kerrick and Wyman, 1990; Nesbitt, 1991).

Nesbitt (1991) notes that most deposits are restricted to greenschist facies metamorphic hosts. Kerrick and Wyman (1990) state that most Phanerozoic mesothermal gold deposits occur in areas of accretion of allochthonous terranes onto continental margins or island arcs. Their model suggests that mesothermal gold is produced by subduction-related underplating of crust, and that deep metamorphism provides a heat source for fluid circulation. Nesbitt (1991) notes that association with felsic plutonism is common in mesothermal gold occurrences, but not ubiquitous.

Manto-type deposits within the North American Cordillera have been described by Beatty (ed., 1990), Thompson and Beatty (1990) and Bradford and Godwin (1988). These deposits have a number of features in common with the Ketz River deposits, and are described briefly below:

Leadville, Colorado

The Leadville deposit is a Ag-Pb-Zn dolomite-hosted deposit, described by Thompson and Beatty (1990). This deposit is one of a number of sulphide deposits hosted by the Leadville Dolomite in this area. The dominant sulphide mineralogy is galena, sphalerite and pyrite, with quartz and siderite gangue. Quartz is found enclosing euhedral

pyrite, as in the PEEL sulphide zone at Ketz River. Fluid inclusion homogenisation temperatures are 220 to 320°C, no CO₂ is reported in these inclusions (Thompson and Beaty, 1990). Mineralogical zoning of the deposit about a central stock is observed, and fluid inclusions from veins proximal to the stock have a homogenisation temperature of 450°C (Thompson and Beaty, 1990). Vertical zoning of $\delta^{18}\text{O}$ and δD seen in the vein minerals are interpreted by Thompson and Beaty (1990) as representing an influx of hot magmatic fluids which produced the mineralisation. Oxygen isotope analysis of carbonates also indicates high $^{18}\text{O}_{\text{fluid}}$ values (Thompson and Beaty, 1990).

Gilman, Colorado

The Gilman deposit is a manto-type deposit which also occurs within the Leadville Dolomite in Colorado. This deposit is described by Beaty (ed., 1990). The deposit is a dolomite hosted sulphide manto and chimney complex. The dominant mineralogy is marmatite, galena, pyrite and siderite. Fluid inclusions from quartz associated with the manto mineralisation show a range in temperature of homogenisation of 174 to 306°C, with an average salinity of 5.2 equivalent weight % NaCl (Naeser et al., 1990). Isotopic composition of the mineralising fluids is given by Beaty and Landis (1990) as $\delta^{18}\text{O}_{\text{fluid}}$ of 4 to 9 ‰ and $\delta\text{D}_{\text{fluid}}$ of -40 to -50 ‰.

Midway, British Columbia

The Midway Ag-Pb-Zn deposit in northern British Columbia is another manto-type deposit within the North American Cordillera, and has been described by Bradford and Godwin (1988). The deposit consists of irregular pipe-like bodies of sulphide mineralisation hosted by mid-Devonian limestone of the Cassiar Terrane. Thrust faulting and imbrication of the deposit have been indicated by drilling (Bradford and Godwin, 1988). Sulphide mineralogy is dominated by pyrite, galena and sphalerite, and shows sharp bleached wallrock contacts. Bradford (1988) reports fluid inclusion homogenisation temperatures of 267 to 334°C from H₂O-NaCl-CO₂±CH₄ inclusions in quartz and sphalerite. Salinities in fluid inclusions range from 2.5 to 10 equivalent weight % NaCl.

The Ketz River deposits show a similar range of fluid homogenisation temperatures and fluid salinities to most manto-type deposits. The morphological characteristics of the deposit are also similar to manto-type deposits elsewhere. However, the presence of significant CO₂ in the fluid and the mineralogy of the Ketz River deposit is significantly different from the majority of manto-type deposits described in the literature.

In these characteristics, the Ketz River deposit more closely fits the mesothermal gold deposit model.

Phanerozoic mesothermal gold mineralisation has been described by Nesbitt (1991). Deposits consist of Au-quartz-carbonate veins containing some sulphides and other silicate minerals. Host rocks are of variable lithology and are generally metamorphosed to greenschist facies. Fluid inclusions are usually $\text{H}_2\text{O}-\text{CO}_2\pm\text{NaCl}\pm\text{CH}_4$ systems, have salinities <5 equivalent weight % NaCl and show homogenisation temperatures of 250 to 350°C. Pressures of formation are in excess of 1000 bars (Nesbitt, 1991). Hydrogen isotope fluid compositions fall in the range -160 to -30‰, $\delta^{18}\text{O}_{\text{quartz}}$ is typically 11 to 18‰. Fluid source for these deposits is controversial; some authors argue in favour of fluids derived from metamorphic devolatilisation (Kerrick and Fyfe, 1981; Goldfarb et al., 1989), others consider that mesothermal deposits are formed by circulation of evolved meteoric water (Nesbitt et al., 1986; Shelton, 1988).

Archean lode gold deposits are described by Groves and Foster (1991). These deposits generally show significant structural control, being hosted in shear zones adjacent to craton margins. Mineralisation takes the form of vein and stockwork systems. Mineralising fluids are low salinity, $\text{H}_2\text{O}-\text{CO}_2$ bearing systems. Isotopic signatures of mineralising fluids are generally in the range 5 to 8‰ for $\delta^{18}\text{O}$ and 0 to -70‰ for δD . Fluid inclusion homogenisation temperatures are typically 250 to 350°C, as for Phanerozoic deposits, and fluid pressures are generally 1-2 kbar (Groves and Foster, 1991).

The Mosquito Creek mine, in the Cariboo district of central British Columbia, is a mesothermal Au deposit described by Alldrick (1983). Mineralisation consists of limestone-hosted replacement sulphide bodies, with vein mineralisation in adjacent clastic hosts. The vein mineralisation is composed of Au-quartz-pyrite, similar to the argillite-hosted Type I mineralisation seen at Ketz River. The replacement ore occurs as stratabound massive pyrite bodies, mostly within limestone. These bodies show evidence of structural control on mineralisation. Contacts between the sulphide and limestone are sharp, possibly indicating that the sulphide filled earlier cavities and fractures (Alldrick, 1983). Au is reported as filling fractures in pyrite (Alldrick, 1983), this is also seen in the Ketz River deposits.

Evidence for meteoric fluids: Deposits of the Canadian Cordillera

Recent studies by Rushton (1991), Nesbitt et al. (1989), Madu et al. (1990) and Shaw et al. (1991) suggest that meteoric fluids play an important part in the formation of many Cordilleran gold deposits.

In a study of Klondike Au-quartz veins, Rushton (1991) reports a $\delta^{18}\text{O}_{\text{fluid}}$ of $7.8 \pm 1.5\text{‰}$, and a $\delta\text{D}_{\text{fluid}}$ of -104 to -179‰. Shaw et al. (1991), in a study of Au-quartz veins in low grade metasediments at Athabasca Pass, Central Rocky Mountains, reports a $\delta^{18}\text{O}_{\text{fluid}}$ of approximately 8‰ and an average $\delta\text{D}_{\text{fluid}}$ of -115‰. These veins contain lower sulphide contents than the Ketza River deposits, but the nature of the hosts (non-carbonate) precludes large-scale dissolution and manto formation. Fluids from quartz veins in the area of the Mosquito Creek mine, Cariboo District, Central British Columbia, also have a meteoric signature (Nesbitt et al., 1989).

It seems that there is an increasing body of evidence to support the involvement of meteoric fluids in gold deposits of the Canadian Cordillera. To date, no fluid studies of manto-type deposits in the Canadian Cordillera have included isotopic analyses of deuterium in inclusion fluids; it is possible that these deposits may also show a degree of involvement of meteoric fluids.

Mineral deposits of the Canadian Cordillera: Fluid composition

Fluid compositions from other deposits in northern British Columbia and Yukon Territory have been described by Bradford (1988), Lynch (1989), Rushton (1991) and Walton (1987). Bradford (1988), in a study of the Midway manto-type deposit, northern British Columbia, reports a fluid composition of $\text{H}_2\text{O}-\text{CO}_2-\text{NaCl} \pm \text{CH}_4$ from primary fluid inclusions within quartz and sphalerite. Calculated salinity is 2.5 to 10 equivalent wt.% NaCl. Lynch (1989) studied the zoned deposits at Keno Hill, Yukon Territory, and described mineralogy in some zones which is similar to that seen at Ketza River. Salinity, calculated from fluid inclusion measurements, is between 0 and 20 equivalent wt.% NaCl, with higher salinities being recorded from fluid inclusions in siderite than from inclusions in quartz.

A recent study of the Au-quartz-sulphide veins in the Klondike, Yukon Territory, by Rushton (1991) documents variable CO_2 contents within inclusions, with possible evidence for CO_2 effervescence during vein formation. Salinity of the inclusions in the Klondike veins is low, with an average of 4.5 equivalent wt.% NaCl. Fluids in the Venus vein, southwestern Yukon Territory, documented by Walton (1987) contain an average XCO_2 of 0.13, and have a salinity of 3.6 equivalent wt.% NaCl. The mineralogy of the

Venus deposit is similar to types I, II and III mineralogy at Ketz River, consisting primarily of quartz-arsenopyrite-pyrite.

A heat source for mineralisation at Ketz River

Evidence for a buried pluton beneath the centre of the Ketz River deposits has been described by Abbott (1986). Hornfelsing is seen in the argillites in the area of the Ketz Uplift, and there is a geomagnetic anomaly centred on this area. Abbott (1986) suggests that this inferred pluton provides the heat source for the hydrothermal mineralisation seen at Ketz River. Other plutons of Cretaceous age are exposed within the Pelly Mountains, including a small granitic stock in the Seagull Creek area, adjacent to the Ketz River deposits (Abbott, 1986). The Seagull Creek stock shows associated skarn mineralisation.

Alternative possible heat sources are metamorphism or tectonic heating. Mesozoic thrusting and imbrication of the Cassiar Platform occurred as a result of terrane collision and is well documented by Abbott (1986) and Gabrielse (1985). However, the low metamorphic grade (sub-greenschist) of the Ketz River area suggests that a widespread tectonic or metamorphic heat source is unlikely for the Ketz River mineralisation.

Thus it appears that the heat source involved in the formation of the Ketz River deposits is a buried Cretaceous pluton, which is situated beneath the Ketz Uplift. Circulation of hydrothermal fluid resulted from emplacement of this pluton; the mineralisation was produced from this fluid. This model has been applied to many other hydrothermal systems within the North American Cordillera, where isotopic zonation about a central area is seen (eg. Criss and Taylor, 1983, 1986).

Mineralising fluid: 1. Fluid source

The main fluid involved in the Ketz River mineralisation (designated Fluid I in Chapter IV) is interpreted as having a meteoric source. This fluid percolated into the rocks along deep faults, was heated by cooling of the pluton, and formed a hydrothermal circulation cell. Such a cell is shown diagrammatically in Figure 19. This is unlike models suggested by the majority of authors for both manto-type deposits and mesothermal gold deposits.

Beatty (ed. 1990) and Thompson and Beatty (1990) suggest that the fluids responsible for the Gilman and Leadville deposits in Colorado are of magmatic origin. This interpretation is based on the stable isotopic systematics of these deposits as described above. The fluids have high calculated $\delta^{18}\text{O}$ and δD values, and the vertical isotopic zoning shown by the hydrothermal minerals. A similar magmatic origin for Fluid I at Ketz River is unlikely, based upon mass balance and hydrogen isotopes, as presented in

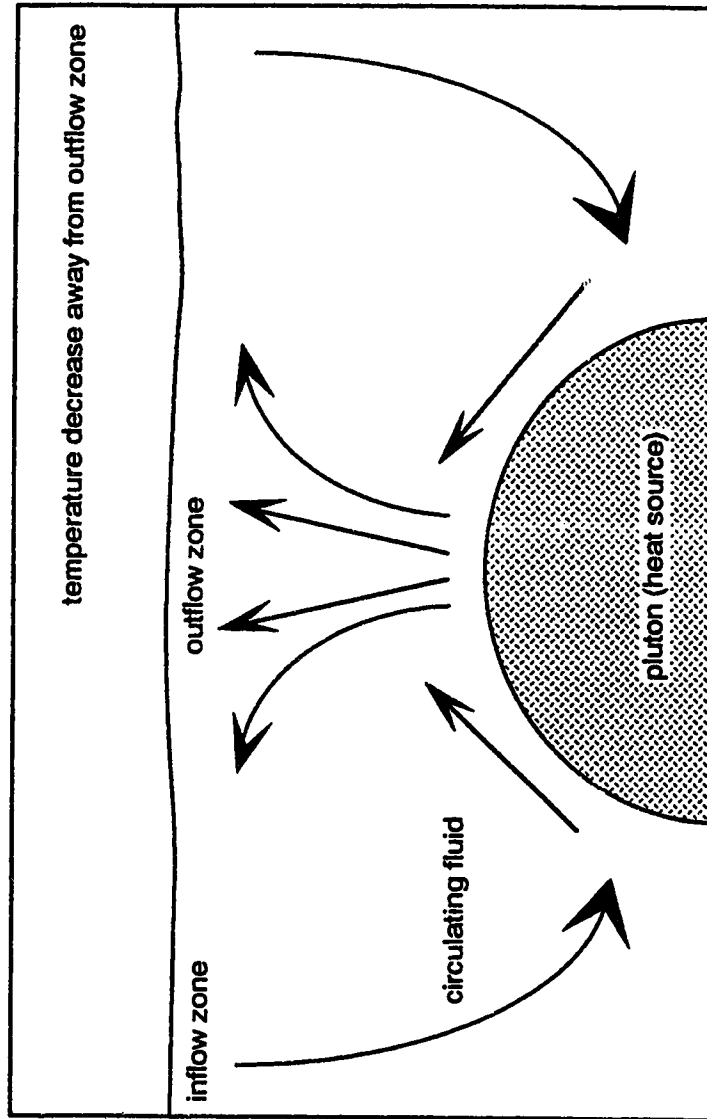


Figure 19: Model of an hydrothermal cell containing circulating meteoric water, driven by an igneous heat source.

Chapter IV. δD values for Ketz River Fluid I lie between -140 and -180‰. ^{18}O depletion in the limestone host to types II and III mineralisation suggests that a large volume of fluid has flowed through the area (see Appendix II for calculations). This volume of fluid would require a very large batholith as a source. A distinction in isotopic signature between meteoric and magmatic fluids at these latitudes is most pronounced, and has been noted in other studies of northern Cordilleran mineral deposits.

Mineralising fluid: 2. Fluid composition

The limited fluid inclusion evidence defines the mineralising fluid composition as $H_2O + NaCl \pm CO_2 \pm CH_4$. The salinity is low (0 to 7 equivalent wt.% NaCl) and XCO_2 is 0 to 0.16. These are unlike the fluids associated with most manto-type deposits. The majority of manto-type deposit studies indicate low to moderate salinity, low XCO_2 fluids.

Fluid I composition at Ketz River appears to be similar to the composition of fluids responsible for other deposits seen in Yukon Territory and northern British Columbia, described above. Evolution of this fluid from pristine meteoric water to a slightly saline, CO_2 -bearing composition occurred during flow through the sedimentary sequence of Cassiar Terrane rocks of the Ketz River area.

A model for the formation of the Ketz River mineral deposits

Mineralisation within the Ketz River deposits shows strong structural control. The regional-scale thrust and normal faulting, related to Mesozoic arc-continent collision (Abbott, 1986) and local normal faulting associated with suggested emplacement of a pluton beneath the Ketz Uplift have produced an extensive fracture network to allow infiltration and circulation of hydrothermal fluids.

Deep circulation of meteoric fluids, which percolated into the system from the surface along fractures, caused the evolution of these fluids. Salinity, CO_2 and metal content of the fluids increased as the fluids moved into deeper, hotter parts of the system. Upflow of fluids in the centre of the hydrothermal cell formed a zone of limestone dissolution and sulphide and gangue deposition. Type I mineralisation, hosted by argillites, takes the form of Au-quartz-sulphide veins which formed along pre-existing fractures. Sericite alteration is evident along the margins of these veins. In the limestone unit, fluid passage is marked by extensive dissolution of the host to form large cavities. This dissolution is likely to have increased fluid pH sufficiently to precipitate sulphides, hence the higher sulphide:gangue ratio seen in Types II and III mineralisation, compared to Type I. Fluid flow within the limestone units was pervasive, and caused resetting of oxygen isotopic values within these limestones throughout a large area. This is further

evident from the many small veins of quartz and calcite within the limestone. Mineralogy within the central parts of the Ketz River deposit is predominantly Fe- and As-sulphides, whilst in more distal areas Pb- and Zn-sulphides are more common. This is likely to be caused by a temperature zonation, also evident in the $\delta^{18}\text{O}_{\text{quartz}}$ values, from a hotter, central upflow zone to cooler distal areas (Figure 20).

After cooling of the pluton and cessation of circulation within the hydrothermal cell described above, infiltration of surface meteoric fluids along some of the large faults caused deep supergene oxidation in some parts of the Ketz River deposits. This oxidation replaced Fe- As-sulphides with hisingerite, limonite, goethite, scorodite and other oxide minerals. Gold grades were enriched by circulation of the oxidising fluids, and further sericite alteration occurred in the argillites hosting Type I mineralisation. Some late stage carbonate was precipitated.

Implications

The deposits at Ketz River do not appear to fit neatly into any current deposit model. However, there are notable features of the deposit which may have important implications.

The ^{18}O depletion halo around the Type II and Type III mineralisation could be a useful tool in the exploration for other carbonate-hosted sulphide deposits. Despite the difference in mineralogy between the Ketz River mantos and other manto-type deposits seen in the Canadian Cordillera, this ^{18}O depletion is likely to be seen around other carbonate-hosted mineralisation where meteoric fluids are involved.

This study, like other recent studies of Cordilleran mineralisation, indicates that the role of evolved meteoric water in the formation of a variety of mineral deposit types may be much greater than previously considered. Light stable isotopic studies of manto-type deposits in Yukon and northern British Columbia may indicate further involvement of evolved meteoric fluids.

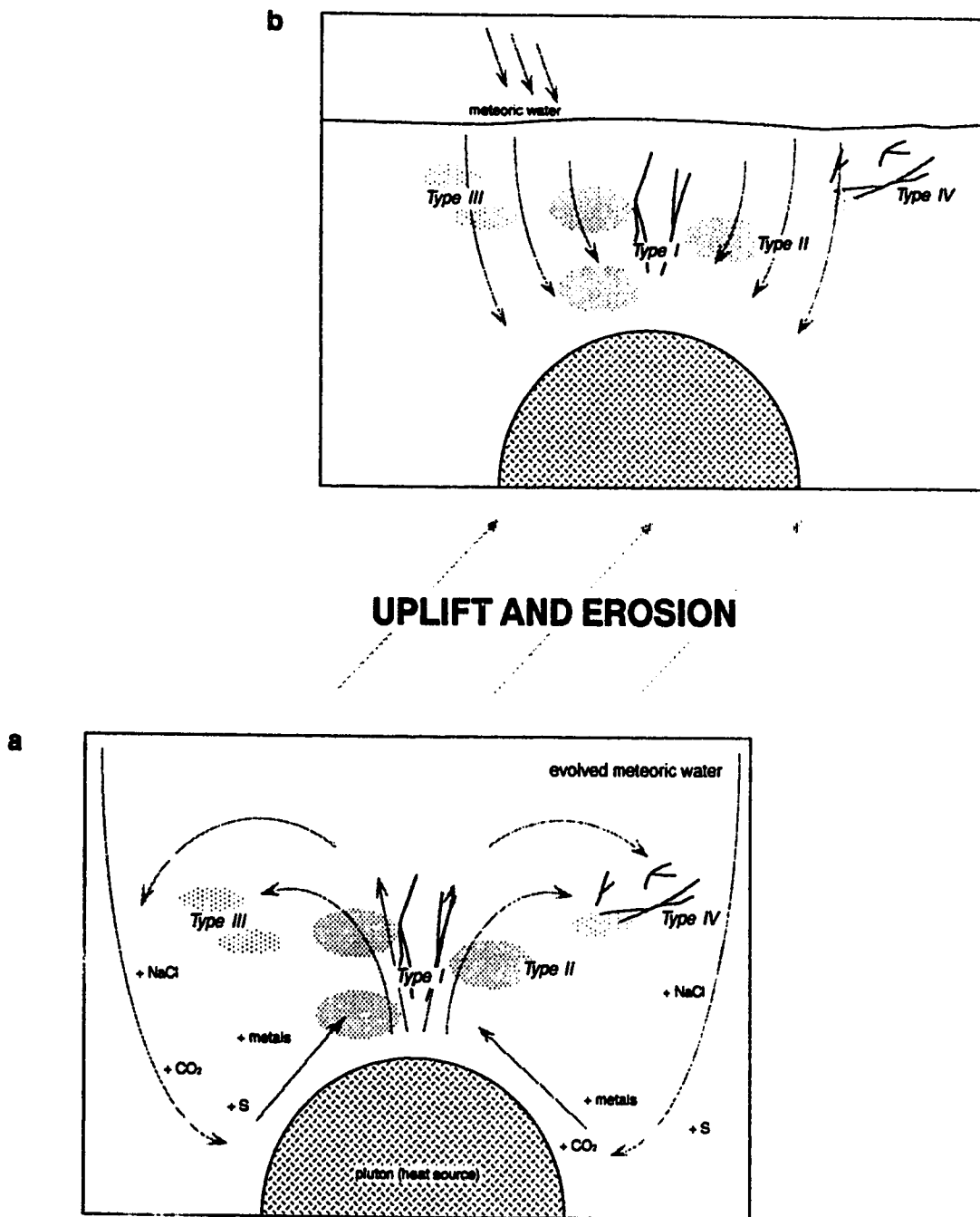


Figure 20: Model of the Ketza River hydrothermal system responsible for producing the mineralisation styles described in the text - Type I: Au-quartz-sulphide veins; Type II: massive sulphide mantos; Type III: quartz-sulphide bodies; Type IV: Ag-Pb veins. a. Main mineralising event, a pluton-driven hydrothermal cell; b. Oxidising event, influx of low temperature meteoric water.

REFERENCES

- Abbott, J.G., 1986, Epigenetic mineral deposits of the Ketzá-Seagull district, Yukon. *In* Yukon Geology, Volume 1, Exploration and Geological Services Division, Yukon, Indian and Northern Affairs Canada, pp. 56-66.
- Abercrombie, S.M., in press, Geology of the Ketzá River gold mine. *In* Yukon Geology, Volume 3, Exploration and Geological Services Division, Yukon, Indian and Northern Affairs Canada.
- Alldrick, D.J., 1983, The Mosquito Creek mine, Cariboo Gold Belt. British Columbia Ministry of Energy, Mines and Petroleum Resources, Paper 1983-1, pp. 399-112.
- Beatty, D.W., Cunningham, C.G., Rye, R.O., Steven, T.A., and Gonzalez-Urien, E., 1986, Geology and geochemistry of the Deer Trail Pb-Zn-Ag-Au-Cu manto deposits, Marysville District, west-central Utah. *Econ. Geol.* v. 81, pp. 1932-1952.
- Beatty, D.W., (ed.) 1990, Origin of the ore deposits at Gilman, Colorado. *Econ. Geol. Mon.* 7, pp. 193-265.
- Beatty, D.W. and Landis, G.P., 1990, Origin of the ore deposits at Gilman, Colorado: Part IV. Stable Isotope Geochemistry. *Econ. Geol. Mon.* 7, pp. 228-245.
- Bozzo, A.T., Chen, H-S, Kass, J.R., and Barduhn, A.J., 1975, The properties of hydrates of chlorine and carbon dioxide. *Desalination* v. 16, pp.303-320.
- Bradford, J.A., 1988, Midway: Hydrothermal environment, and sulphur and metal sources in a high-temperature, carbonate-hosted massive sulphide system. *Geol. Assoc. Canada Program with Abstracts* v. 15, p. A14.
- Bradford, J.A. and Godwin, C.I., 1988, Midway silver-lead-zinc manto deposit, Northern British Columbia. British Columbia Ministry of Energy, Mines and Petroleum Resources, Paper 1988-1, pp. 353-360.
- Cathles, L.M., 1981, Fluid flow and genesis of hydrothermal ore deposits. *Econ. Geol.* v. 75, pp. 424-457.
- Cathro, M.S., 1988, Gold and silver-lead deposits of the Ketzá River District, Yukon: Preliminary results of fieldwork. *In* Yukon Geology, Volume 2, Exploration and Geological Services Division, Yukon, Indian and Northern Affairs Canada, pp. 8-25.
- Clayton, R.N., and Mayeda, T.K., 1963, The use of bromine pentafluoride in the extraction of oxygen from oxides and silicates for isotopic analysis. *Geochim. Cosmochim. Acta* v. 27, pp. 43-52.
- Clayton, R.N., Muffler, L.J.P., and White, D.E., 1968, Oxygen isotope study of calcite and silicates of the River Ranch No. 1 Well, Salton Sea geothermal field, California. *Amer. J. Sci.* v. 266, pp. 968-979.
- Clayton, R.N., Goldsmith, J.R., and Mayeda, T.K., 1989, Oxygen isotope fractionation in quartz, albite, anorthite and calcite. *Geochim. Cosmochim. Acta* v. 53, pp. 725-733.

- Clayton, R.N. and Kieffer, S.W., 1991, Oxygen isotope thermometer calibrations. Geochemical Society, Special Publication No. 3, pp. 3-10.
- Coleman, M.L., Shepherd, T.J., Durham, J.J., Rouse, J.E., and Moore, G.R., 1982, Reduction of water with zinc for isotopic analysis. *Analytical Chem.* v. 54, pp. 993-995.
- Craig, H., 1961, Isotopic variations in meteoric waters. *Science* v. 133, pp. 1702-1703.
- Criss, R.E. and Taylor, H.P.Jr., 1983, An $^{18}\text{O}/^{16}\text{O}$ and D/H study of Tertiary hydrothermal systems in the southern half of the Idaho Batholith. *Geol. Soc. Am. Bull.* v. 94, pp. 640-663.
- Criss, R.E. and Taylor, H.P.Jr., 1986, Meteoric-hydrothermal systems. *Reviews in Mineralogy* v. 16, pp. 373-424.
- Diamond, L.W., 1986, Hydrothermal geochemistry of late-metamorphic gold-quartz veins at Brusson, Val D'Ayas, Pennine Alps, NW Italy. Unpub. PhD thesis, Swiss Federal Institute of Technology, Zurich, Switzerland, 256 pp.
- Field, C.W., and Fife, R.H., 1985, Light stable isotope systematics in the epithermal environment. *Rev. Econ. Geol.* v. 2, pp. 99-128.
- Friedman, I. and O'Neil, J.R., 1977, Compilation of stable isotope fractionation factors of geochemical interest. In *Data of Geochemistry*, Sixth edition, M. Fleischer, ed. U. S. Geological Survey Prof. Pap. 440 KK, pp. KK1-KK12.
- Gabrielse, H., 1985, Major dextral transcurrent displacements along the Northern Rocky Mountain Trench and related lineaments in north-central B.C. *Geol. Soc. America Bull.* v. 196, pp. 1-14.
- Gabrielse, H. and Wheeler, J.O., 1961, Tectonic framework of southern Yukon and northern British Columbia. *Geol. Surv. Canada paper* 60-24, 37 pp.
- Goldfarb, R.J., Leach, D.L., Rose, S.C. and Landis, G.P., 1989, Fluid inclusion geochemistry of gold-bearing quartz veins of the Juneau Gold Belt, southeastern Alaska: Implications for ore genesis. *Econ. Geol. Mon.* 6, pp. 363-375.
- Groves, D.I. and Foster, R.P., 1991, Archean lode gold deposits. In Foster, R.P., ed, *Gold metallogeny and exploration*: Blackie and Sons Limited, Glasgow, pp. 63-103.
- Haas, J.L.Jr., 1976, Physical properties of the coexisting phases and thermochemical properties of the H_2O component in boiling NaCl solutions. *U.S. Geol. Surv. Bull.* 1421-A, 73 pp.
- Hedenquist, J.W., and Henley, R.W., 1985, The importance of CO_2 on freezing point measurements of fluid inclusions: Evidence from active geothermal systems and implications for epithermal ore deposition. *Econ. Geol.* v. 80, pp. 1379-1406.
- Heyen, G., Ramboz, C. and Debussey, J., 1982, Simulation des equilibres de phases dans le systeme $\text{CO}_2\text{-CH}_4$ en dessous de 50°C et de 100 bar. Application aux inclusions de fluides. *Acad. Sci. (Paris) Comptes Rendus.* v. 294, ser. 2, pp. 203-206.

- Kerrick, R.W., 1987, The stable isotope geochemistry of Au-Ag vein deposits in metamorphic rocks. *Mineralog. Assoc. Canada Short Course Handbook v. 13*, pp. 287-336.
- Kerrick, R.W., and Fyfe, W.S., 1981, The gold-carbonate association: source of CO₂ and CO₂-fixation reactions in Archean lode gold deposits. *Chem. Geology v. 33*, pp. 265-294.
- Kerrick, R.W., and Wyman, D., 1990, Geodynamic setting of mesothermal gold deposits: an association with accretionary tectonic regimes. *Geology v. 18*, pp. 882-885.
- Lynch, J.V.G., 1989, Hydrothermal zoning in the Keno Hill Ag-Pb-Zn vein system: A study in structural geology, mineralogy, fluid inclusions and stable isotope geochemistry. Unpub. PhD. thesis, Univ. of Alberta, 217 pp.
- Madu, B.E., Nesbitt, B.E., and Muehlenbachs, K., 1990, A mesothermal gold-stibnite-quartz vein occurrence in the Canadian Cordillera. *Econ. Geol. v. 85*, pp. 1260-1268.
- Matsuhisa, Y., Goldsmith, J.R., and Clayton, R.N., 1979, Oxygen isotope fractionation in divalent metal carbonates. *J. Chem. Physics v. 51*, pp. 5547-5558.
- McCrea, J.M., 1950, On the isotopic chemistry of carbonates and a paleotemperature scale. *J. Chem. Physics v. 18*, pp. 849-857.
- Naeser, C.W., Cunningham, C.G. and Beaty, D.W., 1990, Origin of the ore deposits at Gilman, Colorado: Part III. Fission track and fluid inclusion studies. *Econ. Geol. Mon. 7.*, pp. 219-228.
- Nelson, J.L., 1991, Carbonate-hosted lead-zinc (\pm silver, gold) deposits of British Columbia. *In Ore Deposits, tectonics and metallogeny of the Canadian Cordillera*, British Columbia Ministry of Energy, Mines and Petroleum Resources, Paper 1991-4, pp. 71-86.
- Nesbitt, B.E., 1990, Fluid flow and chemical evolution in the genesis of hydrothermal ore deposits. *Mineralog. Assoc. Canada Short Course Handbook v. 18*, pp. 261-292
- Nesbitt, B.E., 1991, Phanerozoic gold deposits in tectonically active continental margins. *In Foster, R.P., ed. Gold metallogeny and exploration: Blackie and Sons Limited*, Glasgow, pp. 104-132.
- Nesbitt, B.E., Murowchick, J.B. and Muehlenbachs, K., 1986, Dual origins of lode gold deposits in the Canadian Cordillera. *Geology v.14*, pp. 506-509.
- Nesbitt, B.E. and Muehlenbachs, K., 1989, Geology, geochemistry and genesis of mesothermal lode gold deposits of the Canadian Cordillera: Evidence for ore formation from evolved meteoric water. *Econ. Geol. Mon. 6*. pp. 553-563.
- Nesbitt, B.E., Muehlenbachs, K., and Murowchick, J.B., 1989, Genetic implications of stable isotope characteristics of mesothermal Au deposits and related Sb and Hg deposits in the Canadian Cordillera. *Econ. Geol. v. 84*, pp. 1489-1506.
- O'Neil, J.R., Clayton, R.N., and Mayeda, T.K., 1969, Oxygen isotope fractionation in divalent metal carbonates. *J. Chem. Phys. v. 51*, pp. 5547-5558.

- Potter, R.W.II, and Brown, D.L., 1977, The volumetric properties of aqueous sodium chloride solutions from 0° to 500°C at pressures up to 2000 bars based on a regression of available data in the literature. U.S. Geol. Surv. Bull. 1421-C, 36 pp.
- Potter, R.W.II, Clynnne, M.A., and Brown, D.L., 1978, Freezing point depression of aqueous sodium chloride solutions. *Econ. Geol.* v. 73, pp. 284-285.
- Rushton, R.W., 1991, A fluid inclusion and stable isotope study of mesothermal Au-quartz veins in the Klondike schists, Yukon Territory. Unpub. MSc. thesis, Univ. of Alberta, 192 pp.
- Schwartz, M.O., Determining phase volumes of mixed CO₂-H₂O inclusions using microthermometric measurements. *Mineralium Deposita* v. 24, pp. 43-47.
- Shaw, R.P., Morton, R.D., Gray, J., and Krouse, H.R., 1991, Origins of metamorphic gold deposits: Implications of stable isotope data from the Central Rocky Mountains, Canada. *Mineralogy and Petrology* v. 43, pp. 193-209.
- Shelton, K.L., So, C.-S., and Chang, J.-S., 1988, Gold rich mesothermal vein deposits of the Republic of Korea: Geochemical studies of the Jungwon gold area. *Econ. Geol.* v.83, pp. 1221-1237.
- Sheppard, S.M.F., Nielsen, R.L. and Taylor, H.P.Jr., 1971, Hydrogen and oxygen isotopic ratios in minerals from porphyry copper deposits. *Econ. Geol.* v. 66, pp. 515-542.
- Sheppard, S.M.F., 1986, Characterization and isotopic variations in natural waters. *Reviews in Mineralogy* v. 16, pp. 165-183.
- Swanenberg, H.E.C., 1979, Phase equilibria in carbonic systems and their application to freezing studies of fluid inclusions. *Contr. Mineralogy. Petrology* v. 68, pp. 303-306.
- Taylor, H.P.Jr., 1979, Oxygen and hydrogen isotope relationships in hydrothermal mineral deposits. *In* *Geochemistry of hydrothermal ore deposits*, second edition, H.L. Barnes, *ed.* J. Wiley and Sons, New York, pp. 236-277.
- Templeman-Kluit, D.J., Abbott, G., Gordey, S., and Read, B.C., 1975, Stratigraphic and structural studies in the Pelly Mountains, Yukon Territory. *In* Report of activities, Part A, Geol. Surv. Canada Paper 75-1A, pp. 45-48.
- Templeman-Kluit, D.J., Gordey, S.P., and Read, B.C., 1976, Stratigraphic and structural studies in the Pelly Mountains, Yukon Territory. *In* Report of activities, Part A, Geol. Surv. Canada Paper 76-1A, pp. 97-106.
- Thompson, T.B., and Beaty, D.W., 1990, Geology and the origin of ore deposits in the Leadville district, Colorado: Part II. Oxygen, hydrogen, carbon, sulfur and lead isotope data and the development of a genetic model. *Econ. Geol. Mon.* 7, pp. 156-179.
- Vezier, J., 1983, Trace elements and isotopes in sedimentary carbonates. *Reviews in Mineralogy* v. 11, pp. 265-300.
- Walton, L.A., 1987, Geology and geochemistry of the Venus Au-Ag-Pb-Zn vein deposit, Yukon Territory. Unpub. MSc. Thesis, University of Alberta, 113 pp.

- Wheeler, J.O. and McFeely, P. (comp.), 1991, Tectonic assemblage map of the Canadian Cordillera and adjacent parts of the United States of America. Geol. Surv. Canada, Map 1712A.
- Whitney, J.A., 1989, Origin and emplacement of silicic magmas. Rev. Econ. Geol. v. 4, pp. 183-201.

APPENDICES

Appendix I

Fractionation equations used in oxygen isotopic calculations, Chapter IV

N.B. The approximation $1000 \ln \alpha_{A-B} \approx \Delta_{A-B}$ was used in all calculations.

$\Delta_{\text{calcite-water}} = 2.78(10^6/T^2) - 3.39$	0 - 500°C <i>O'Neil et al. (1969)</i>
$\Delta_{\text{quartz-water}} = 3.34(10^6/T^2) - 3.31$	250 - 500°C <i>Matsuhisa et al. (1979)</i>
$\Delta_{\text{quartz-calcite}} = 0.56(10^6/T^2) - 0.42$	<i>Friedman and O'Neil (1977)</i>
$\Delta_{\text{quartz-calcite}} = 0.38(10^6/T^2)$	>500°C <i>Clayton et al. (1989)</i>
$\Delta_{\text{quartz-calcite}} = 0.335(10^6/T^2) - 0.05(10^6/T^2)^2 + 0.035(10^6/T^2)^3$	<500°C <i>Clayton and Kieffer (1991)</i>

where: T is temperature in Kelvins

$$\Delta_{A-B} = \delta_A - \delta_B$$

Appendix II

Water:rock ratio and mass balance calculations from isotopic data

The equation of Field and Fifarek (1985) was used in these calculations. This equation uses final and initial fluid isotopic values, initial rock isotopic values and fluid-rock fractionation factors to calculate a water:rock ratio for the system.

For this system: final $\delta^{18}\text{O}_{\text{fluid}} = 9.5\text{‰}$, initial $\delta^{18}\text{O}_{\text{rock}} = 22\text{‰}$, $\Delta_{\text{r-w}} = 4.5$

$$\delta^{18}\text{O}_{\text{w}} = \frac{22 - \Delta_{\text{r-w}} + 1.8R(\delta^{18}\text{O}_{\text{w}}^i)}{1 + 1.8R}$$

where R is the water:rock ratio.

For ^{18}O depletion of the limestones by a magmatic fluid with an initial $\delta^{18}\text{O}_{\text{fluid}} \approx 7\text{‰}$

$$9.5 = \frac{22 - 4.5 + 1.8R \times 7}{1 + 1.8R}$$

$$R = 1.67$$

the water:rock ratio ≈ 1.7

For ^{18}O depletion of the limestones by a meteoric fluid with an initial $\delta^{18}\text{O}_{\text{fluid}} \approx -22\text{‰}$

$$9.5 = \frac{22 - 4.5 + 1.8R \times -22}{1 + 1.8R}$$

$$R = 0.132$$

the water:rock ratio ≈ 0.1

Depletion of limestone over a 75km^2 area, assuming a depth of depletion of 1km, would thus require the quantities of fluid calculated below:

$$\text{volume of } ^{18}\text{O} \text{ depleted limestone} = 75\text{km}^3 = 75 \times 10^{15} \text{ cm}^3$$

$$\text{mass of fluid required (in grams)} = 75 \times 10^{15} \times \rho_{\text{limestone}} \times R$$

where R = water:rock ratio and $\rho_{\text{limestone}} = 2.6 \text{ g/cm}^3$

for a magmatic fluid system: $R = 1.7$; mass of fluid required = 3.3×10^{17} g.

Assuming that a granitic pluton contains 5 wt.% water, this translates to a minimum pluton size of $2.5 \times 10^3 \text{ km}^3$ to provide a source for the fluid system.

for a meteoric fluid system: $R = 0.1$; mass of fluid required = 2.0×10^{16} g.

From computer models of hydrothermal fluid circulation, Cathles (1981) calculates that an intrusion can drive a hydrothermal circulation system containing a fluid mass of up to 22% of the mass of the pluton. Thus a minimum pluton size of 33 km^3 would be necessary to drive this mass of fluid.

Appendix III

Equations used in fluid inclusion salinity calculations, Chapter V

1. Aqueous inclusions: essentially H₂O-NaCl systems (XCO₂<0.01), salinity calculated from depression of the ice melting point.

$$\text{Salinity} = 0.00 + 1.76958 T - 4.2384 \times 10^{-2} T^2 + 5.2778 \times 10^{-4} T^3$$

Potter et al. (1978)

where the salinity is expressed as equivalent weight percent of NaCl in solution and T = depression of ice melting temperature (T_{m_{ice}}) in °C.

2. CO₂-bearing inclusions: H₂O-CO₂-NaCl systems, salinity calculated from the melting point of CO₂-hydrate (clathrate).

$$\text{Salinity} = 15.52023 - 1.02342 (T_{m_{clath}}) - 0.05286 (T_{m_{clath}})^2$$

Bozzo et al. (1975)

where the salinity is expressed as equivalent weight percent of NaCl in solution and T_{m_{clath}} = final melting temperature of clathrate in °C.

The equation of Bozzo et al. (1975) is only valid for T_{m_{clath}}<10°C

Appendix IV: Ketz River surface samples

Location¹	Sample number	Description²	UTM ref.³
Peel Zone	KR-90-79	qtz vein, po, aspy, py	451 251
	KR-90-80	po, py, qtz	451 251
	KR-90-81	po, py, qtz	451 251
	KR-90-82	po, py, oxide	455 255
	KR-90-83	po, py, oxide	455 255
	KR-90-84	po, py, cc, qtz	455 255
	KR-90-85	po, py	455 255
	KR-90-86	calcite	451 254
Break Zone	KR-90-66	limestone	457 256
	KR-90-67	oxide	457 256
	KR-90-68	sulphide	457 256
Lab/Hoodoo	KR-90-33	qtz vein, lst host	444 254
	KR-90-34	sulphide, qtz, cc	442 252
	KR-90-35	cc vein	442 252
Cliff Zone	KR-90-32	sulphide	449 244
Penguin Zone	KR-90-29	qtz, aspy, lim	437 245
	KR-90-30	po, aspy, py	437 245
	KR-90-31	po, py (oxidised)	437 245
	KR-90-76	qtz vein (026/85°W)	438 244
	KR-90-77	cc vein, lst host	438 244
	KR-90-109	qtz vein, lim	440 241
	KR-90-110	qtz vein, lim	440 241
Mount Fury	KR-90-60	qtz vein, lim	432 267
	KR-90-61	qtz vein, lim	435 267
Sauna Zone	KR-90-23	qtz vein, lim	435 244
	KR-90-24	qtz vein, lim	435 244
	KR-90-25	qtz, po, py, aspy	435 244
	KR-90-26	po, py (oxidised)	435 246
	KR-90-52	qtz vein, lst host	437 244
	KR-90-53	qtz vein, lst host	437 244
	KR-90-54	limestone	435 246
Tarn Zone	KR-90-27	boxwork (oxide)	435 248
	KR-90-28	aspy (oxidised)	435 248
Upper Tarn	KR-90-78	qtz vein, lst	430 230

Appendix IV: Ketz River surface samples (continued)

Location ¹	Sample number	Description ²	UTM ref. ³
Next Valley	KR-90-44	qtz vein	422 245
	KR-90-45	qtz vein	422 245
	KR-90-46	cc vein	422 245
	KR-90-88	qtz, sulphide, arg host	417 252
	KR-90-89	massive py	400 234
	KR-90-90	qtz vein, py	400 234
	KR-90-91	qtz vein, py	400 234
	KR-90-92	py, arg	400 234
White Creek (N trib)	KR-90-107	qtz vein, aspy, oxide	439 234
	KR-90-108	qtz-cc vein	439 234
White Creek	KR-90-97	qtz, cc, lim	436 195*
	KR-90-98	qtz, sulphides, arg host	444 199*
	KR-90-99	qtz-cc vein, arg host	444 199*
	KR-90-100	qtz vein	457 204*
Peel Creek	KR-90-69	qtz, lim, sulphides	456 259
	KR-90-70	qtz vein (006/70°W), lim	456 259
	KR-90-71	cc, Fe-oxides	456 259
	KR-90-72	hematite breccia	456 259
Gully Zone	KR-90-62	qtz, aspy	454 266
	KR-90-63	argillite	454 266
	KR-90-64	qtz vein	452 266
	KR-90-65	qtz vein	454 267
	KR-90-73	qtz vein	
	KR-90-74	qtz vein (brecciated)	451 269
	KR-90-114	qtz vein, lim	457 266
	KR-90-115	qtz, py	457 266
	KR-90-116	qtz vein, lim	457 266
MMM Zone	KR-90-75	qtz vein	456 269
	KR-90-119	qtz, aspy, lim	457 268
	KR-90-123	qtz-cc vein	455 270
	KR-90-124	qtz-cc vein, lim	455 270
	KR-90-125	qtz-cc vein, lim	457 270
	KR-90-126	aspy, scor	459 270
	KR-90-127	qtz vein, scor	459 270
	KR-90-128	qtz vein, scor	459 270
QB Zone	KR-90-19	scorodite	436 264
	KR-90-20	qtz vein	436 264
	KR-90-21	qtz vein, scor	436 264
	KR-90-22	qtz, aspy, lim	462 265
	KR-90-117	qtz vein, sulphide	463 265
	KR-90-118	qtz vein, lim	460 267

Appendix IV: Ketz River surface samples (continued)

Location ¹	Sample number	Description ²	UTM ref. ³
Knoll Zone	KR-90-120	qtz-cc vein, lim	466 273
	KR-90-121	qtz-cc vein, lim	466 273
	KR-90-122	argillite	466 273
Misery Creek	KR-90-58	qtz vein	477 278
	KR-90-59	py, aspy	477 278
	KR-90-129	qtz-cc vein, host	448 279
	KR-90-130	qtz, sulphide, lim	448 279
	KR-90-131	py, host	448 279
	KR-90-132	qtz vein, lim	450 280
	KR-90-133	qtz vein	456 278
	KR-90-134	qtz vein, lim	464 276
East Cache Creek	KR-90-13	cc, sid	504 271
	KR-90-14	siderite	500 267
	KR-90-15	galena	500 267
	KR-90-16	gal, sphal (oxidised)	500 267
	KR-90-17	py, qtzite host	500 275
	KR-90-18	cc, py, lst host	505 268
	KR-90-38	qtz vein, (006/90°)	503 280
	KR-90-39	qtz vein	503 280
	KR-90-40	py, aspy, gal, cpy	503 280
	KR-90-41	py, aspy, gal, sphal	501 280
	KR-90-42	qtz-cc vein	501 297
	KR-90-43	qtz-cc vein	501 297
	KR-90-47	qtz vein	500 267
	KR-90-48	qtz-cc vein, gal	502 270
	KR-90-56	limestone	503 280
	KR-90-57	limestone	503 280
Oxo Showing	KR-90-101	py, gal, cc vein, lst host	475 230
	KR-90-102	po, py, gal	475 230
	KR-90-103	qtz vein	475 230
	KR-90-104	cc vein, lst host	475 230
	KR-90-105	cc vein	475 230
	KR-90-106	qtz vein, lim	473 251
Oxo Flats	KR-90-135	qtz cein	450 215
	KR-90-136	calcite	450 215
	KR-90-137	boxwork (oxide)	450 215
Stump Mine	KR-90-5	qtz-cc vein	512 260
	KR-90-6	qtz-cc vein, gal	512 260
	KR-90-7	qtz-cc vein, gal	510 250
	KR-90-8	qtz vein, lim	510 250
	KR-90-9	qtz vein, gal	510 250

Appendix IV: Ketz River surface samples (continued)

Location¹	Sample number	Description²	UTM ref.³
Ketz River South	KR-90-2	limestone	511 288
	KR-90-3	qtz vein	514 283
	KR-90-4	qtz vein	510 281
	KR-90-10	qtz-cc vein, sulphides	511 288
	KR-90-11	cc vein, host	511 288
	KR-90-12	qtz vein, lim	511 288
	KR-90-49	sulphides	517 278
	KR-90-50	qtz-ank vein	517 278
	KR-90-51	qtz vein	517 278
Ketz River North	KR-90-1	limestone	
	KR-90-93	green-grey tuff	482 340
	KR-90-94	qtz-cc vein	482 340
	KR-90-95	massive py	482 240
	KR-90-96	py, gal	482 340
	KR-90-111	po, py, cpy	488 297
	KR-90-112	qtz vein, lim	482 298
	KR-90-113	po, py	482 298

Notes:

¹ Location names used in Figure 6, page 14.

² Abbreviations used:

- qtz: quartz
- cc: calcite
- sid: siderite
- ank: ankerite
- po: pyrrhotite
- py: pyrite
- aspy: arsenopyrite
- cpy: chalcopyrite
- gal: galena
- sphal: sphalerite
- lim: limonite + other Fe-oxides/hydroxides
- scor: scorodite
- lst: limestone
- arg: argillite
- qtzite: orthoquartzite

³ Universal Transverse Mercator grid reference. All sample locations are from map sheet 105 F-9 except those marked * which are from sheet 105 F-8

Appendix V: Sample suites taken along traverses close to underground workings

Location¹	Sample number	Description²
Peel Zone - underground	KR-90-U-1	qtz vein, sulphides
	KR-90-U-2	qtz vein, sulphides
	KR-90-U-3	qtz vein, sulphides
	KR-90-U-4	sulphide, qtz
	KR-90-U-5	sulphide, qtz
	KR-90-U-6	sulphide, qtz, lst
	KR-90-U-7	sulphide, qtz, lst
1510, series 1	KR-90-138	sulphide
	KR-90-139	sulphide
	KR-90-140	lst with cc veins
	KR-90-141	lst with cc veins
	KR-90-142	lst with cc veins
	KR-90-143	oxide boxwork
	KR-90-144	sulphide, lst
	KR-90-145	lst with cc veins
	KR-90-146	lst with cc veins
	KR-90-147	qtz, sulphide, lst
	KR-90-148	lst with cc veins
	KR-90-149	lst with cc veins
	KR-90-150	lst with cc veins
	KR-90-151	cc, sulphide
	KR-90-152	lst with cc veins
	KR-90-153	lst with cc veins
	KR-90-154	sulphide
	KR-90-155	lst with cc veins
	KR-90-156	lst with cc veins
	KR-90-157	lst with cc veins
	KR-90-158	lst with cc veins
	KR-90-159	calcite
	KR-90-160	lst with cc veins
1510, series 2	KR-90-161	argillite
	KR-90-162	argillite
	KR-90-163	lst with cc veins
	KR-90-164	lst with cc veins
	KR-90-165	lst with cc veins
	KR-90-166	argillite
1510, series 3	KR-90-167	lst with cc veins
	KR-90-168	cc, qtz
	KR-90-169	lst with cc, py
	KR-90-169a	oxide
	KR-90-169b	oxide

Appendix V: Sample suites taken along traverses close to underground workings
(continued)

Location ¹	Sample number	Description ²
1430, series 1	KR-90-170	lst with cc veins
	KR-90-171	lst with cc veins
	KR-90-172	lst with cc veins
	KR-90-173	calcite
	KR-90-174	cc, sulphide
	KR-90-175	cc, sulphide
	KR-90-176	lst with cc veins
	KR-90-177	calcite
	KR-90-178	lst with cc veins
	KR-90-179	limestone
	KR-90-180	argillite
	KR-90-181	lst with cc veins
	KR-90-182	lst with cc veins
	KR-90-183	lst with cc veins
	KR-90-184	lst with cc veins
1430, series 2	KR-90-185	lst with cc veins
	KR-90-186	lst with cc veins
	KR-90-187	lst with cc veins
	KR-90-188	lst with cc veins
	KR-90-189	lst with cc veins
	KR-90-190	lst with cc veins
	KR-90-191	lst with cc veins
	KR-90-192	lst with cc veins
	KR-90-193	lst with cc veins
	KR-90-193a	lst with cc veins
1550 area	KR-90-184	calcite
	KR-90-195	oxide

Notes:

¹ Location of traverses given in Figure 21.

² Abbreviations used: qtz: quartz
 cc: calcite
 py: pyrite
 lst: limestone

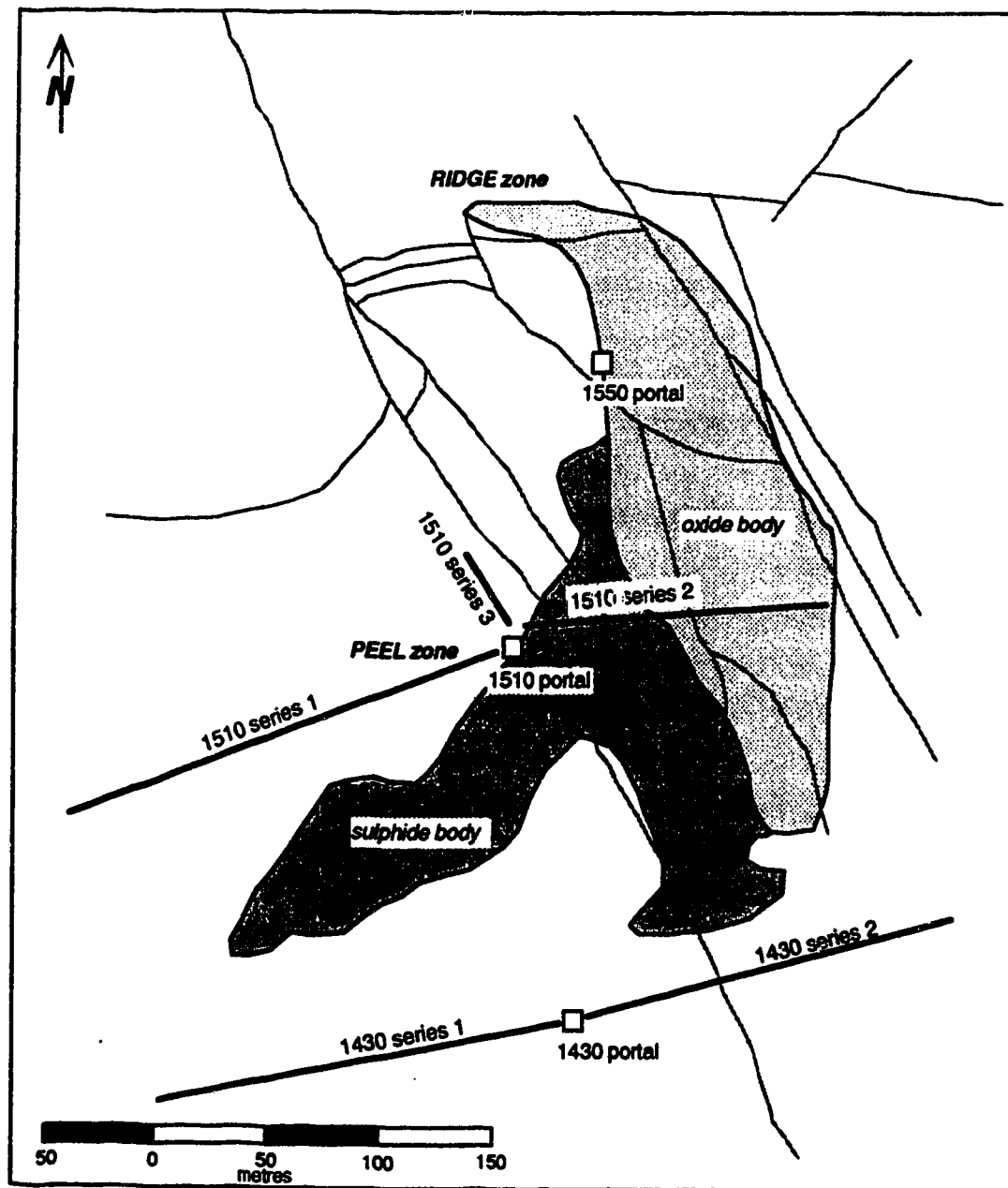


Figure 21: Map as in Figure 7, showing also entrances to the underground workings and the surface traces of sample traverses near the underground workings. (After Abercrombie, in press.)